(12) B.S.

NOSC

NOSC / TR 141

Technical Report 141

EFFECTIVE ELECTRON DENSITY DISTRIBUTIONS DESCRIBING VLF/LF PROPAGATION DATA

DG Morfitt

21 September 1977

Prepared for
Defense Communications Agency (DCA)
and Defense Nuclear Agency (DNA)

Approved for public release; distribution is unlimited

NAVAL OCEAN SYSTEMS CENTER
SAN DIEGO, CALIFORNIA 92152

BLANK PAGES
IN THIS
DOCUMENT
WERE NOT
FILMED

NAVAL OCEAN SYSTEMS CENTER, SAN DIEGO, CA 92152

AN ACTIVITY OF THE NAVAL MATERIAL COMMAND

RR GAVAZZI, CAPT USN
Commander

HL BLOOD
Technical Director

ADMINISTRATIVE INFORMATION

Work was performed from January 1973 to June 1977 by the Propagation Technology Division with funding provided by the following agencies: the Defense Communications Agency (DCA), Code 962, UNDT, O, DCA (NOSC M216) and the Defense Nuclear Agency (DNA), DNA, S99QAXHB042, Work Unit 19 (NOSC M402). This report was approved for publication on 21 September 1977.

Released by
Dr JH Richter, Head
EM Propagation Division

Under authority of
JD Hightower, Head
Environmental Sciences
Department

UNCLASSIFIED

SECURITY CLASSIFICATION OF THIS PAGE *(When Data Entered)*

REPORT DOCUMENTATION PAGE

READ INSTRUCTIONS BEFORE COMPLETING FORM

1. REPORT NUMBER: NOSC Technical Report 141 (TR 141)

2. GOVT ACCESSION NO.: (9)

3. RECIPIENT'S CATALOG NUMBER: Technical rept.

4. TITLE *(and Subtitle)*: (6) Effective Electron Density Distributions Describing VLF/LF Propagation Data.

5. TYPE OF REPORT & PERIOD COVERED: January 1973 - June 1977

6. PERFORMING ORG. REPORT NUMBER:

7. AUTHOR(s): (10) D. G. Morfitt

DG Morfitt

8. CONTRACT OR GRANT NUMBER(s):

9. PERFORMING ORGANIZATION NAME AND ADDRESS: Naval Ocean Systems Center, San Diego, CA 92152

10. PROGRAM ELEMENT, PROJECT, TASK AREA & WORK UNIT NUMBERS: UNDT, 0, DCA (NOSC M216) and DNA, S99QAX HB042 Work Unit 19 (NOSC M402)

62704H

11. CONTROLLING OFFICE NAME AND ADDRESS: Defense Communications Agency, Washington, DC 20305

(12) 109p. (11)

12. REPORT DATE: 21 September 1977

13. NUMBER OF PAGES: 88

14. MONITORING AGENCY NAME & ADDRESS *(if different from Controlling Office)*: (14) NOSC/TR-141

15. SECURITY CLASS. *(of this report)*: UNCLASSIFIED

15a. DECLASSIFICATION/DOWNGRADING SCHEDULE:

16. DISTRIBUTION STATEMENT *(of this Report)*: (16) S99QAXH

Approved for public release; distribution is unlimited. (17) B042

17. DISTRIBUTION STATEMENT *(of the abstract entered in Block 20, if different from Report)*:

18. SUPPLEMENTARY NOTES:

19. KEY WORDS *(Continue on reverse side if necessary and identify by block number)*:

Vlf/lf Propagation
Electron Density Profiles
Computer Programs
Predictions

20. ABSTRACT *(Continue on reverse side if necessary and identify by block number)*:

This report presents vlf/lf field strength measurements obtained between 9 and 60 kHz for several radio propagation paths. These include several radials outward from Hawaii, several transmission paths across the continental United States, and high latitude propagation over the Greenland Ice Cap. Effective exponential electron density profiles are derived yielding predicted signal levels that simulate the experimental data.

DD FORM 1 JAN 73 1473 EDITION OF 1 NOV 65 IS OBSOLETE
S/N 0102-LF-014-6601

UNCLASSIFIED

SECURITY CLASSIFICATION OF THIS PAGE *(When Data Entered)*

293 159

OBJECTIVE

Determine the effective ionospheric electron density profiles describing the propagation environment at vlf and lf.

RESULTS

Effective ionospheric electron density profiles are defined describing vlf/lf radio wave propagation under daytime and/or nighttime conditions over the following paths:

1. Mid-latitude-Pacific for various radials outward from Hawaii.
2. Across the continental United States.
3. High latitude and across the Greenland Ice Cap.

RECOMMENDATIONS

1. Determine a multiparameter profile of the ionospheric electron density which will describe radio wave propagation simultanously on many vlf/lf frequencies.

2. Obtain additional signal level measurements for the propagation paths examined in this report and over new paths which include various ionospheric inhomogenuities and anisotropicities in addition to varying ground conductivities.

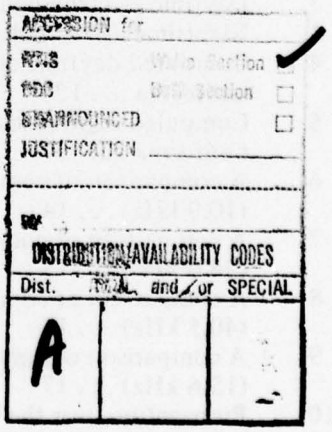

CONTENTS

ILLUSTRATIONS

ILLUSTRATIONS (Continued)

ILLUSTRATIONS (Continued)

TABLES

INTRODUCTION

The propagation of low frequency (lf, 30–60 kHz) and very low frequency (vlf, 10–30 kHz) radio waves is of considerable practical importance for strategic communications, for worldwide navigation systems, and for worldwide frequency and time comparisons.

The propagation of vlf/lf radio waves is characterized by high stability in both phase and amplitude. Little attenuation of the waves occurs in the ionospheric reflection process and as a result they can be propagated to very great distances. These waves also penetrate further into seawater than do waves of higher frequencies. The signals are not greatly affected by most natural-occurring ionospheric disturbances apart from the polar cap events, and radio communications can usually be maintained under conditions (including some nuclear conditions) that make communication very difficult at higher frequencies.

Because of the above propagation characteristics, vlf and low-lf systems are prime components in the Minimum Essential Emergency Communications Network (MEECN). The Navy is highly dependent upon the vlf radio frequency band for broadcast communications to the Fleet and to Navy Tacamo aircraft. Concurrently, the US Air Force has specific interest in propagation on frequencies at the lower end of the lf range and particularly for use with its airborne command posts.

In order to design, deploy, and maintain the essential communications circuits required by MEECN, a reliable knowledge of radio signal amplitude and phase characteristics together with the properties of atmospheric noise is required. For these reasons the Tri-service propagation program was established by the Defense Communications Agency (DCA) to develop reliable and accurate propagation prediction techniques. The Naval Oceans Systems Center (NOSC) is one of the contributing laboratories to the program.

Considerable theoretical work to develop a mathematical model which will accurately predict signal levels for vlf/lf frequencies has been conducted since the early 1960s. References 1, 2, 3, and 4 describe the basic theory of radio wave propagation at long wavelengths. Detailed computational models (computer programs) based on the multimode theory, which is characteristic of propagation at vlf/lf frequencies, have been developed in recent years. These models have been found to account for the signal variability as a function of propagation distance that occurs in nature.

Computed results are, however, very sensitive to the choice of model parameters used as inputs to the calculations. In particular, the ionospheric electron density, ion density and collision frequency profiles along with proper values of the earth's magnetic field parameters, ground conductivity, and dielectric constant are important quantities which are required to adequately depict the real propagation environment if reliable predictions of signal levels are to be made. In order to uniquely identify the ionospheric profiles, signal level data must be available from measurements made at many distances along a given propagation path for transmission on at least one frequency. This type of data are usually obtained by recording the transmitted fields aboard an inflight aircraft. Alternately, data may be recorded at a fixed receiver site which gives the signal levels for several frequencies transmitted simultaneously over a single propagation path.

---

1. Budden, KG, Radio Waves in the Ionosphere, Cambridge University Press, 1961
2. Budden, KG, The Waveguide Mode Theory of Wave Propagation, Prentice Hall, Inc, Englewood Cliffs, NJ, 1961
3. Wait, JR, Electromagnetic Waves in a Stratified Media, Pergamon Press, Inc, Elmsford, NY, 1962
4. Galejs, J, Terrestrial Propagation of Long Electromagnetic Waves, Pergamon Press, Inc. Elmsford, NY, 1972

Only a small quantity of existing published data satisfies the above requirements. These measurements are mostly of vlf and are for propagation at midlatitudes. The data, however, also include signal levels recorded for propagation into the high latitudes and across the Greenland Ice Cap for some lower lf as well as vlf transmissions. Attempts to determine the ionospheric profiles which describe some of these data are shown to be generally successful.

This report presents a summary of the comparisons obtained between predictions made using the NOSC multimode propagation models and available experimental data recorded over various propagation paths. Although a comprehensive study to find the 'best-fit' profiles to the propagation data has not been undertaken, several simple exponential ionospheric profiles used in the calculations describe the observed fields well enough to be used for preliminary estimates of median signal strengths available to MEECN system receivers.

VLF/LF PROPAGATION MODELS

Propagation models and computer programs used to calculate signal levels have been developed at NOSC. These models are referred to as the NOSC multimode propagation models. These models allow the full-wave solution to be obtained for a waveguide whose upper boundary has arbitrary electron and ion density distributions with height and an adjustable surface conductivity. The models also allow for earth curvature, ionospheric inhomogeneity, and anisotropy (resulting from the earth's magnetic field).

The basic theory of the NOSC multimode propagation models is described in reference 5. In this theory the electromagnetic waves are considered to propagate between the earth and the ionosphere as normal modes, analogous to microwave propagation in a lossy waveguide. The modal equation for propagation within the earth's ionosphere waveguide is solved for as many modes as required. The eigenvalues so obtained are then used in a modal summation to compute the total field at some distant point from the transmitter. In many instances, the earth-ionosphere waveguide can be considered to have constant propagation properties along the transmission path. The mode sum calculations made for these cases are referred to as horizontally homogeneous. In instances where the earth-ionosphere waveguide cannot be considered as horizontally homogeneous but instead varies slowly along the propagation path, a WKB* form of the mode sum is used (ref 6). This procedure was utilized in reference 7 to predict vlf signals as measured aboard an inflight aircraft.

For those cases where the changes in the propagation environment are too abrupt to be adequately simulated by the WKB procedure, mode conversion techniques must be applied. This type of computation is required for propagation through sunrise or sunset transition periods and in instances where the ground parameters change rapidly along the propagation

---

* WKB – Mathematical method for approximating the fields of a vlf/lf radio signal in regions where the propagation coefficients, such as excitation, phase velocity, and attenuation, are slowly varying functions of distance.

5. Pappert, RA, EE Gossard, and IJ Rothmuller, A Numerical Investigation of Classical Approximations Used in VLF Propagation, Radio Science, v 2, p 387-400, April 1967
6. Wait, JR, Two-Dimensional Treatment of the Mode Theory of the Propagation of VLF Radio Waves, Radio Science, v 68D, p 81-95, January 1964
7. Bickel, JE, JA Ferguson, and GV Stanley, Experimental Observation of Magnetic Field Effects on VLF propagation at Night, Radio Science, p 19-25, January 1970.

path. References 8 and 9 describe the NOSC mode-conversion computer program and some results obtained when this model was applied to experimental data.

The NOSC propagation models provide for the calculation of both vertical and horizontal electromagnetic fields as excited by dipoles of arbitrary orientation and elevation. The relevant equations and characteristic results are discussed in references 10, 11, and 12, and the computer program is discussed in references 13 and 14.

For simplicity in modeling vlf-lf signal levels, the propagation path should be horizontally homogenous. That is, the path should consist of all seawater or all of a specific conductivity land mass. The earth's magnetic field parameters (magnetic azimuth and magnetic dip angle) should remain nearly constant over the complete transmission path. The propagation path between Hawaii and Southern California satisfies this condition very well. The path between Hawaii and Samoa illustrates (fig 1) a considerable change ($\sim 70^\circ$) in magnetic dip angle between the two terminals.

The propagation path between Hawaii and Southern California could be modeled by the horizontally homogenous mode sum option of the NOSC propagation models. The path between Hawaii and Samoa would need to utilize the WKB option. For a path containing a dramatic change in conductivity parameters, eg, a path which crosses the Greenland Ice Cap, the mode conversion option should be incorporated.

All field strength measurements and computations presented in this report are normalized to 1 killowatt of radiated power.

---

8. Naval Electronics Laboratory Center Interim Report 722, Mode Conversion Program for an Inhomogeneous Anisotropic Ionosphere, by RA Pappert and LR Shockey, 1 May 1972
9. Pappert, RA and FP Snyder, Some Results of a Mode-Conversion Program for VLF, Radio Science, v 7, p 913-923, October 1972
10. Pappert, RA, Effects of Elevation and Ground Conductivity on Horizontal Dipole Excitation of the Earth-Ionosphere Waveguide, Radio Science, v 5, p 579-590, March 1970
11. Pappert, RA and JE Bickel, Vertical and Horizontal VLF Fields Excited by Dipoles of Arbitrary Orientation and Elevation, Radio Science, v 5, p 1445-1452, December 1970
12. Naval Electronics Laboratory Center Technical Report 1833, Measurements of Vertical and Horizontal VLF Fields Excited by an Elevated, Arbitrarily Oriented Antenna, by JE Bickel, 21 July 1972
13. Naval Electronics Laboratory Center Interim Report 702, A Fortran Program for Waveguide Propagation Which Allows for Both Vertical and Horizontal Dipole Excitation, by RA Pappert and LR Shockey, 15 June 1970
14. Naval Electronics Laboratory Center Interim Report 713, WKB Mode Summing Program for VLF/ELF Antennas of Arbitrary Length, Shape and Elevation, by RA Pappert and LR Shockey, 2 June 1971

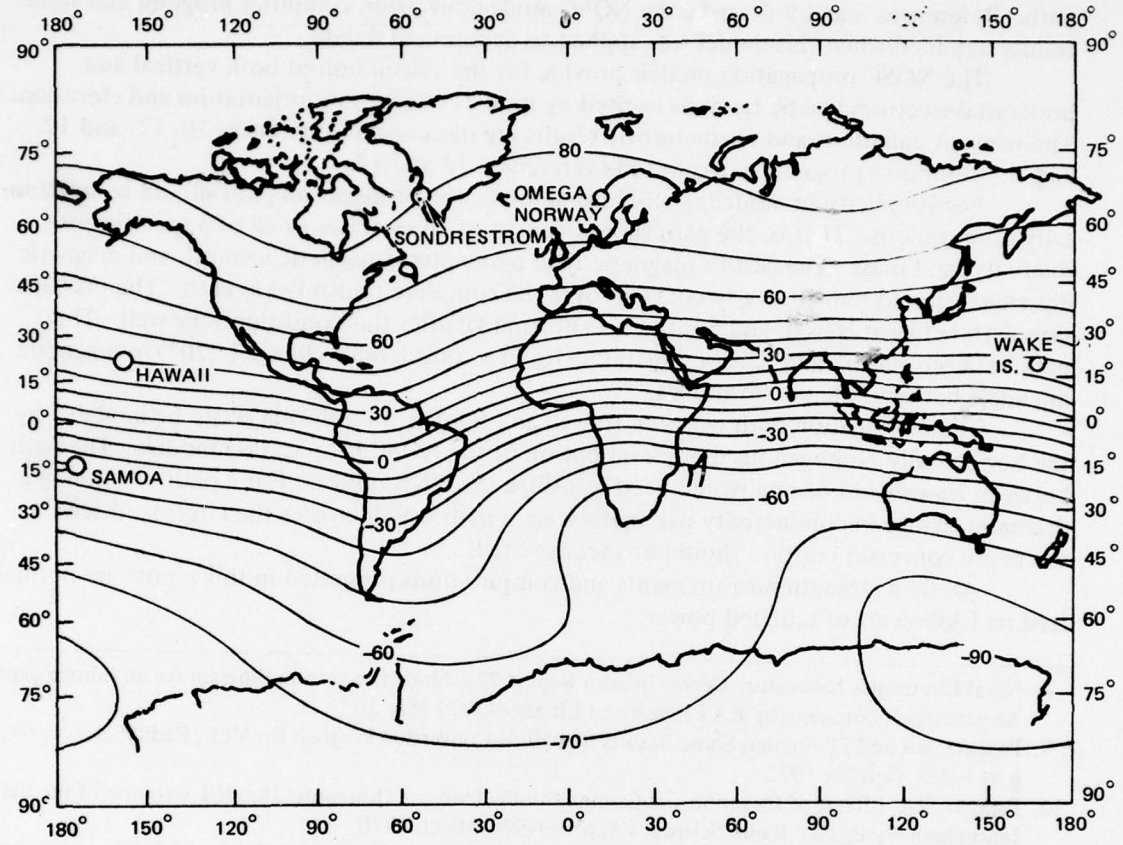

Figure 1. World map of magnetic dip angle.

DATA ANALYSIS

IONOSPHERIC PARAMETERS

The important ionospheric parameter needed to simulate actual propagation data is the conductivity profile below which the radio waves must pass. This parameter is defined as the ratio of the ionospheric electron plasma frequency to the electron-neutral particle collision frequency and is a function of ionospheric height. The plasma frequency is related to the density of free electrons at each height. The ionospheric conductivity ω_r, as a function of height Z, is given by:

$$\omega_r(Z) = \frac{\omega^2_p(Z)}{\nu(Z)} = \left[\frac{N(Z)q^2}{\epsilon_0 m}\right] \Big/ \nu(Z) \qquad (1)$$

where

$\omega_p(Z)$ is the electron plasma frequency

$N(Z)$ is the electron density in electrons per cubic centimeter

$\nu(Z)$ is the electron-neutral particle collision frequency

q is the electron charge

m is electron mass

ϵ_0 is the permittivity of free space.

Following Wait (ref 15), the conductivity parameter $\omega_r(Z)$ may be considered of the exponential form

$$\omega_r(Z) = \omega_0 \exp[\beta(Z - H')] \tag{2}$$

where

β is a gradient parameter in inverse height units

and

H' is a reference height

The ionospheric parameters needed as inputs to the multimode computer programs, then, are the electron density profile and the effective electron-neutral particle collision frequency profile. These terms may be assigned exponential relationships with height and are identified by the terms β, km^{-1} and H', km.

The value of the electron density N(Z), in electrons/cubic centimetres, is calculated as a function of height Z in kilometres by the equation:

$$N(Z) = \left\{1.43 \cdot 10^7 \ \frac{el}{cm^3} \cdot \exp(-0.15\ H')\right\} \left\{\exp[(\beta - 0.15)(Z - H')]\right\} \tag{3}$$

The collision-frequency profile for the computations was taken as

$$\nu(Z) = \nu_0 \exp(-\alpha Z) \tag{4}$$

where

Z is the height in km

ν_0 is $1.82 \times 10''$ collisions/sec

α is $0.15\ km^{-1}$

The exponential form of these profiles was chosen for the computations as attempts to find more complex shapes would likely require much additional effort. This is true because the state-of-the-art in analysis procedures allows for an almost infinite variety of profile shapes to be examined. It is possible that profiles of more complex forms than the exponential could be found to produce a better fit to the data in some instances, but since the propagation paths being considered are quite long, any profile determined to produce a best fit to the data is really an average profile for the total path.

---

15. Wait, JR and KP Spies, Characteristics of the Earth-Ionosphere Waveguide for VLF Radio Waves, National Bureau of Standards Technical Note 300, 30 December 1964

The characteristic relationship, as a function of height, for some exponential profiles is illustrated in figure 2 for daytime conditions and in figure 3 for nighttime conditions.

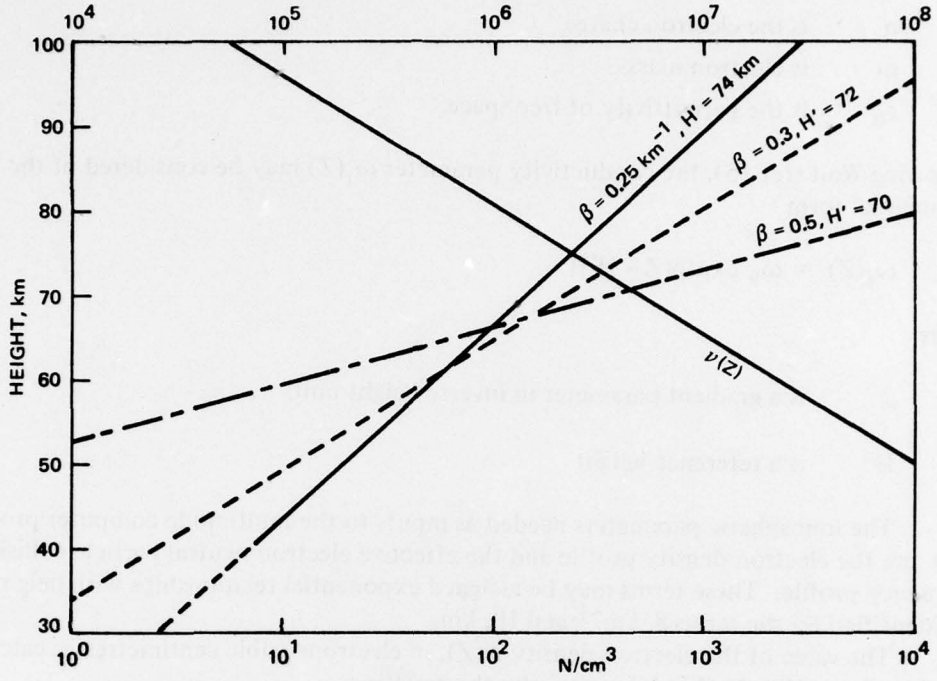

Figure 2. Daytime electron density profiles and collision frequency profile.

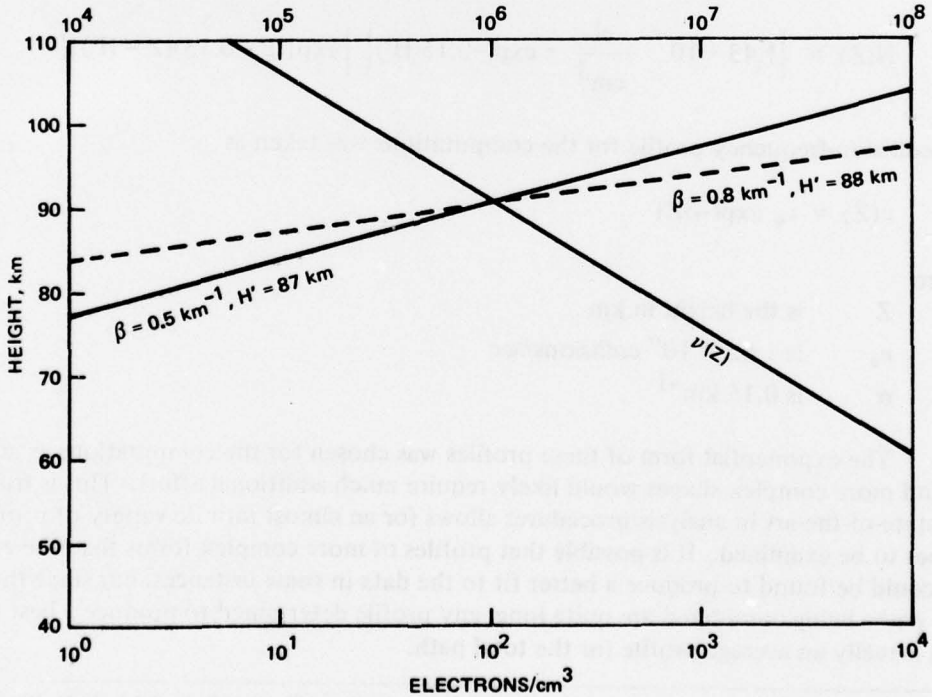

Figure 3. Nighttime electron density profiles and collision frequency profile.

FIELD STRENGTH VS DISTANCE CHARACTERISTICS

Examples of computed signal levels for the Hawaii to Southern California path are shown in figure 4 for daytime propagation and in figure 5 for nighttime propagation.

The frequencies are those frequently used for vlf sounder experiments and are listed below.

TABLE 1. VLF SOUNDER FREQUENCIES.

kHz	kHz
9.340	21.794
10.897	24.908
14.010	26.464
15.567	28.020
17.124	31.134

It has been determined (ref 7) that the propagation path from Hawaii to Southern California could be treated as horizontally homogeneous in terms of the earth's magnetic-field parameters. Therefore, in the field-strength computations these parameters were assigned their values at the midpoint of the great circle propagation path. They are: magnetic azimuth = 50.6°, dip angle = 50°, and magnetic intensity = 4.25×10^{-5} weber/m^2.

These field strength curves give typical representation of the modal interference patterns characteristic of propagation at vlf and lf. The electron density profile of β = 0.5 km^{-1}, H′ = 70 km was used to compute the daytime fields of figure 4 while the parameters β = 0.5 km^{-1}, H′ = 87 km were used for the nighttime fields of figure 5. It is instructive to note certain characteristics of these curves: First, the excursions in modal interference structure increase with propagation frequency up to about 25 kHz for daytime and up to 15 kHz for nighttime. Second, the modal interference structure, as a function of distance, is more prominent for nighttime propagation than for daytime propagation. Third, the propagation path from Hawaii to Southern California is approximately 4 megametres (Mm) long. Examination of the figures illustrates that there should be a deep minimum in signal level at the California terminal on 25 kHz for daytime propagation and on 15 kHz and 28 kHz for nighttime propagation.

The field strength levels produced by multimode computations, using various values of the β and H′ parameters of the electron density profile, are illustrated in figures 6 through 9 for the vertical electric field. These computations of field strength are for the Hawaii to Southern California path and are for an assumed horizontally homogeneous waveguide where no ionospheric (or ground) variation along the propagation path is considered. Figure 6 shows a plot of received signal amplitude versus propagation distance for 10.9 kHz transmissions. The variation in signal level produced by varying the gradient value, $\beta(km^{-1})$ while maintaining the reference height (H′ km) at a constant value is presented. In this case, β is assigned values between 0.2 to 0.7 km^{-1} and H′ is held at 87 km. Observation shows that an increase in β produces an increase in mode structure. That is, the signal level is found to vary over a

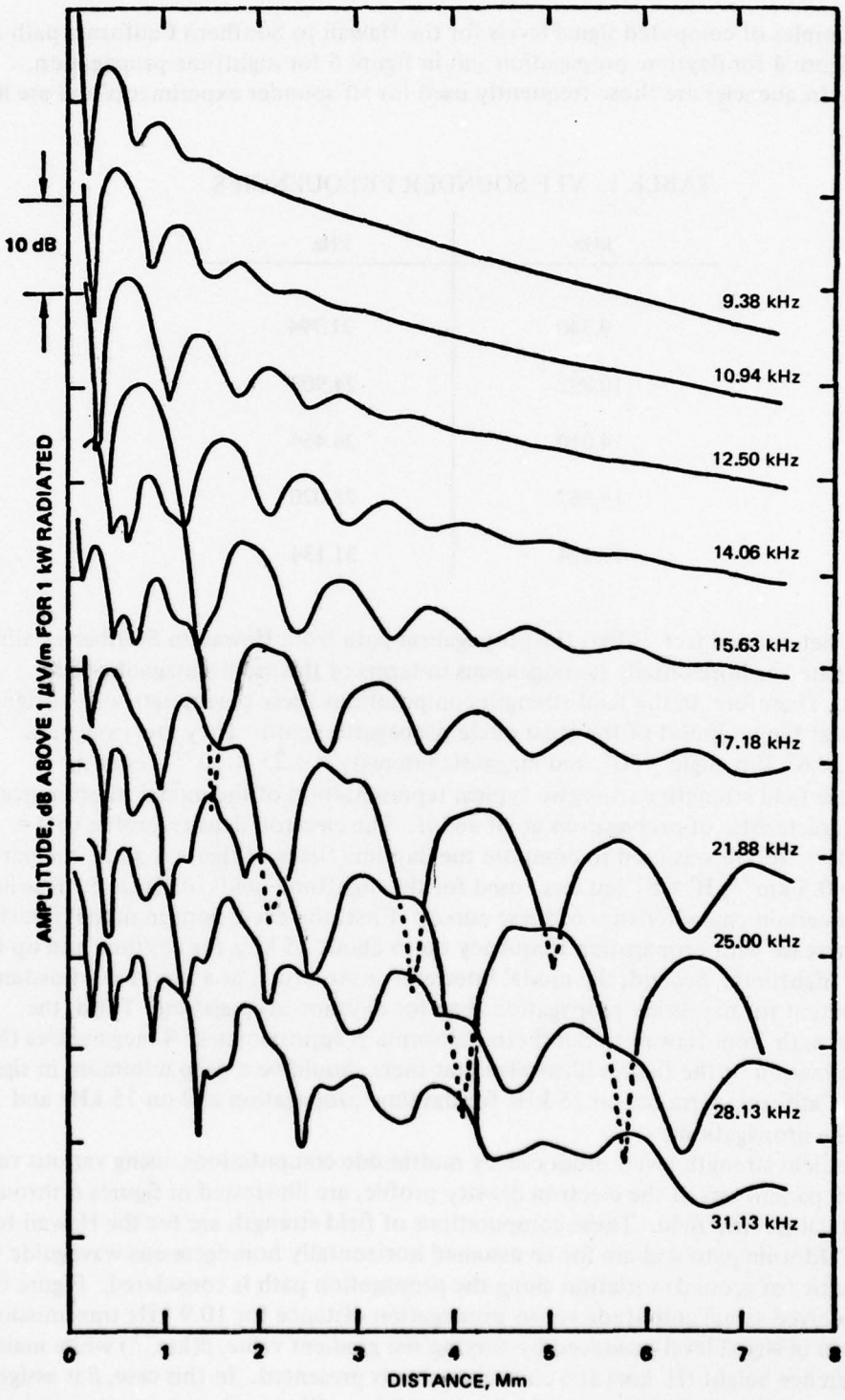

Figure 4. Computed daytime amplitude for propagation from Hawaii through Southern California.

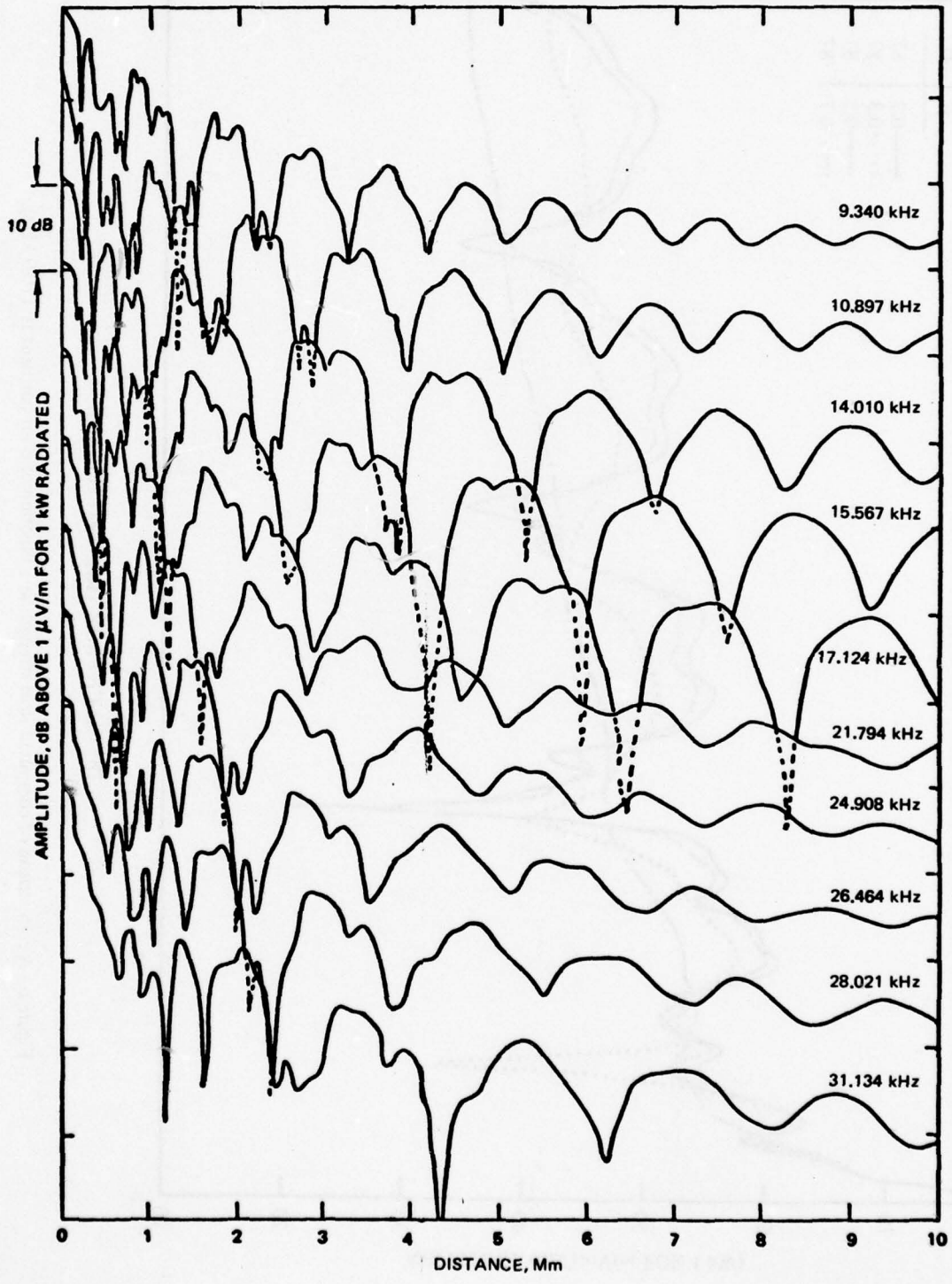

Figure 5. Computed nighttime amplitude for propagation from Hawaii through Southern California.

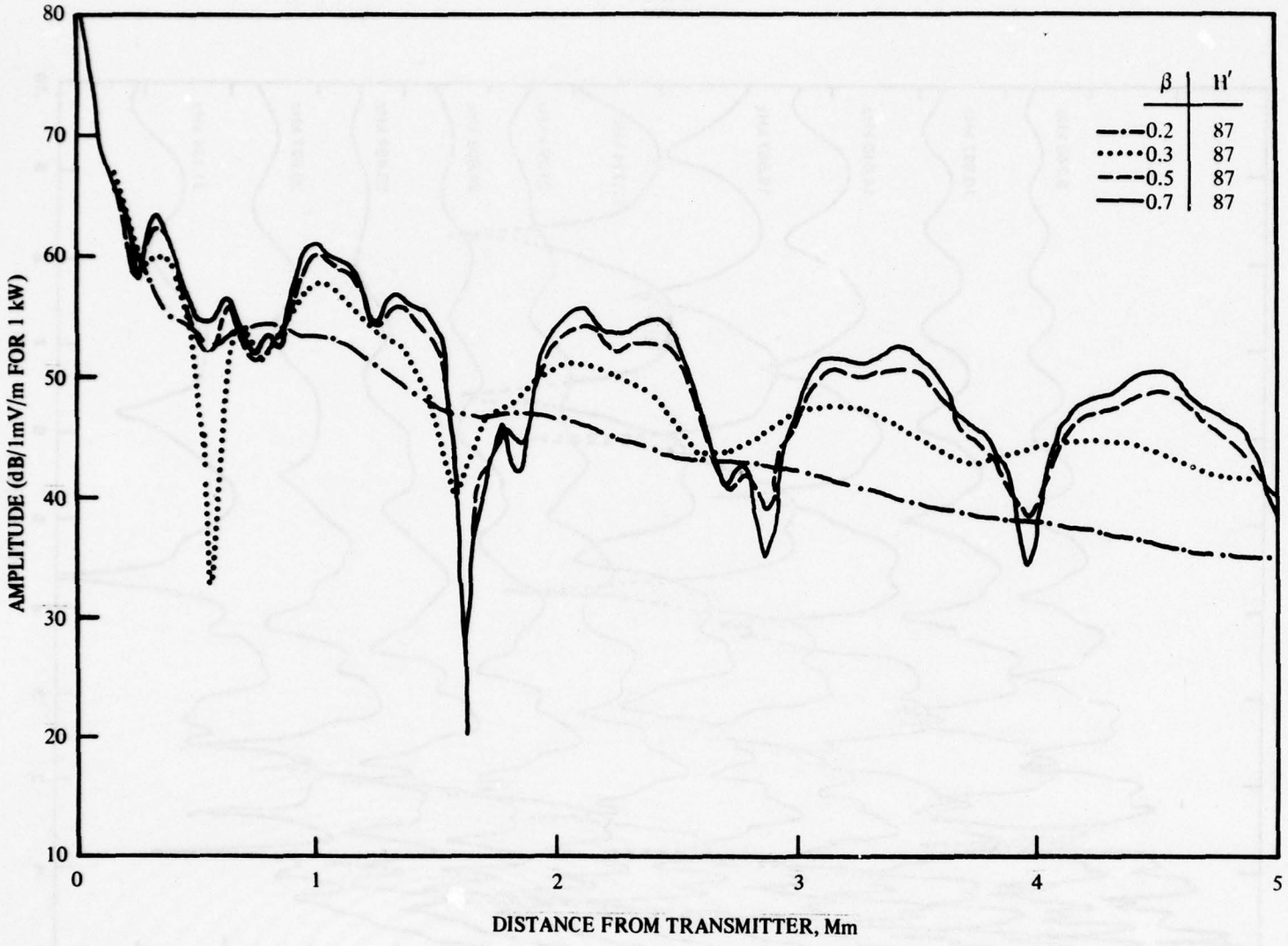

Figure 6. A comparison of computed field strength as a function of β for constant H′ (10.9 kHz).

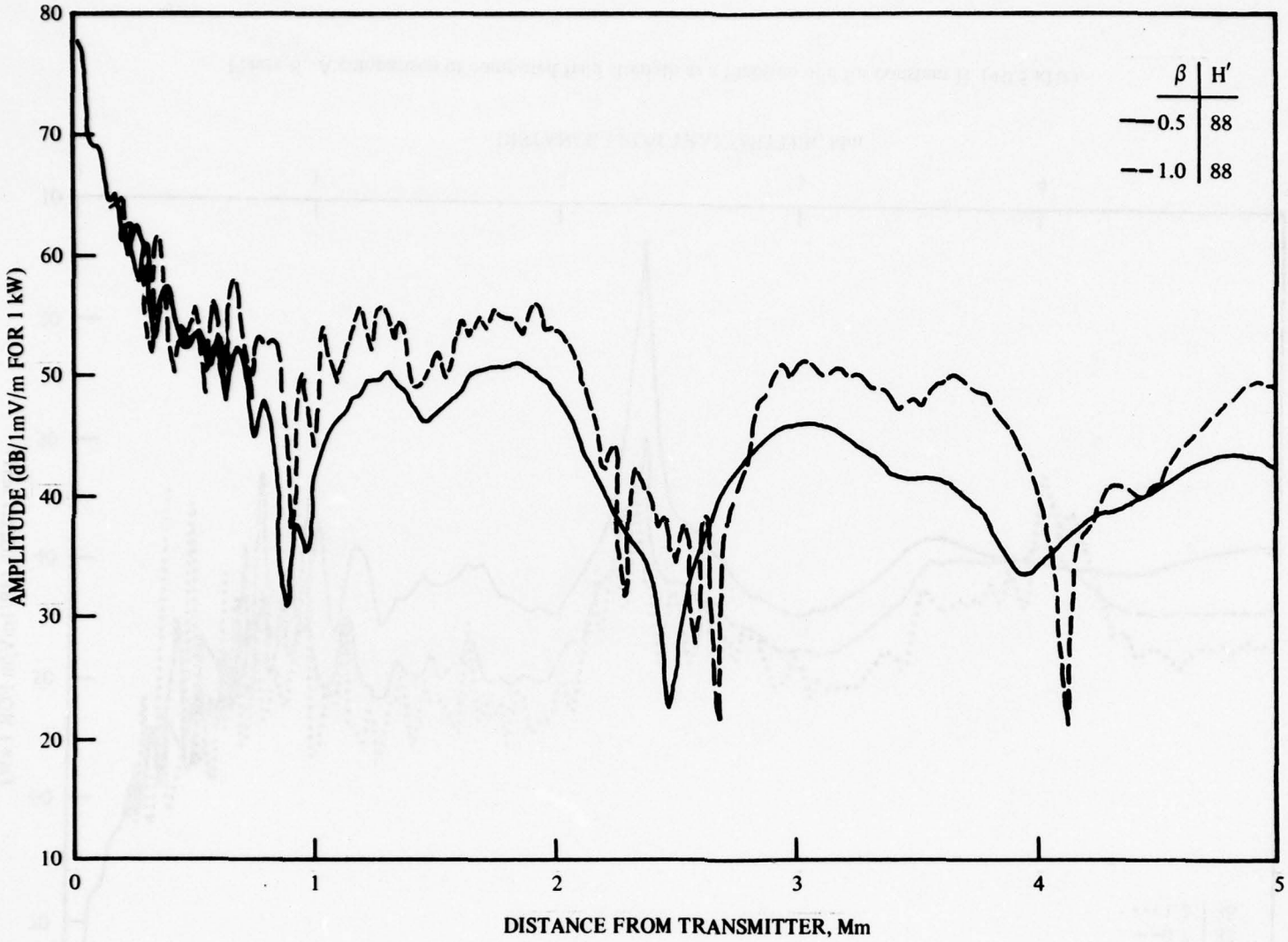

Figure 7. A comparison of computed field strength as a function of β for constant H′ (28.0 kHz).

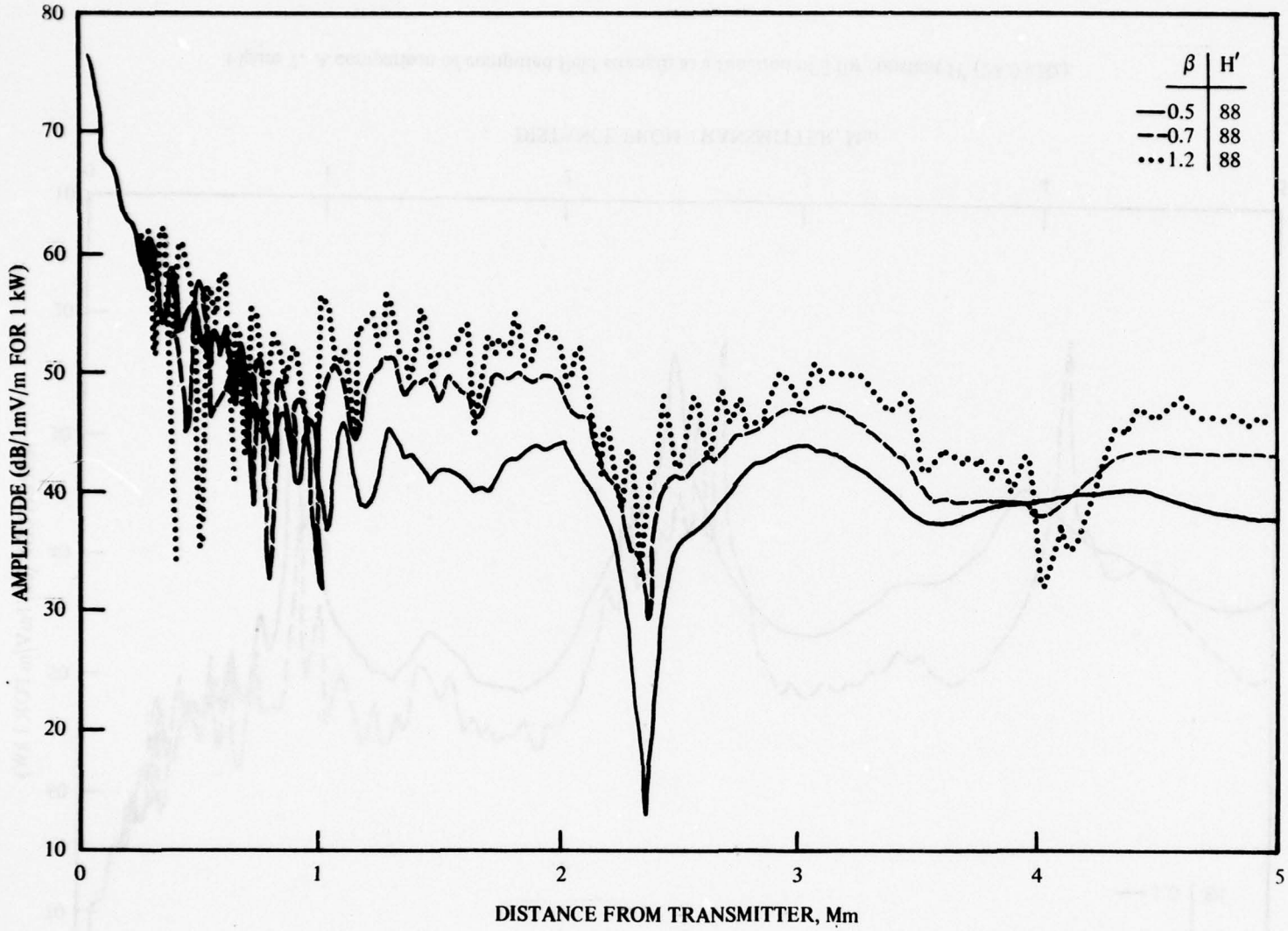

Figure 8. A comparison of computed field strength as a function of β for constant H′ (40.5 kHz).

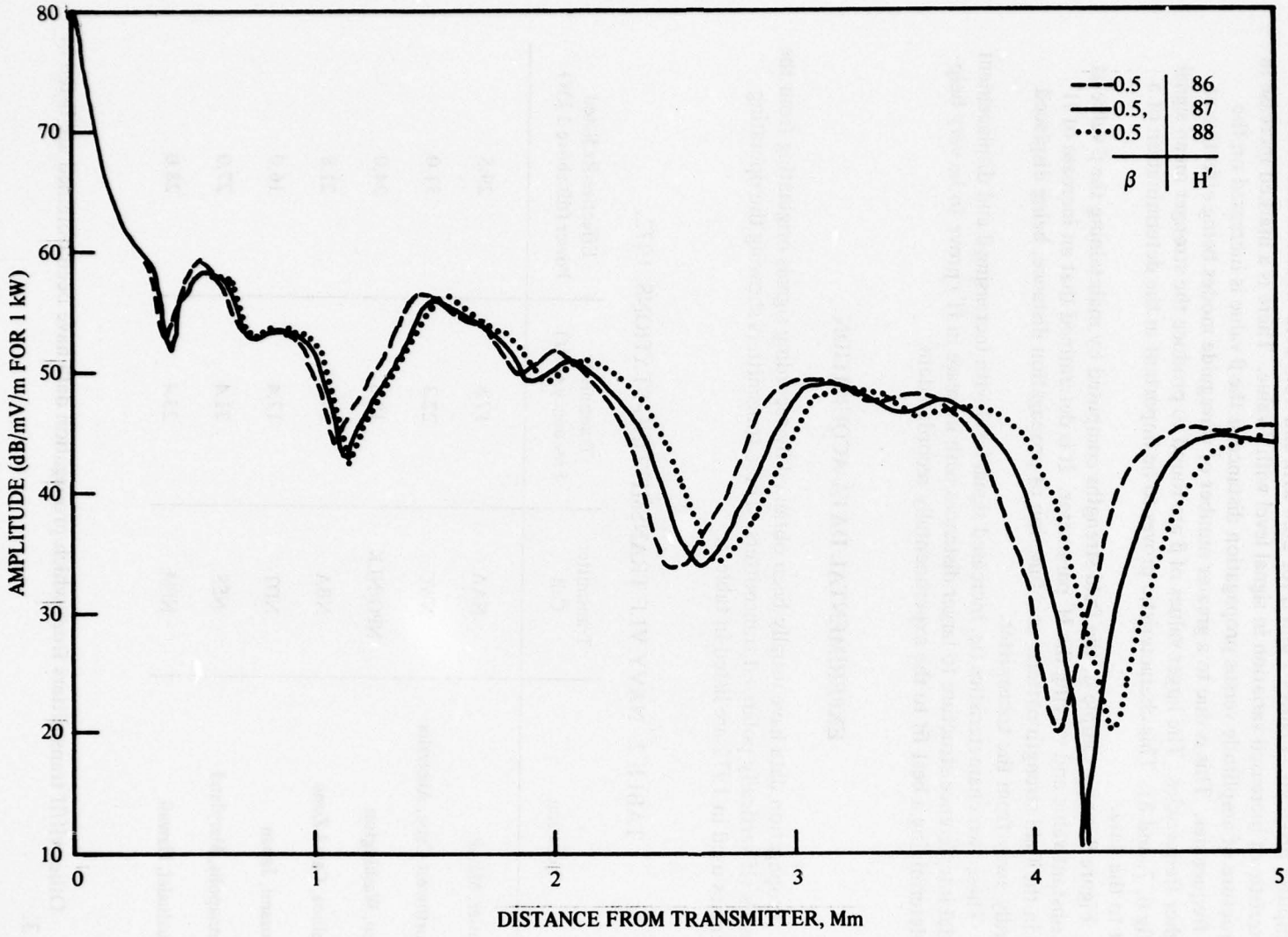

Figure 9. A comparison of computed field strength as a function of H′ for constant β (15.6 kHz).

wider range in the regions of strong modal interference when the larger values of β are input to the computer program. Figures 7 and 8 for 28.0 kHz and 40.5 kHz illustrate this same characteristic of increased variation in signal level with β value. There is a marked increase in fine structure of amplitude versus propagation distance as the β value is increased on the higher frequencies. This is due to a greater number of waveguide modes being effective at the higher frequencies. The larger values of β are found to produce the stronger mean signal level (fig 6, 7, and 8). This characteristic proves to be important in the determination of a best fit to the data.

Figure 9 is an example of the field strengths computed by maintaining the β value at some constant value and varying the H′ parameter. It is determined that an increase of H′ results in the field strength pattern, as a function of propagation distance, being displaced outwardly away from the transmitter.

These two characteristics (ie, increased signal level with increasing β and displacement of modal interference structure to larger distances with increase in H′) prove to be very helpful in determining a best fit to the experimentally recorded data.

EXPERIMENTAL DATA ACQUISITION

Propagation data have usually been obtained by recording signals originating from the US Navy's vlf vertically polarized transmitters. These transmitters showing the operating frequencies used in 1972 are listed in table 2.

TABLE 2. NAVY VLF TRANSMITTING STATIONS, 1972.

Location	Transmitter Call	Transmitter Frequency (kHz)	Effective Radiated Power (dB above 1 kW)
Cutler, Maine	NAA	17.8	29.5
Northwest Cape, Australia	NWC	22.3	31.0
Oso, Washington	NPG/NLK	18.6	24.0
Balboa, Canal Zone	NBA	24.0	21.8
Yosami, Japan	NDT	17.4	16.0
Annapolis, Maryland	NSS	21.4	27.0
Lualualei, Hawaii	NPM	23.4	28.0

Other vlf/lf transmitters from which propagation data have been obtained are listed in table 3.

TABLE 3. OTHER VLF/LF TRANSMITTING STATIONS.

Location	Transmitter Call	Transmission Frequency (kHz)
Fort Collins, Colorado	WWVL	20
Fort Collins, Colorado	WWVB	60
Rugby, England	MSF	60 (1970)
Preston, England	GYN	45 (1970)
Rugby, England	GBZ	19.6 (1958)
Bodo, Norway	OMEGA	10.2, 11.3, 13.6
Haiku, Hawaii	OMEGA	10.2, 13.6
Annapolis, Maryland	NSS	15.5 (1958)
Lualualei, Hawaii	NPM	24.0 (1965) 26.1 (1965) 16.6 (1955)

A further source of vlf/lf propagation data is the NOSC multifrequency sounder. This system is described in detail in references 16 and 17. The sounder has been used for recording both vertical incidence and oblique incidence propagation data.

The data available for comparison between computer model computations and experimentally recorded data consist of that recorded aboard an inflight aircraft as a function of distance from the transmitter and that recorded at fixed sites as a function of time.

PROPAGATION IN THE PACIFIC AREA

DAYTIME AIRCRAFT DATA

Figures 10 and 11 show the comparison between fields as computed by the NOSC horizontally homogenous waveguide program and data recorded aboard an inflight aircraft. These data were recorded by the Naval Research Laboratory (NRL) and are described in references 18 and 19. Figures 10 and 11 indicate that the profile $\beta = 0.5$ km^{-1}, $H' = 70$ km gives signal levels in close agreement with the recorded data. Figure 12 gives a summary of other comparisons using this profile to data recorded by NOSC (ref 20) and by NRL (ref 18 and 19) at various frequencies for propagation over midlatitude seawater paths in the summer.

16. Naval Ordnance Laboratory Corona Report 722, Multiple-Frequency Oblique-Incidence VLF Ionospheric Sounder, by DA Wulfing and VE Hildebrand, 5 May 1967
17. Naval Weapons Center TWC TP 5038, VLF-Propagation Measurement Technique Using Repetitive-Pulse Spectral Lines, by VE Hildebrand and DJ Adrian, February 1971
18. Naval Research Laboratory Report 6359, An Investigation of the Modal Interference of Very-Low-Frequency Radio Waves, by FJ Rhoads and WE Garner, 27 October 1965
19. Rhoads, FJ, and WE Garner, An Investigation of the Modal Interference of VLF Radio Waves, Radio Science, v 2, p 539-546, June 1967
20. Naval Electronics Laboratory Report 767, An Experimental Measurement of VLF Field Strength as a Function of Distance, Using an Aircraft, by JE Bickel, JL Heritage, and S Weisbrod, 28 January 1957

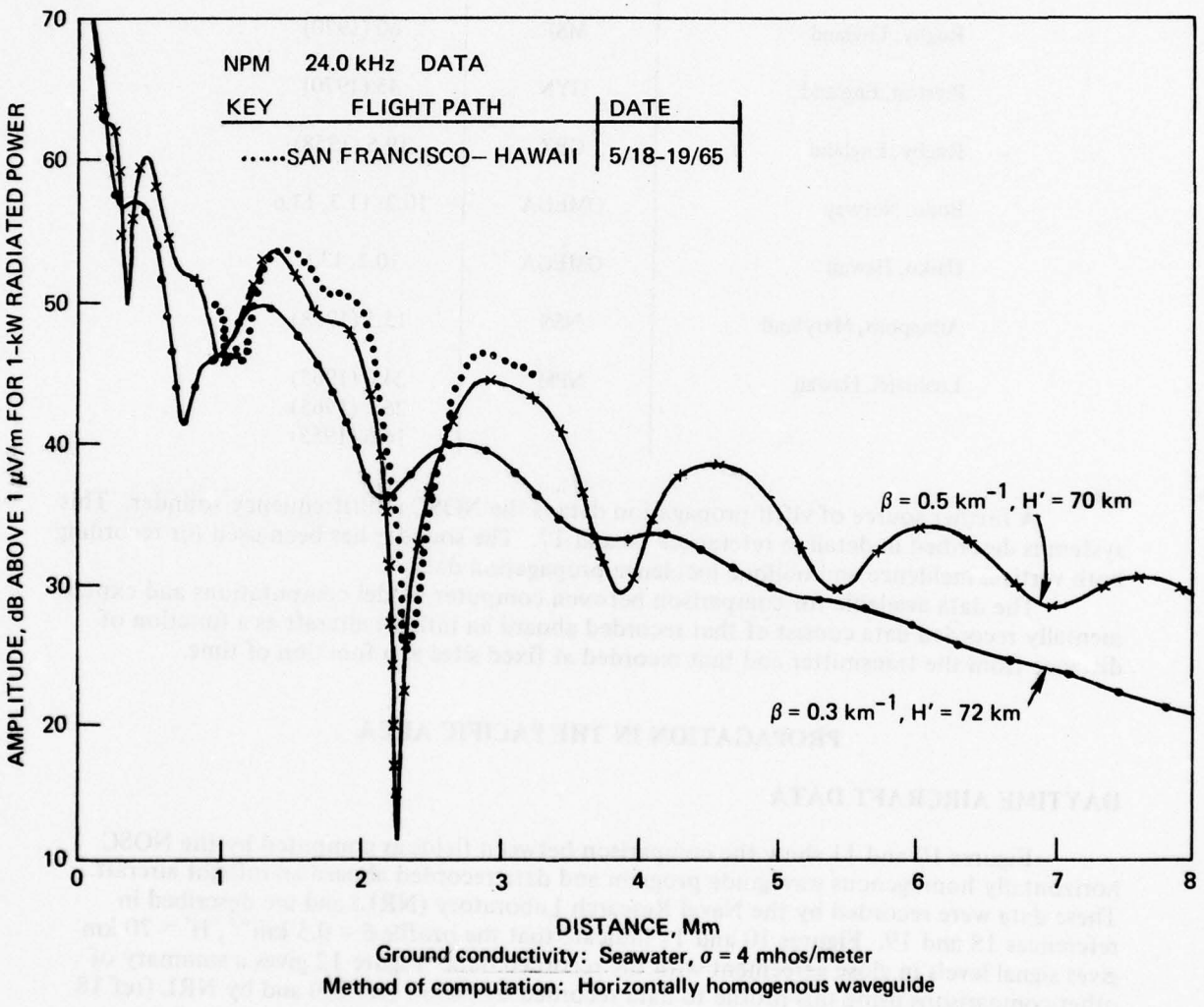

Figure 10. Propagation over the Pacific Ocean (daytime, summer), (NPM 24 kHz).

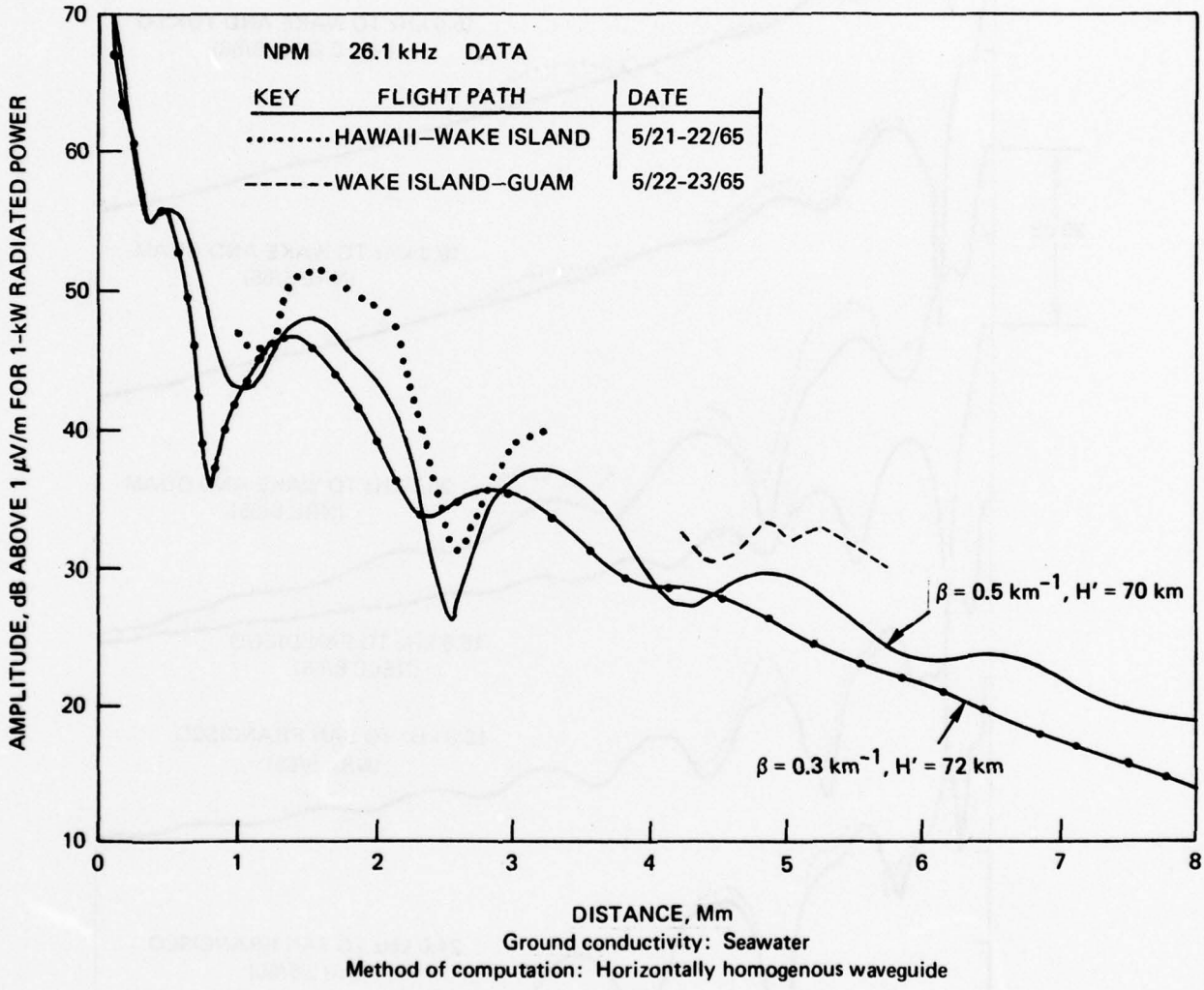

Figure 11. Propagation over the Pacific Ocean (daytime, summer) (NPM 26.1 kHz).

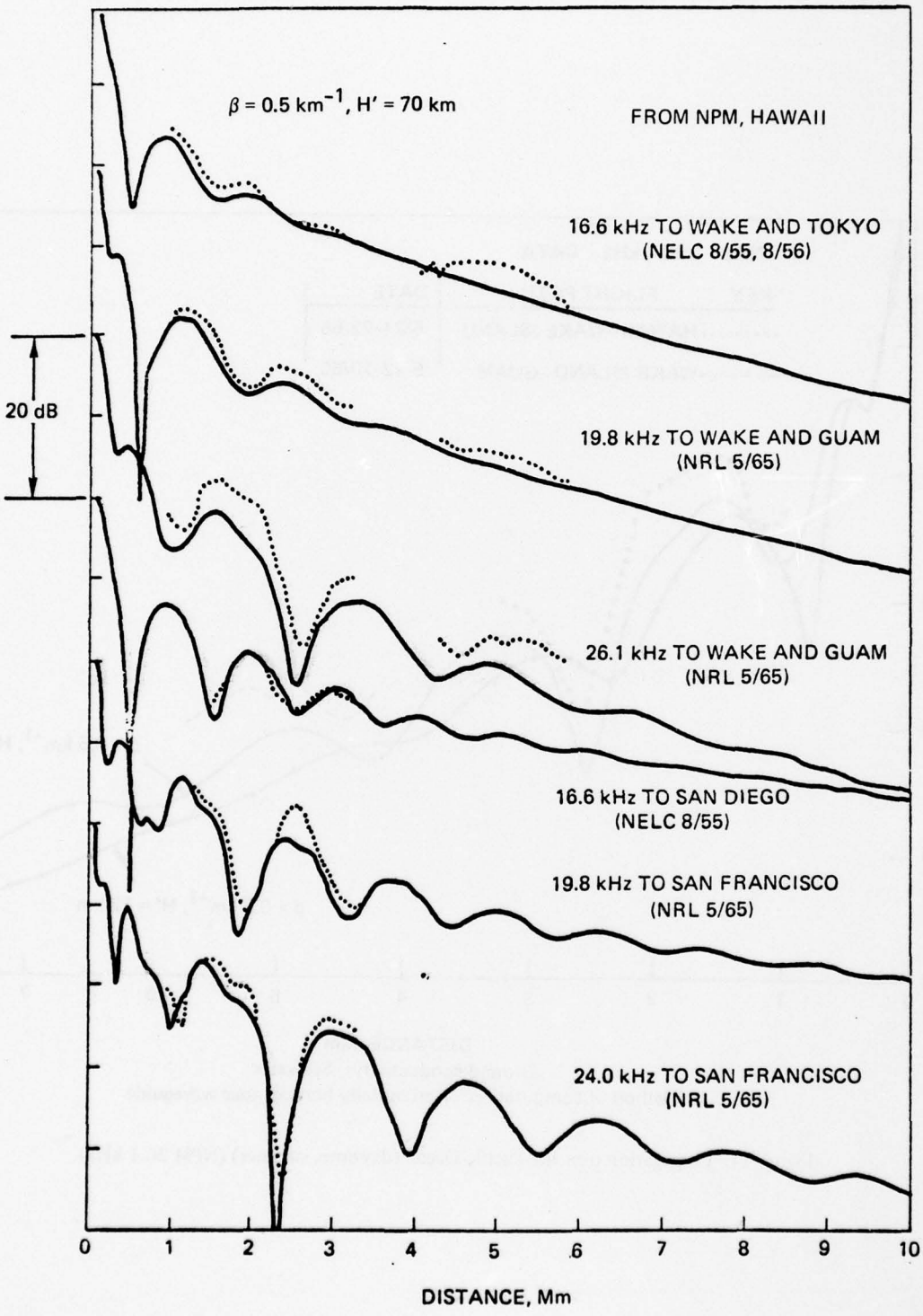

Figure 12. Propagation over the Pacific Ocean (daytime, summer) (various vlf frequencies).

Propagation measurements were also made on 2 and 3 February 1974. Vlf/lf (10–60 kHz) signals were recorded aboard an inflight aircraft at an altitude of 9 km (30,000 ft) as it flew between Hawaii and Southern California. The signals were transmitted and recorded by NOSC multifrequency sounders located at each end of the propagation path (ie, one sounder transmitter was located on the island of Hawaii and the other at Sentinel, Arizona).

The propagation frequencies used for the sounder transmissions are shown in table 4.

TABLE 4. FREQUENCY SETS FOR NOSC MULTIFREQUENCY SOUNDER TRANSMISSIONS (kHz).

Hawaii Transmitter	Sentinel Transmitter
9.340	9.336
10.897	14.003
15.567	17.115
21.794	24.895
28.021	28.007
37.361	34.231
40.475	38.898
46.702	43.566
52.929	49.790
56.042	56.104

The times for which propagation data were recorded are given in table 5.

TABLE 5. DAYTIME AIRCRAFT FLIGHT PATHS FOR JANUARY–FEBRUARY 1974.

Date 1974	Julian Day	Origin	Destination	Times of Recorded Data, UT
2 Feb	33	March AFB	Hickam AFB	1830 - 2350
3 Feb	34	Hickam AFB	March AFB	1830 - 2320

The total path was in daylight from 1430 UT until 0130 UT. Both the Hawaii and Sentinel, Arizona, transmitters were in operation simultaneously for the flights. In general, the Hawaii transmissions were such that acceptable data were obtained on the flights. The data recorded from the Sentinel sounder system was not of as high a quality as that from Hawaii. Most of the problems in the Sentinel system appear to have originated from the inability of the aircraft receiver to gain and remain in synchronization with the transmitted signals. This was due to the poor signal-to-noise ratio available from the Sentinel antenna at the ranges for which data acquisition was attempted.

Figures 13, 14, and 15 show the experimental data values and corresponding predicted fields. The results illustrate that the summer electron density profile, (β = 0.5 km^{-1}, H′ = 70 km), needs to be replaced by a profile with β = 0.3 km^{-1} and H′ = 72–75 kHz for daytime propagation over the Pacific during winter.

Table 6 presents a summary of the best fit daytime profiles obtained for propagation over the Hawaii to Southern California path during winter.

TABLE 6. "BEST-FIT" EXPONENTIAL ELECTRON DENSITY PROFILES –DAYTIME WINTER DATA RECORDER ABOARD AN AIRCRAFT, HAWAII TO SOUTHERN CALIFORNIA PROPAGATION PATH.

Hawaii Transmitter					Sentinel Transmitter		
	2 February 1974		3 February 1974			2 February 1974	
kHz	β (km^{-1})	H′ (km)	β (km^{-1})	H′ (km)	kHz	β (km^{-1})	H′ (km)
9.340	0.3	72	0.3	75	9.336	0.3	74
10.897	0.3	72	0.3	75	14.003	0.3	74
15.567	0.3	72	0.3	75	17.115	0.3	74
21.794	0.3	72	0.3	75	24.895	0.3	74
28.020	0.3	73	0.3	75	28.007	0.3	74
37.361	0.35	73	0.3	75	34.231	0.3	74
40.475	0.35	73	0.3	75	38.898	0.3	74
46.702	0.35	73	0.3	75	43.566	0.3	74
52.929	0.35	73	0.3	75	49.790	0.3	75
56.042	0.35	73	0.3	75	56.104	0.3	75

Observation of figures 13, 14, and 15 illustrates that fields computed, using either the best-fit profile from table 6 or β = 0.5, H′ = 70, are almost identical for frequencies below 15 kHz. The fact that the best-fit profiles for the aircraft flights of 2 February and 3 February are not the same illustrates the variability characteristic of daytime ionospheric propagation.

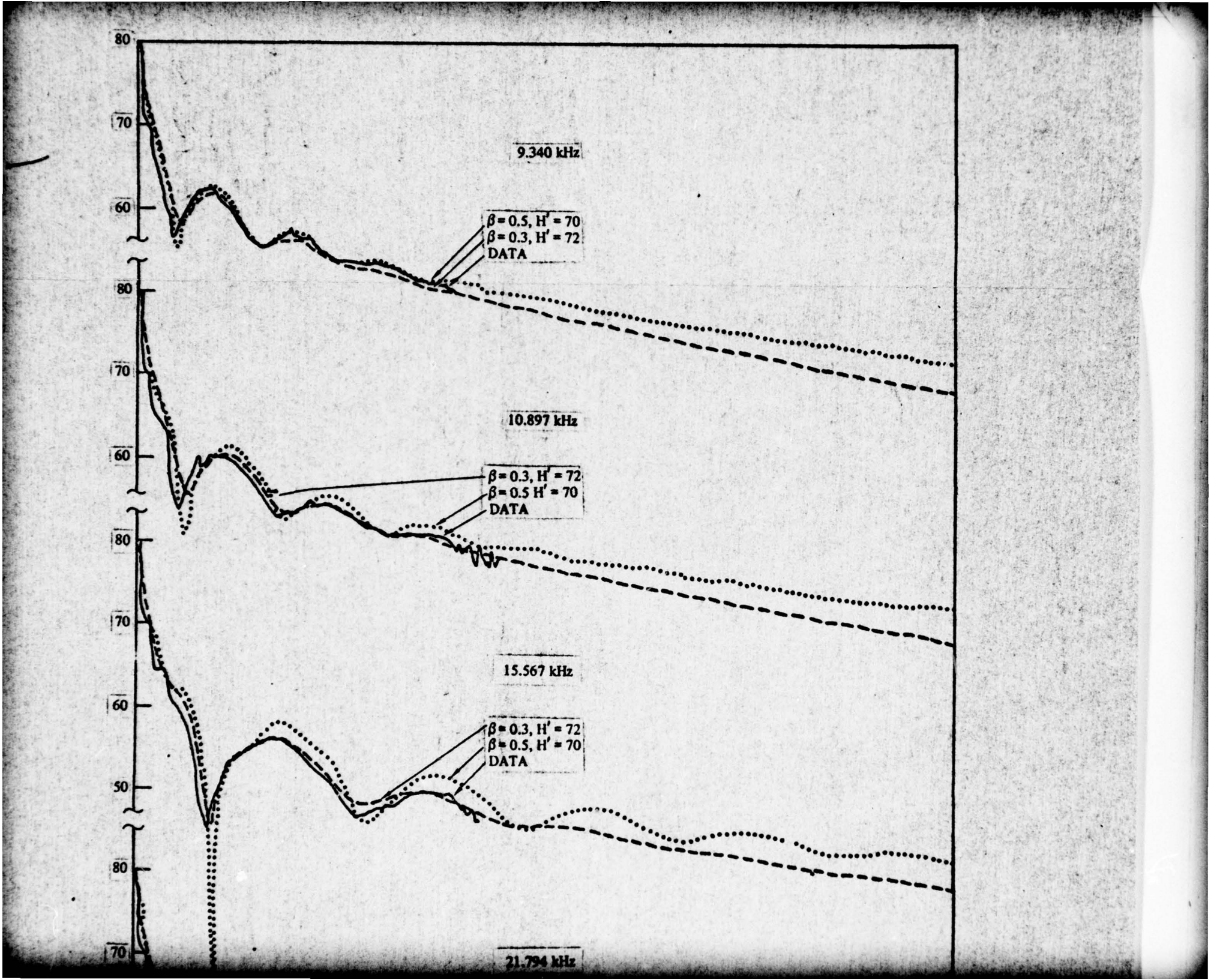
80
70
60
9.340 kHz
β = 0.5, H' = 70
β = 0.3, H' = 72
DATA
80
70
60
10.897 kHz
β = 0.3, H' = 72
β = 0.5 H' = 70
DATA
80
70
15.567 kHz
60
50
β = 0.3, H' = 72
β = 0.5, H' = 70
DATA
80
70
21.794 kHz

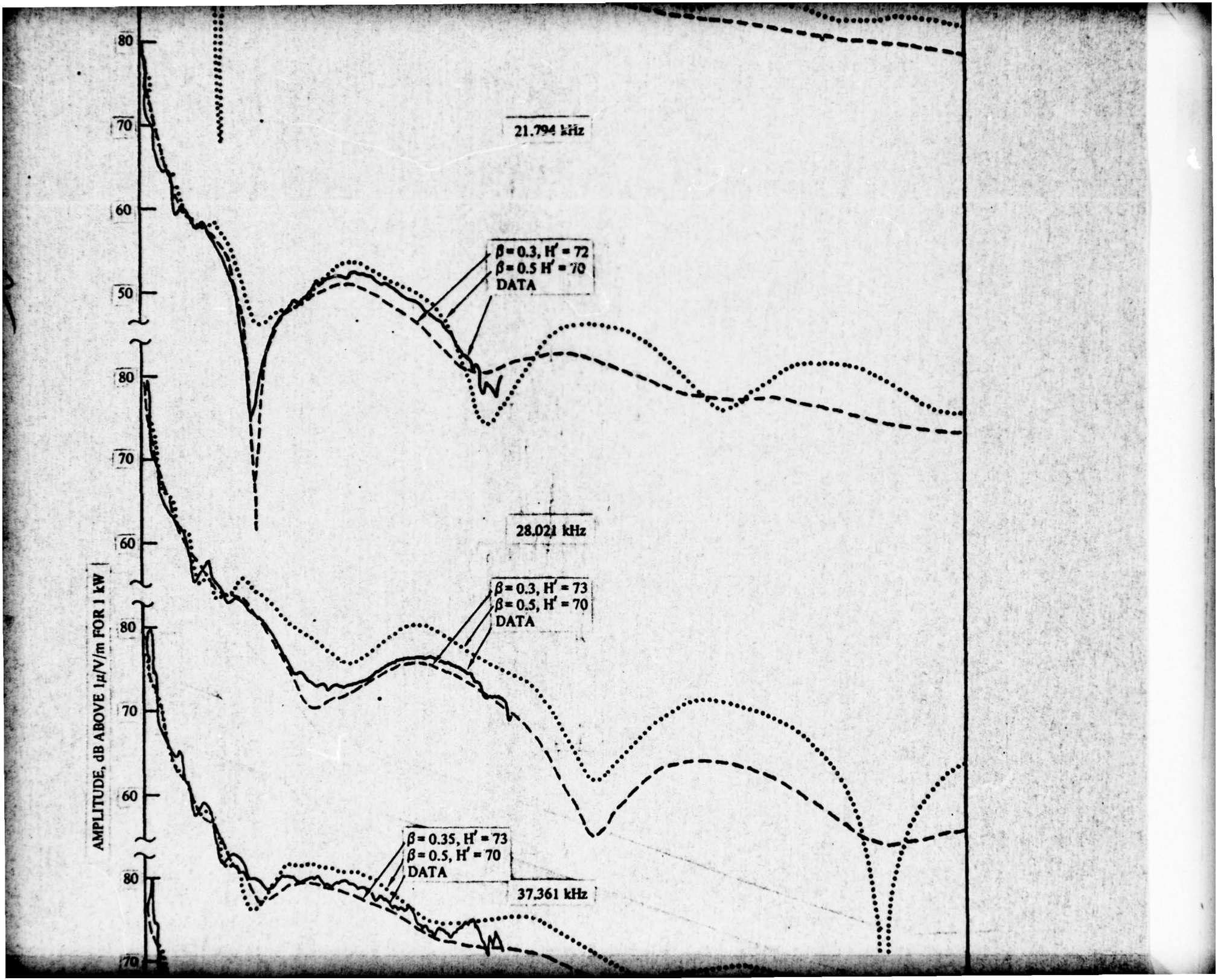
AMPLITUDE, dB ABOVE 1μV/m FOR 1 kW
80
70
60
50
21.794 kHz
β = 0.3, H' = 72
β = 0.5 H' = 70
DATA
28.021 kHz
β = 0.3, H' = 73
β = 0.5, H' = 70
DATA
37.361 kHz
β = 0.35, H' = 73
β = 0.5, H' = 70
DATA

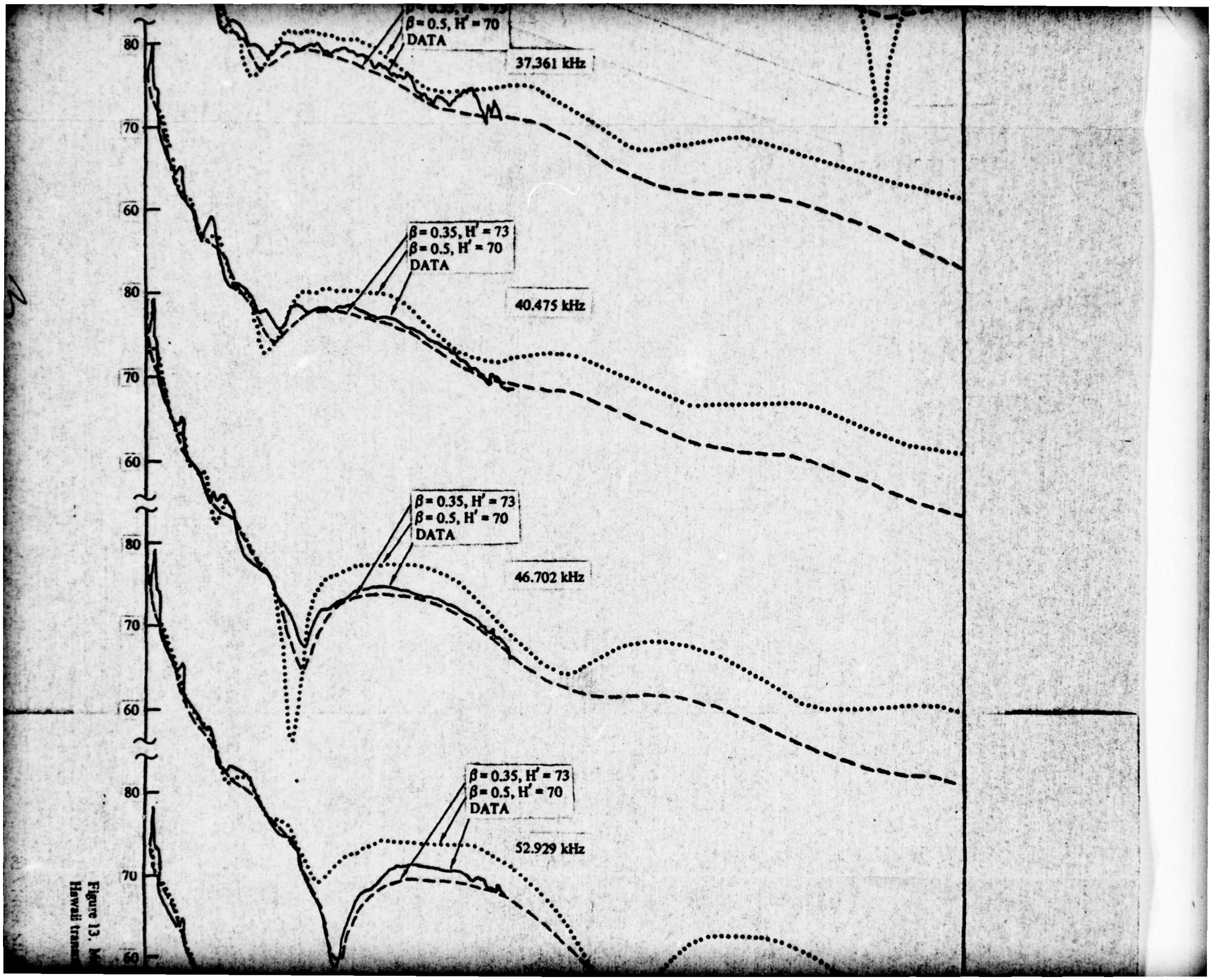

Figure 13. M
Hawaii trans

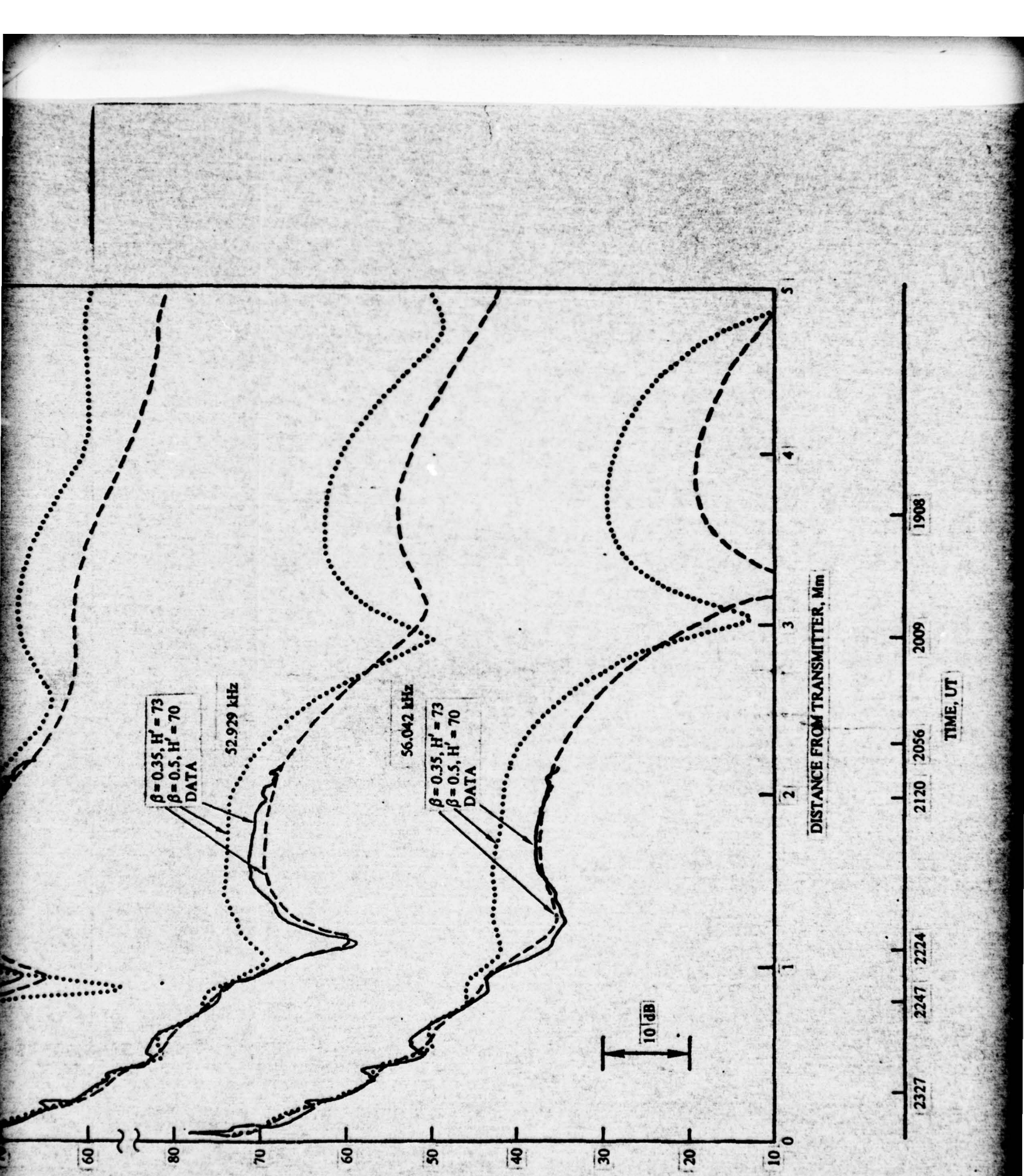

Figure 13. Measured and computed daytime signal levels on the Hawaii to Sentinel, Arizona, path. Hawaii transmitter, 2 February 1974.

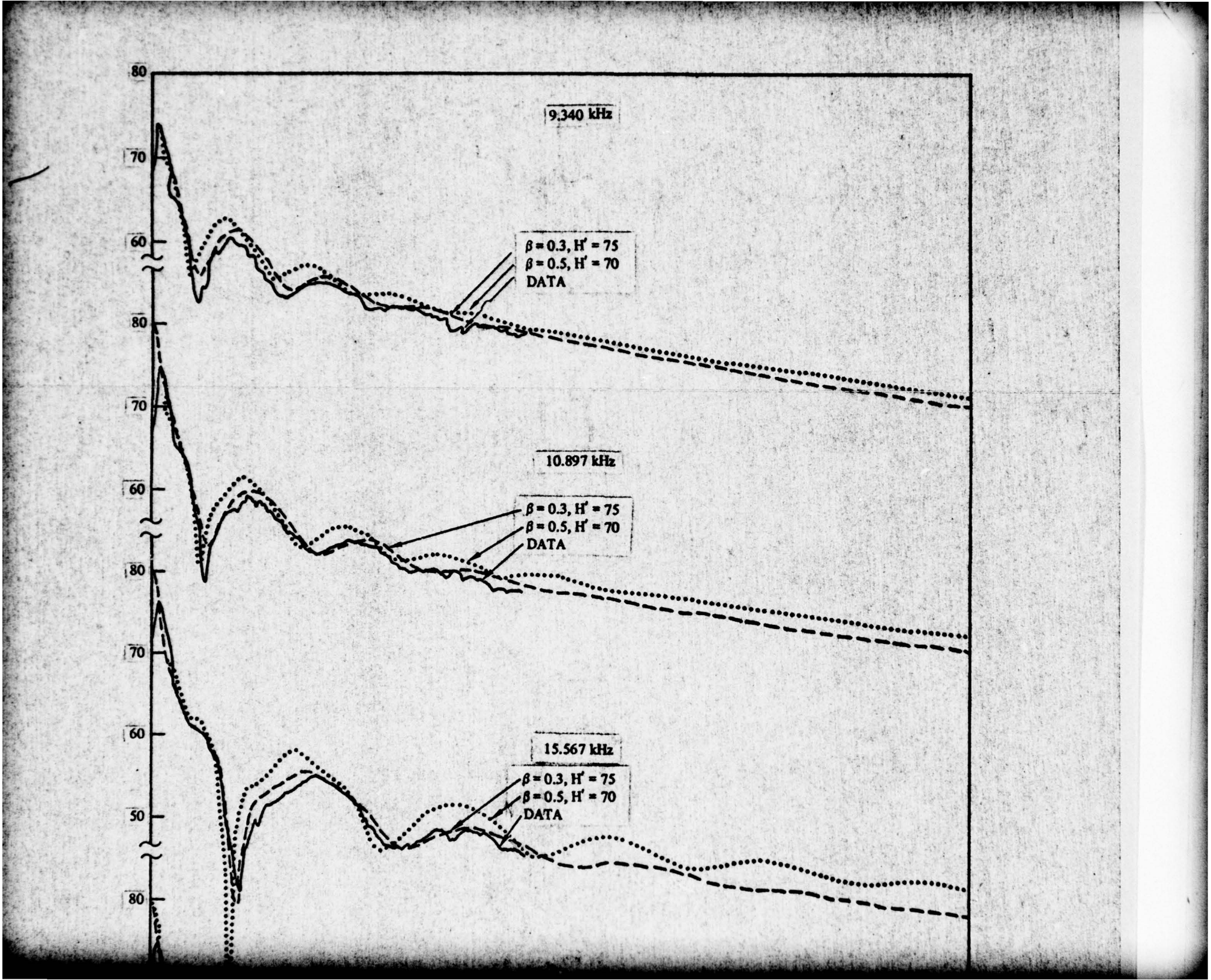
9.340 kHz
β = 0.3, H' = 75
β = 0.5, H' = 70
DATA
10.897 kHz
β = 0.3, H' = 75
β = 0.5, H' = 70
DATA
15.567 kHz
β = 0.3, H' = 75
β = 0.5, H' = 70
DATA
80
70
60
80
70
60
80
70
60
50
80

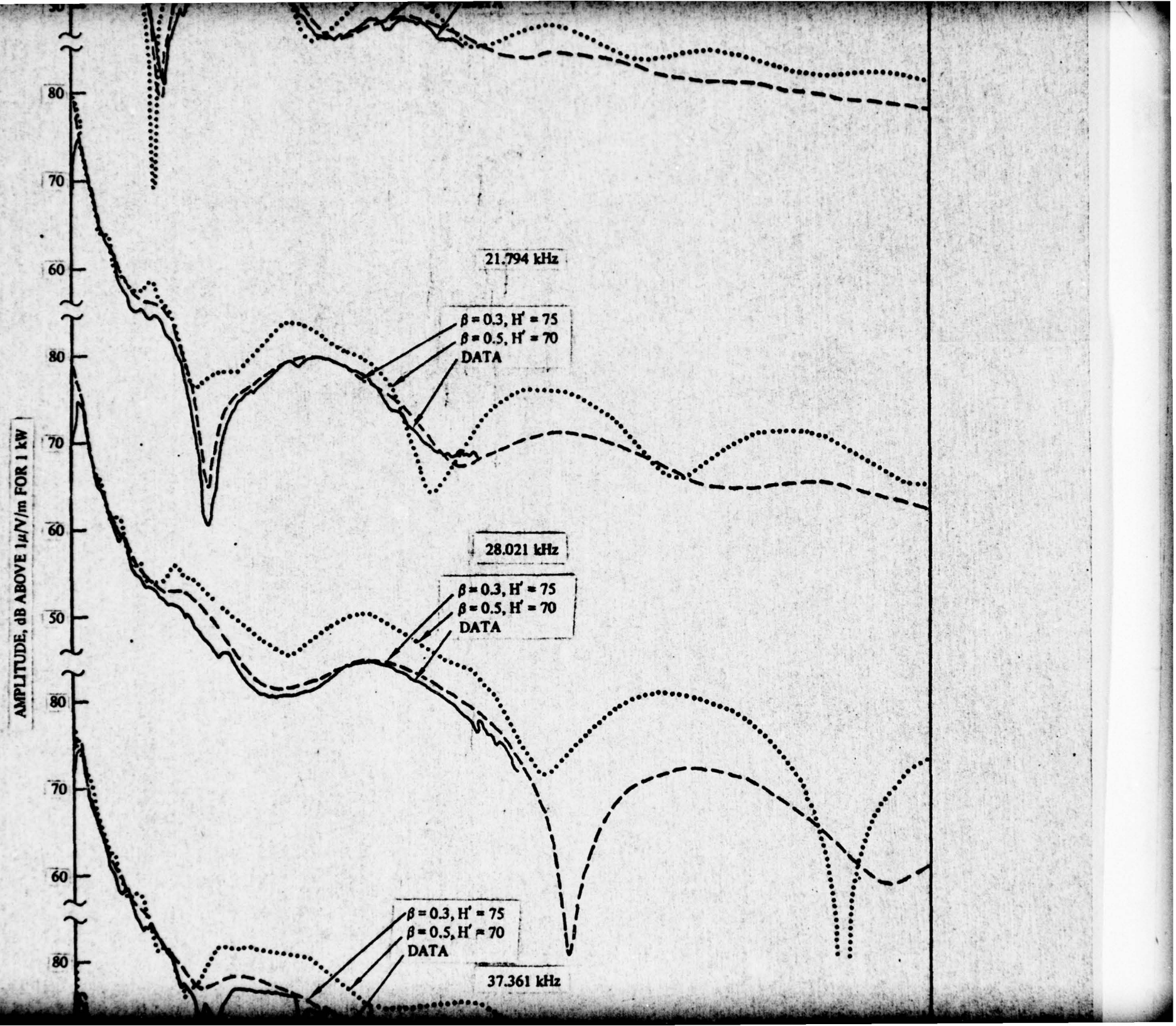
AMPLITUDE, dB ABOVE 1μV/m FOR 1 kW
80
70
60
21.794 kHz
β = 0.3, H' = 75
β = 0.5, H' = 70
DATA
80
70
60
28.021 kHz
β = 0.3, H' = 75
β = 0.5, H' = 70
DATA
50
80
70
60
β = 0.3, H' = 75
β = 0.5, H' = 70
DATA
37.361 kHz
80

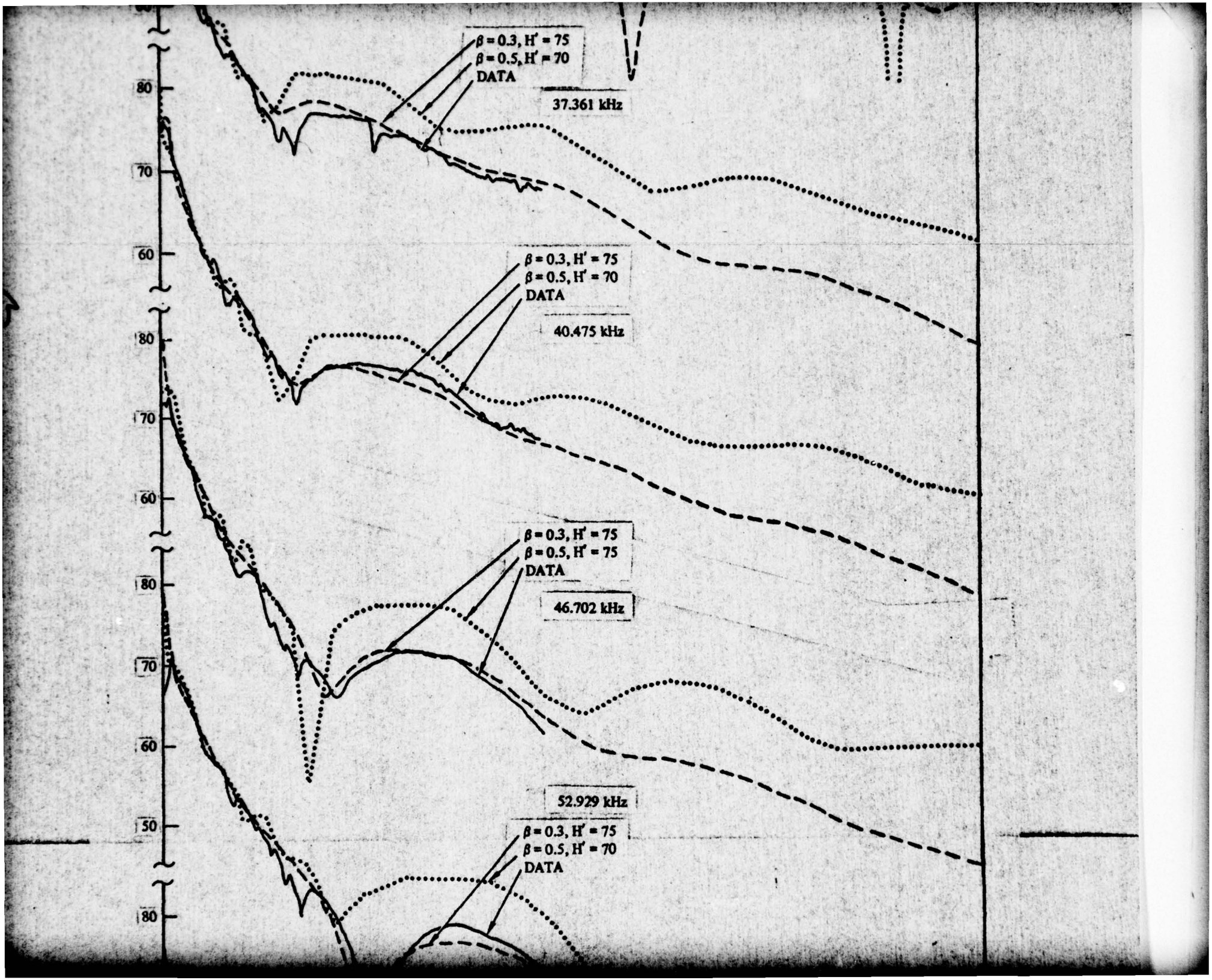
β = 0.3, H' = 75
β = 0.5, H' = 70
DATA
37.361 kHz
β = 0.3, H' = 75
β = 0.5, H' = 70
DATA
40.475 kHz
β = 0.3, H' = 75
β = 0.5, H' = 75
DATA
46.702 kHz
52.929 kHz
β = 0.3, H' = 75
β = 0.5, H' = 70
DATA
80
70
60
80
70
60
80
70
60
50
80

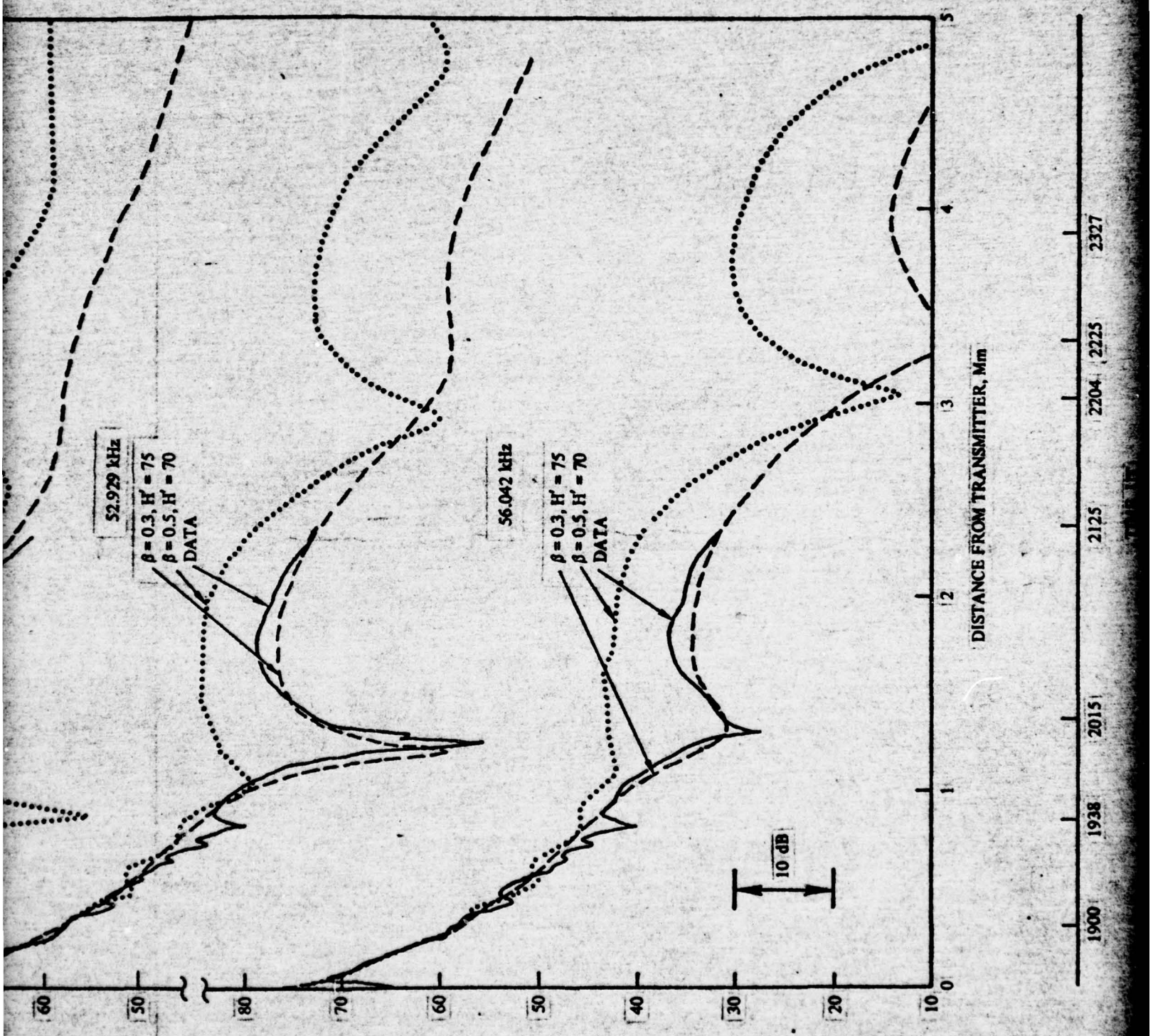

Figure 14. Measured and computed daytime signal levels on the Hawaii to Sentinel, Arizona, path. Hawaii transmitter, 3 February 1974.

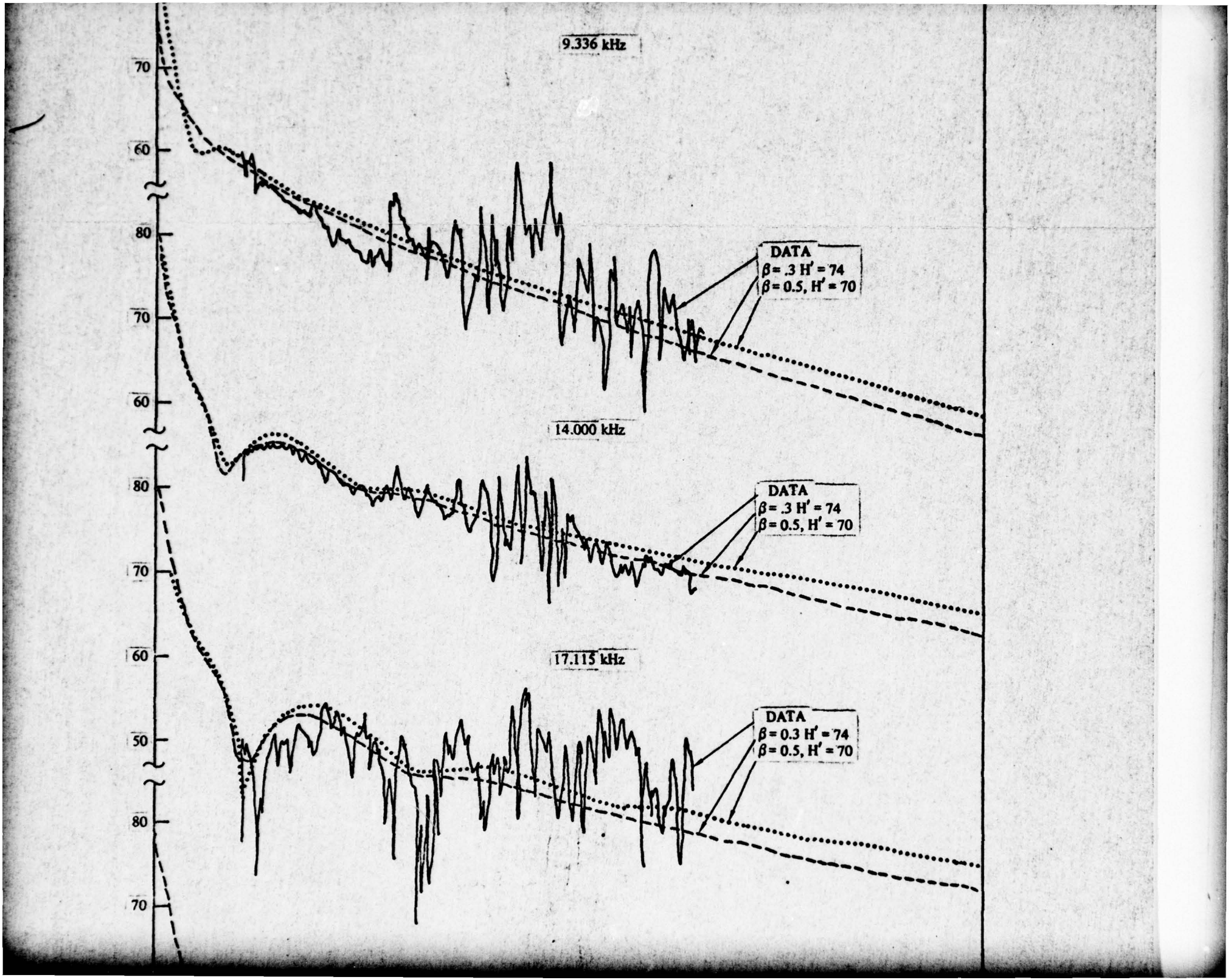
9.336 kHz
70
60
80
70
60
DATA
β = .3 H' = 74
β = 0.5, H' = 70
14.000 kHz
80
70
60
DATA
β = .3 H' = 74
β = 0.5, H' = 70
17.115 kHz
50
80
70
DATA
β = 0.3 H' = 74
β = 0.5, H' = 70

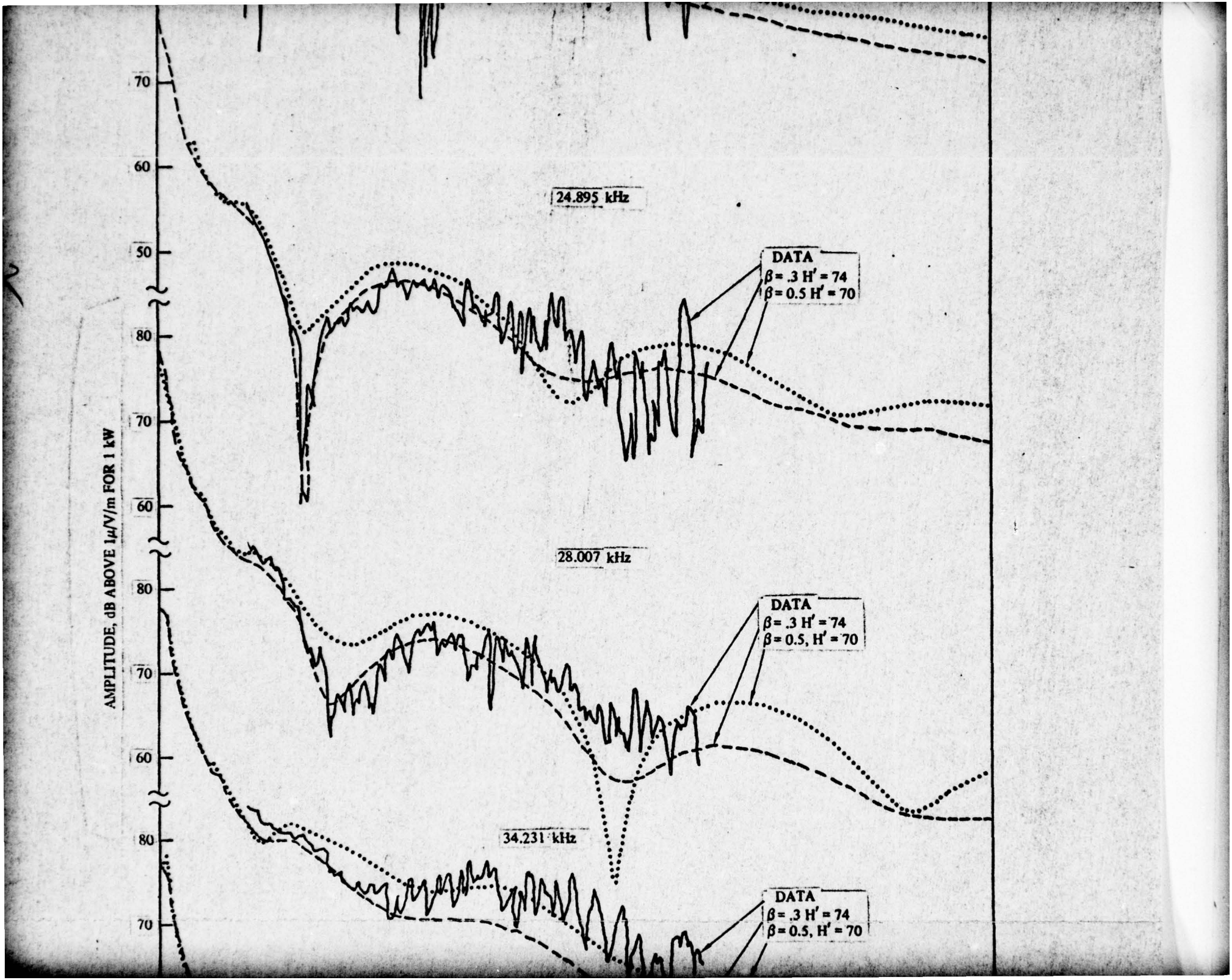
AMPLITUDE, dB ABOVE 1μV/m FOR 1 kW
70
60
50
80
70
60
80
70
60
80
70
24.895 kHz
DATA
β = .3 H′ = 74
β = 0.5 H′ = 70
28.007 kHz
DATA
β = .3 H′ = 74
β = 0.5, H′ = 70
34.231 kHz
DATA
β = .3 H′ = 74
β = 0.5, H′ = 70

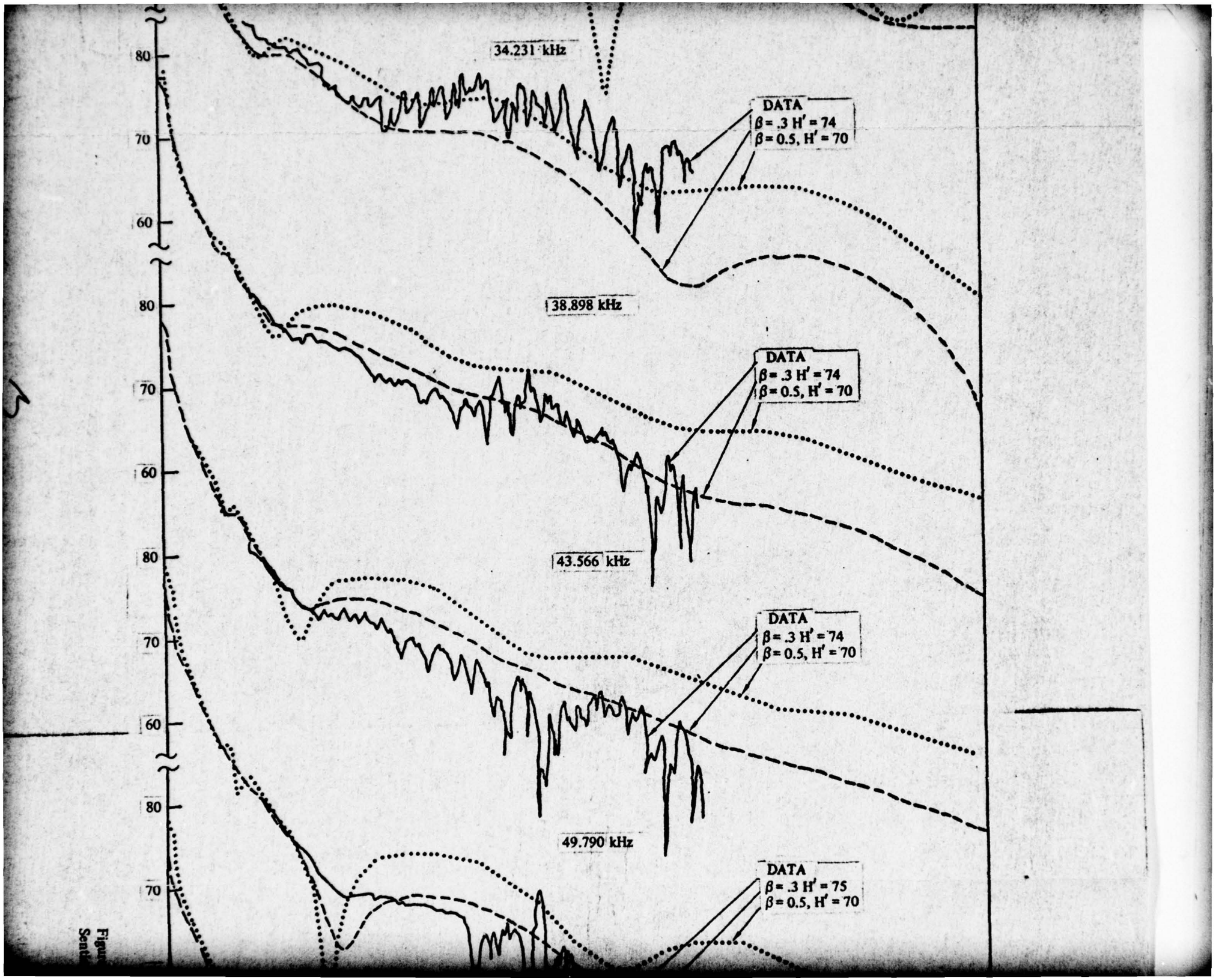
34.231 kHz
DATA
β = .3 H' = 74
β = 0.5, H' = 70
38.898 kHz
DATA
β = .3 H' = 74
β = 0.5, H' = 70
43.566 kHz
DATA
β = .3 H' = 74
β = 0.5, H' = 70
49.790 kHz
DATA
β = .3 H' = 75
β = 0.5, H' = 70
80
70
60

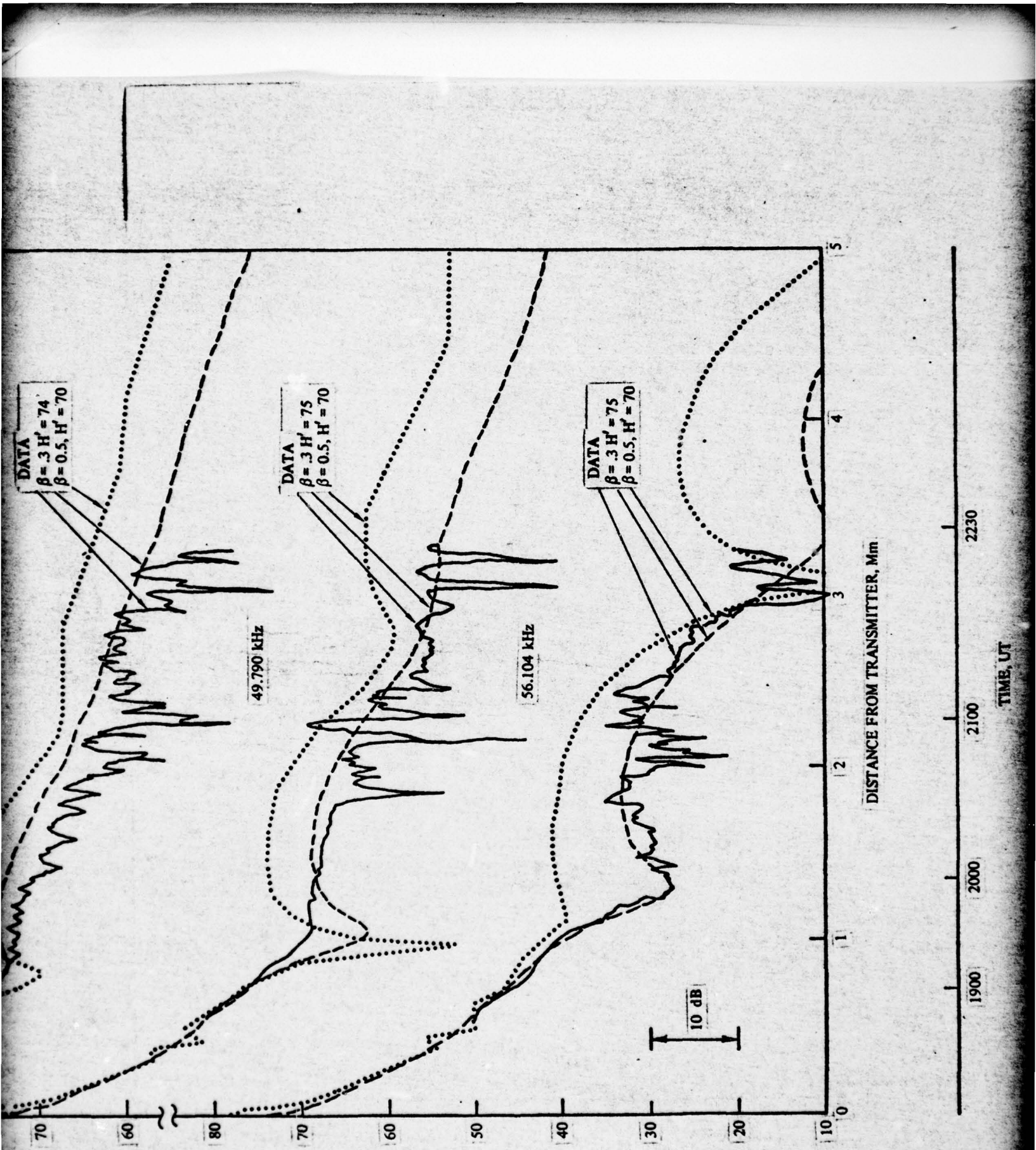

Figure 15. Measured and computed signal levels on the Hawaii to Sentinel, Arizona, path. Sentinel transmitter, 2 February 1974.

NIGHTTIME AIRCRAFT DATA

To examine the characteristics of vlf signal strengths for propagation during nighttime conditions, measurements were made aboard inflight aircraft, at an altitude of 3 km (10 000 ft), during January and February 1969. The signals monitored included NPM on 23.4 kHz as radiated from Oahu, Hawaii; OMEGA on 10.2 and 13.6 kHz as radiated from Haiku, Hawaii; and transmissions from the NOSC multifrequency sounder on ten frequencies between 9 and 31 kHz. The propagation paths considered are listed in table 7 and shown in figure 16.

TABLE 7. NIGHTTIME AIRCRAFT FLIGHT PATHS, 1969.

Flight		Flight Time, GMT	Data Flight Number
Origin	*Destination*	*Beginning* *End*	
Seattle, WA	Hawaii	27 Jan from 0522 to 1701	1
Hawaii	Samoa	29 Jan from 0240 to 1521	2
Samoa	Hawaii	31 Jan from 0755 to 1902	3
Hawaii	Wake	2 Feb from 0731 to 1420	4
Wake	Hawaii	3 Feb from 0730 to 1756	5
Hawaii	Ontario, CA	7 Feb from 0341 to 1514	6

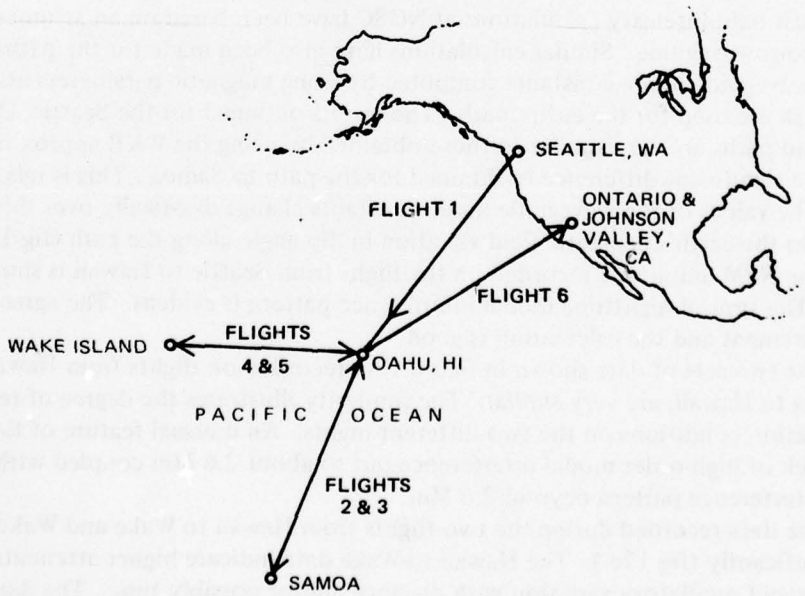

Figure 16. Nighttime aircraft flight paths in the Pacific area.

The geographic parameters chacteristic of the various propagation paths are given in table 8. Also presented are the times for which propagation data were recorded aboard the aircraft.

TABLE 8. GEOGRAPHIC PARAMETERS FOR AIRCRAFT FLIGHTS, 1969.

Flight	Origin-Destination	Flight Data Times, UT	Midpath/Midnight, UT	Range (km)	Times Path in Total Daylight, UT	Times Path in Total Darkness, UT
1	Seattle-Oahu	0600-1630	1000	4329	1700-0100	0415-1440
2	Oahu-Samoa	0430-1500	1100	4100	1700-0130	0415-1440
3	Samoa-Oahu	0800-1830	1100			
4	Oahu-Wake	0730-1400	1200	4028	1930-0415	0650-1700
5	Wake-Oahu	0730-1730	1200			
6	Oahu-Ontario	0430-1500	0930	4100	1710-0415	0415-1430

Figure 17 illustrates the simulation of nighttime propagation as obtained on the radials outward from the 23.4 kHz NPM Hawaii transmitter during the winter of 1969. These data are reproduced from reference 7. The theoretical curves were all computed using the WKB form of the mode sum. The electron density profile was $\beta = 0.5\ km^{-1}$, $H' = 85.5$ km.

Most field-intensity calculations at NOSC have been based on an assumed horizontally homogeneous waveguide. Similar calculations have also been made for the paths included here; the waveguide mode constants computed by using magnetic parameters associated with the midpath are used for the entire path. The results obtained for the Seattle, Ontario, and Wake Island paths are very similar to those obtained by using the WKB approximation. However, a significant difference is obtained for the path to Samoa. This is related to the fact that the values of the waveguide mode constants change drastically over this propagation path due to the earth's magnetic field variation in dip angle along the path (fig 1).

The NPM amplitude recorded on the flight from Seattle to Hawaii is shown in figure 17a. The typical nighttime modal interference pattern is evident. The agreement between the measurement and the calculation is good.

The two sets of data shown in figure 17b, recorded on flights from Hawaii to Samoa and Samoa to Hawaii, are very similar. The similarity illustrates the degree of reproducibility of propagation conditions on the two different nights. An unusual feature of these data is the relative lack of high-order modal interference out to about 2.6 Mm coupled with the rapidly varying interference pattern beyond 2.6 Mm.

The data recorded during the two flights from Hawaii to Wake and Wake to Hawaii differ significantly (fig 17c.). The Hawaii-to-Wake data indicate higher attenuation and show the more rapid oscillatory variation with distance and/or possibly time. The data recorded on the return flight have many of the characteristics of the WKB calculations shown. A profile 2 or more km higher would provide computed results with a modal interference pattern that would fit this particular data better.

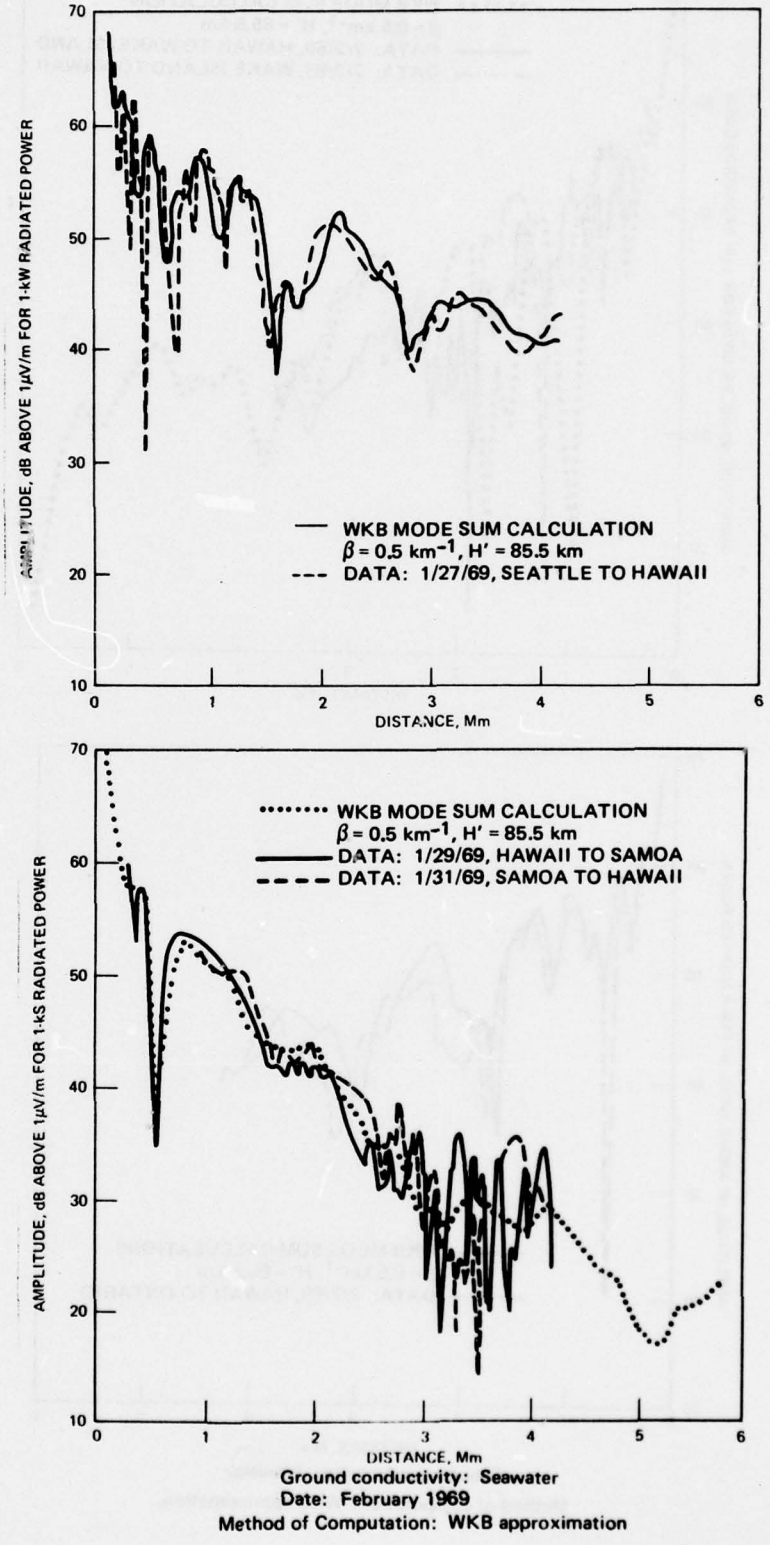

Figure 17. Nighttime propagation over the Pacific Ocean (winter) (NPM 23.4 kHz). (Sheet 1 of 2)

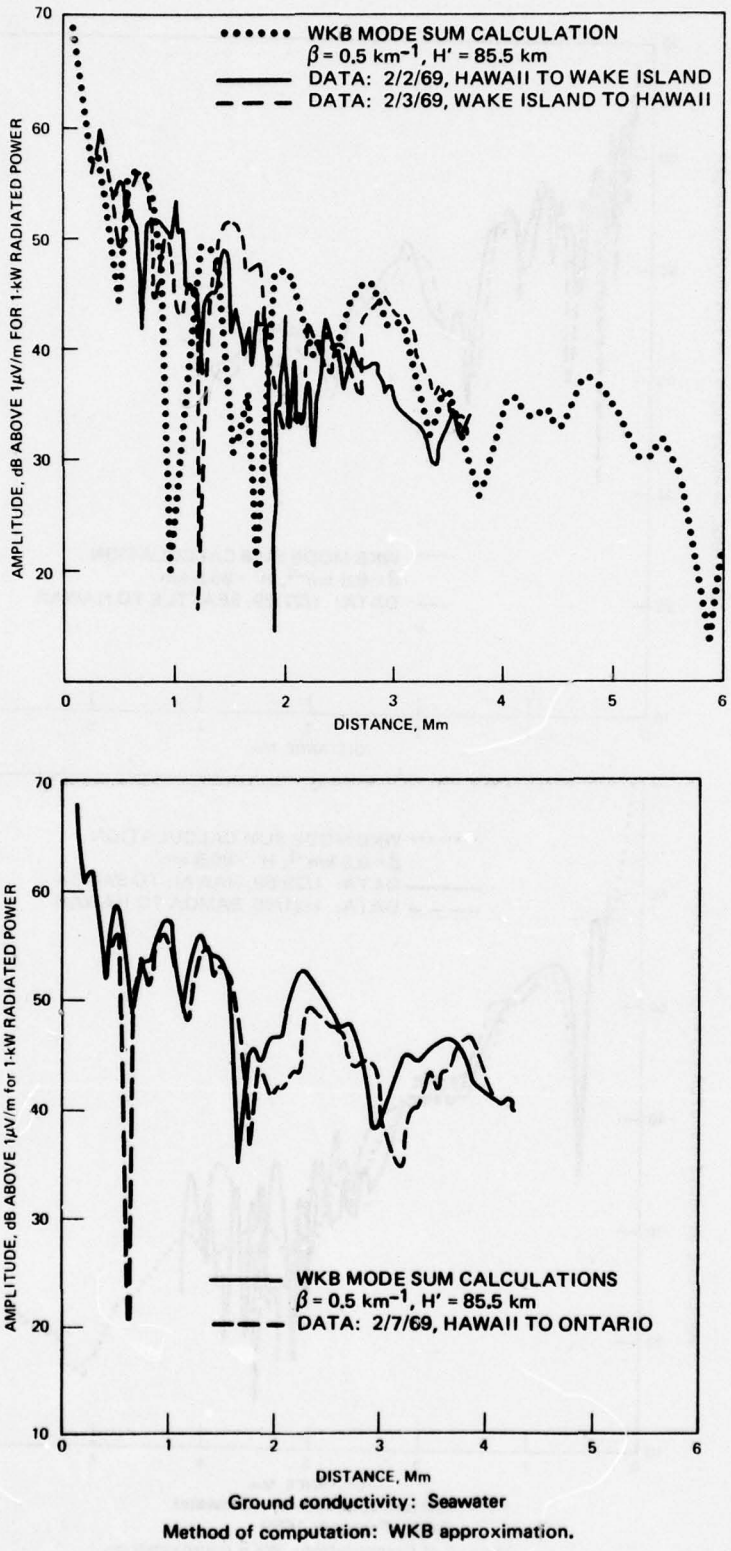

Figure 17. Nighttime propagation over the Pacific Ocean (winter) (NPM 23.4 kHz). (Sheet 2 of 2)

The data and calculations for the Hawaii-to-Ontario path are compared in figure 17d. The characteristics are relatively similar. However, again, a relative shift of the modal interference pattern, such as would be produced by an increase of the ionospheric profile height by about 1 or 2 km, is needed to obtain better agreement.

The vlf data presented here indicate some variation of propagation conditions from night to night and throughout a given night. Such nighttime variability is well known; eg, the variability of phase of 10.2 kHz, as has been measured using the Omega system, is equivalent to a change of phase velocity of the dominant waveguide mode of the order of ±2 to 3 parts in 10^4. This change can be produced by a change in H′ of about ±2 to 3 km. This height variability is within the range of the profile change needed to provide better agreement between computations and data recorded during the flights from Wake to Hawaii (fig 17c.) and Hawaii to Ontario (fig 17d.). The former data indicate that the ionospheric reflection height was changing throughout the flight; the latter data indicate that the reflection height was relatively stationary.

The data recorded on the flight from Hawaii to Wake (fig 17c.) which deviate significantly from the computations for this path and from the other data recorded on the same path, indicate that the ionospheric conditions differed significantly and possibly changed with time. A geomagnetic storm was reported to have started at 1503 UT on 2 February, which was about 40 minutes after the flight terminated and a premagnetic storm disturbance of the nighttime D layer may have occurred.

The relatively rapid oscillatory amplitude variation with distance observed beyond 2.6 Mm on the Hawaii-to-Samoa propagation path is not understood. It may be a spatial variation or a time variation. Note that both the geographic and the geomagnetic equators intersect this path at about 2.45 Mm.

Radio transmissions from the Hawaii OMEGA navigation transmitter at 10.2 and 13.6 kHz were also being recorded during these flights. Results of measured signal levels along with computed fields are shown in figures 18, 19, and 20.

For the Hawaii to Samoa path, the WKB calculation procedure was required. The comparison between prediction and measurement is shown in figure 18 where the β = 0.5 km^{-1}, H′ 85.5 km profile is used as input. The Hawaii to Wake Island path (fig 19) proved to be difficult to model when using any of several β, H′ combinations. Again the WKB procedure was employed. Very encouraging results were obtained for the Hawaii to Southern California path (fig 20) on both 10.2 and 13.6 kHz. The horizontally homogenous form of the calculations were utilized, but the required β value of the profile was found to be different for the two frequencies (10.2 and 13.6 kHz). The values used for the exponential parameters were β = 0.4 km^{-1}, H′ = 87 km for 10.2 kHz and β = 0.5 km^{-1}, and H′ = 87 km for 13.6 kHz.

Propagation data were also recorded during the February 1969 flights using the NOSC multifrequency sounder simultaneously with the NPM data shown in figure 17. These sounder data were recorded aboard the inflight aircraft for vlf transmissions from a horizontal vlf antenna located on the large island of Hawaii. Ten vlf frequencies were transmitted and recorded. These were approximately: 9.3, 10.9, 14.0, 15.6, 17.1, 21.8, 24.9, 26,5, 28.0, and 31.2 kHz. A detailed discussion of the data acquired and the theoretical results obtained from these data are reported in reference 21. Comparisons between horizontally homogenous waveguide predictions and some of the multifrequency sounder data are shown in figure 21. Here it is observed that the profile β = 0.5 km^{-1}, H′ = 87 km represents these actual measured fields very well at 14.0, 17.1, and 21.8 kHz. A somewhat modified profile would be required to obtain better fits to the data at 10.9, 24.9, and 28.0 kHz.

21. Naval Electronics Laboratory Report 1798, Analysis of a Multimode Propagation Concept for Predicting VLF Signal Strengths at Night, by DG Morfitt, 9 December 1971

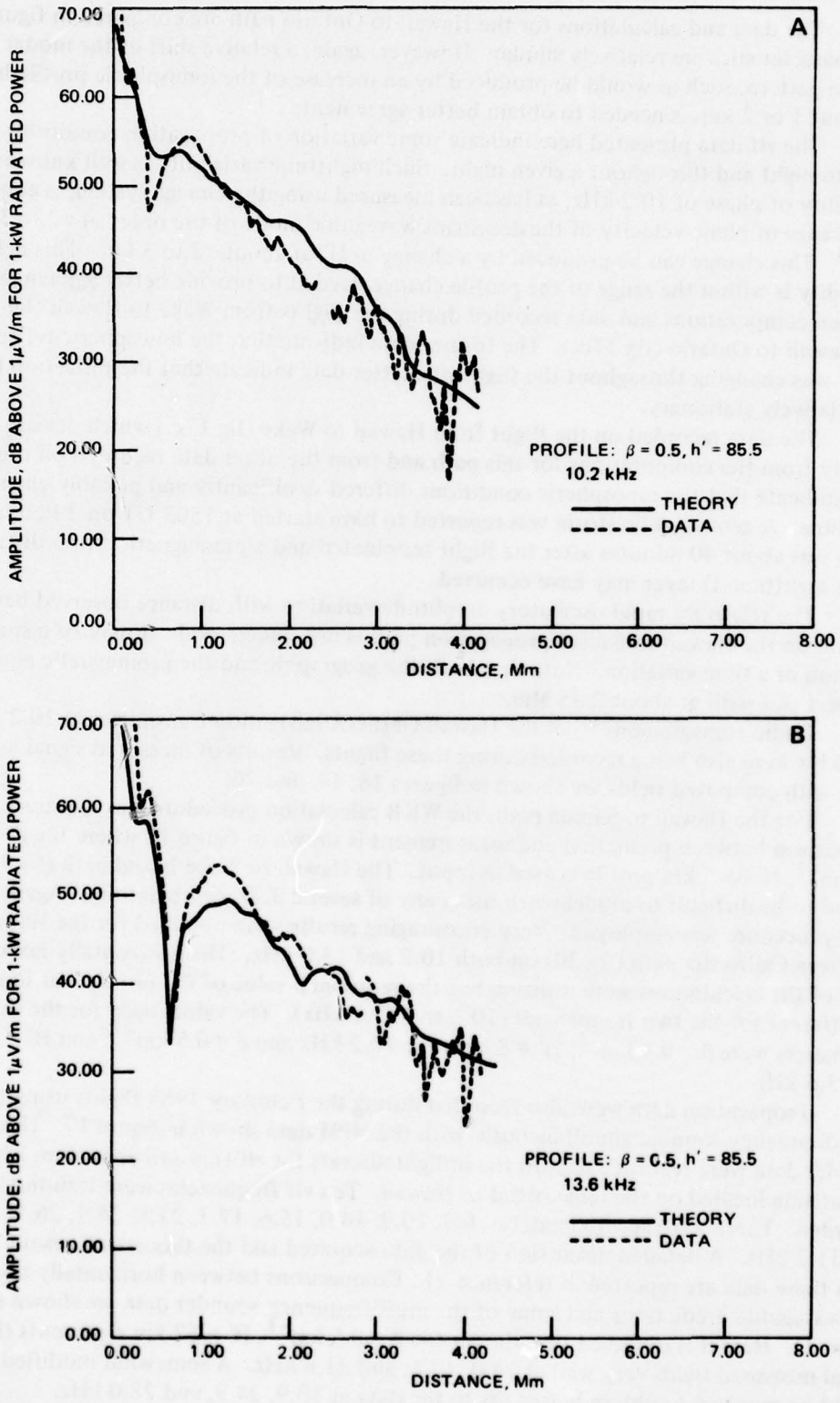

Figure 18. Nighttime Hawaii to Samoa flight data and computed amplitude for 10.2 and 13.6 kHz.

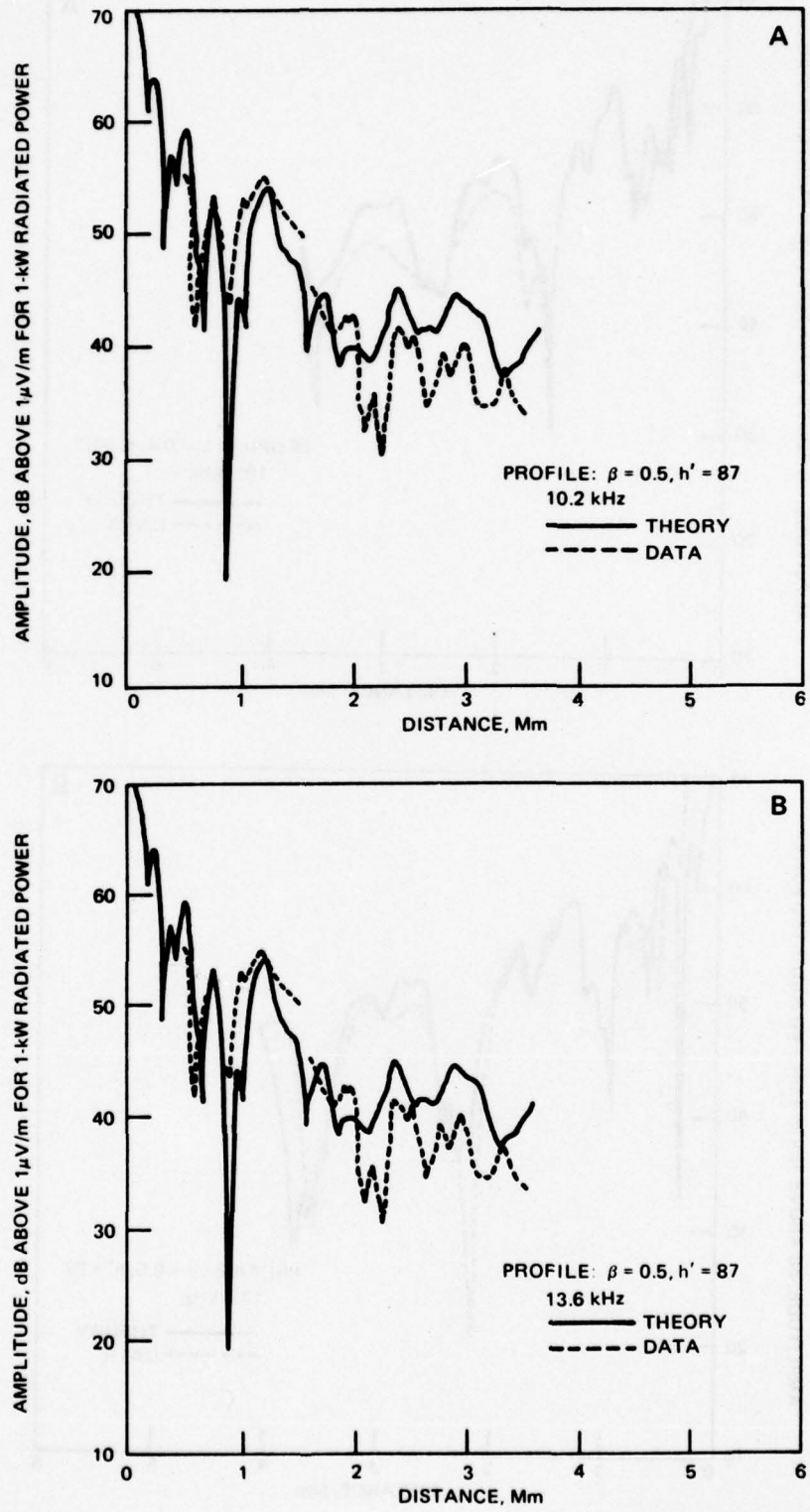

Figure 19. Nighttime Wake to Hawaii flight data and computed amplitude for 13.6 kHz.

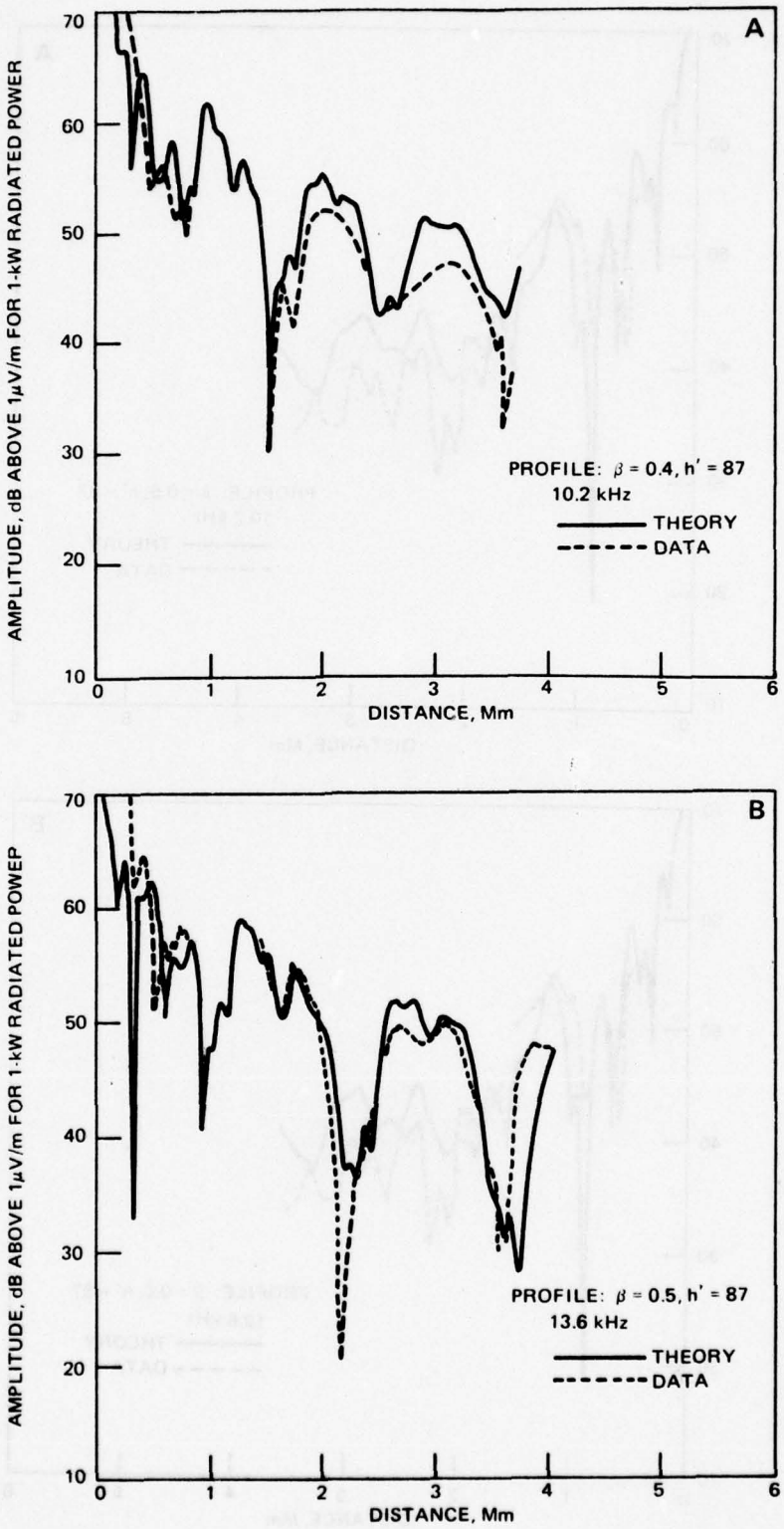

Figure 20. Nighttime Hawaii to Southern California flight data and computed amplitude for 10.2 and 13.6 kHz.

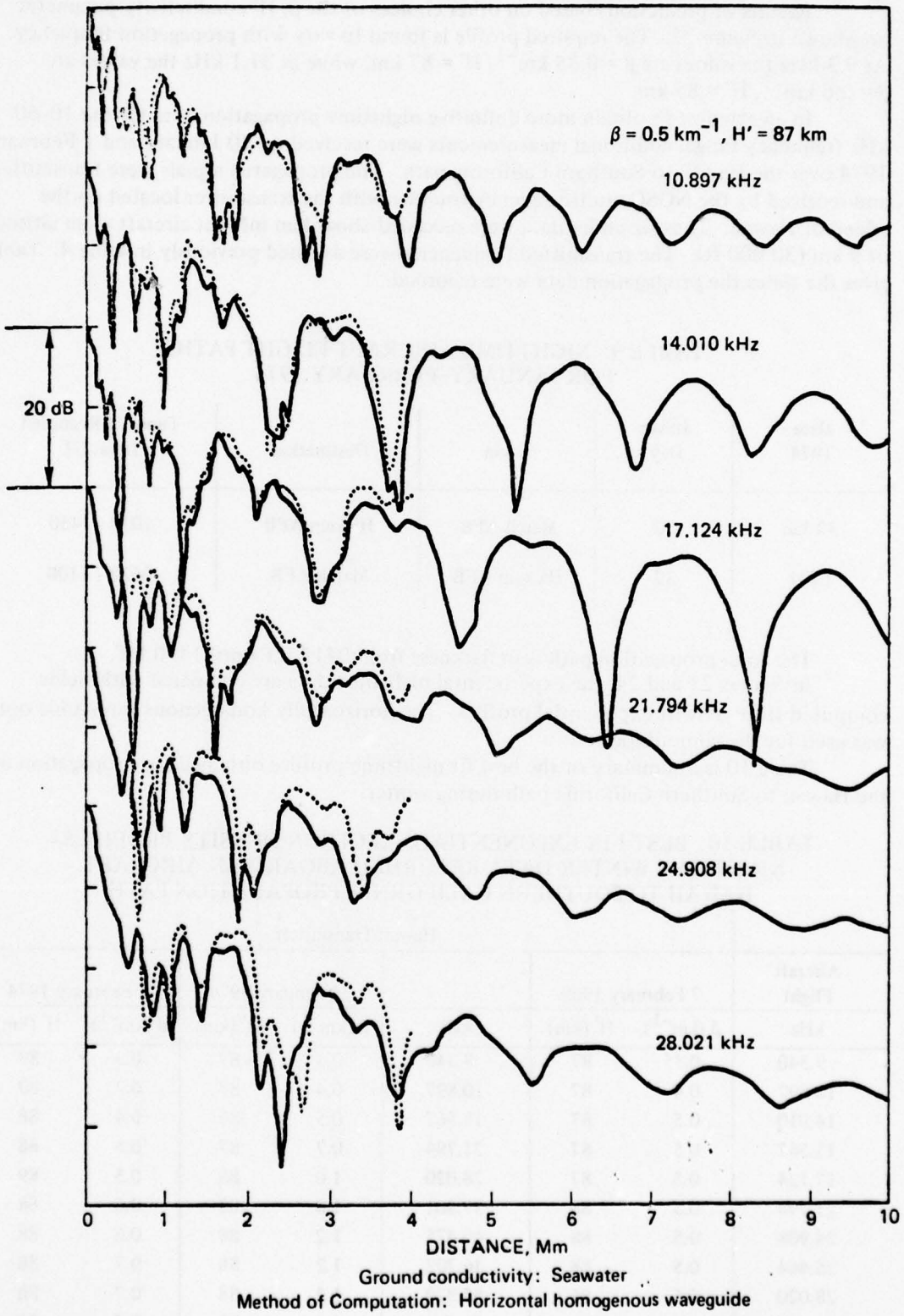

Figure 21. Multifrequency sounder data over the Pacific; Hawaii to Southern California path (Nighttime, winter).

Results of predictions based on other choices of the β, H′ conductivity parameter are shown in figure 22. The required profile is found to vary with propagation frequency. At 9.3 kHz the values are $\beta = 0.35\ km^{-1}$, H′ = 87 km, while at 31.1 kHz the values are $\beta = 0.6\ km^{-1}$, H′ = 88 km.

In an attempt to obtain more definitive nighttime propagation data for the 10–60 kHz frequency range, additional measurements were received on 30 January and 1 February 1974 over the Hawaii to Southern California path. The propagated signals were transmitted and received by the NOSC multifrequency sounder with the transmitter located on the Island of Hawaii. These sounder data were recorded aboard an inflight aircraft at an altitude of 9 km (30 000 ft). The transmitted frequencies were as listed previously in table 4. Table 9 gives the times the propagation data were recorded.

TABLE 9. NIGHTTIME AIRCRAFT FLIGHT PATHS FOR JANUARY–FEBRUARY 1974

Date 1974	Julian Day	Origin	Destination	Times of Recorded Data, UT
30 Jan	30	March AFB	Hickam AFB	1030 - 1450
1 Feb	32	Hickam AFB	March AFB	0620 - 1100

The total propagation path is in darkness from 0415 UT until 1430 UT.

In figures 23 and 24, the experimental nighttime data are compared with fields computed from best-fit exponential profiles. The horizontally homogenous waveguide option was used for the computations.

Table 10 is a summary of the best fit nighttime profiles obtained for propagation over the Hawaii to Southern California path during winter.

TABLE 10. BEST-FIX EXPONENTIAL ELECTRON DENSITY PROFILES– NIGHTTIME WINTER DATA RECORDED ABOARD AN AIRCRAFT, HAWAII TO SOUTHERN CALIFORNIA PROPAGATION PATH

	Hawaii Transmitter						
Aircraft Flight	7 February 1969			30 January 1974		1 February 1974	
kHz	β (km^{-1})	H′ (km)	kHz	β (km^{-1})	H′ (km)	β (km^{-1})	H′ (km)
9.340	0.35	87	9.340	0.3	87	0.3	89
10.897	0.4	87	10.897	0.4	87	0.3	89
14.010	0.5	87	15.567	0.5	86	0.4	88
15.567	0.5	87	21.794	0.7	87	0.5	88
17.124	0.5	87	28.020	1.0	88	0.5	89
21.794	0.5	88	37.361	1.0	88	0.6	88
24.908	0.5	88	40.475	1.2	88	0.6	88
26.464	0.5	88	46.702	1.2	88	0.7	88
28.020	0.5	88	52.929	1.2	88	0.7	88
31.134	0.6	88	56.042	1.2	88	0.7	88

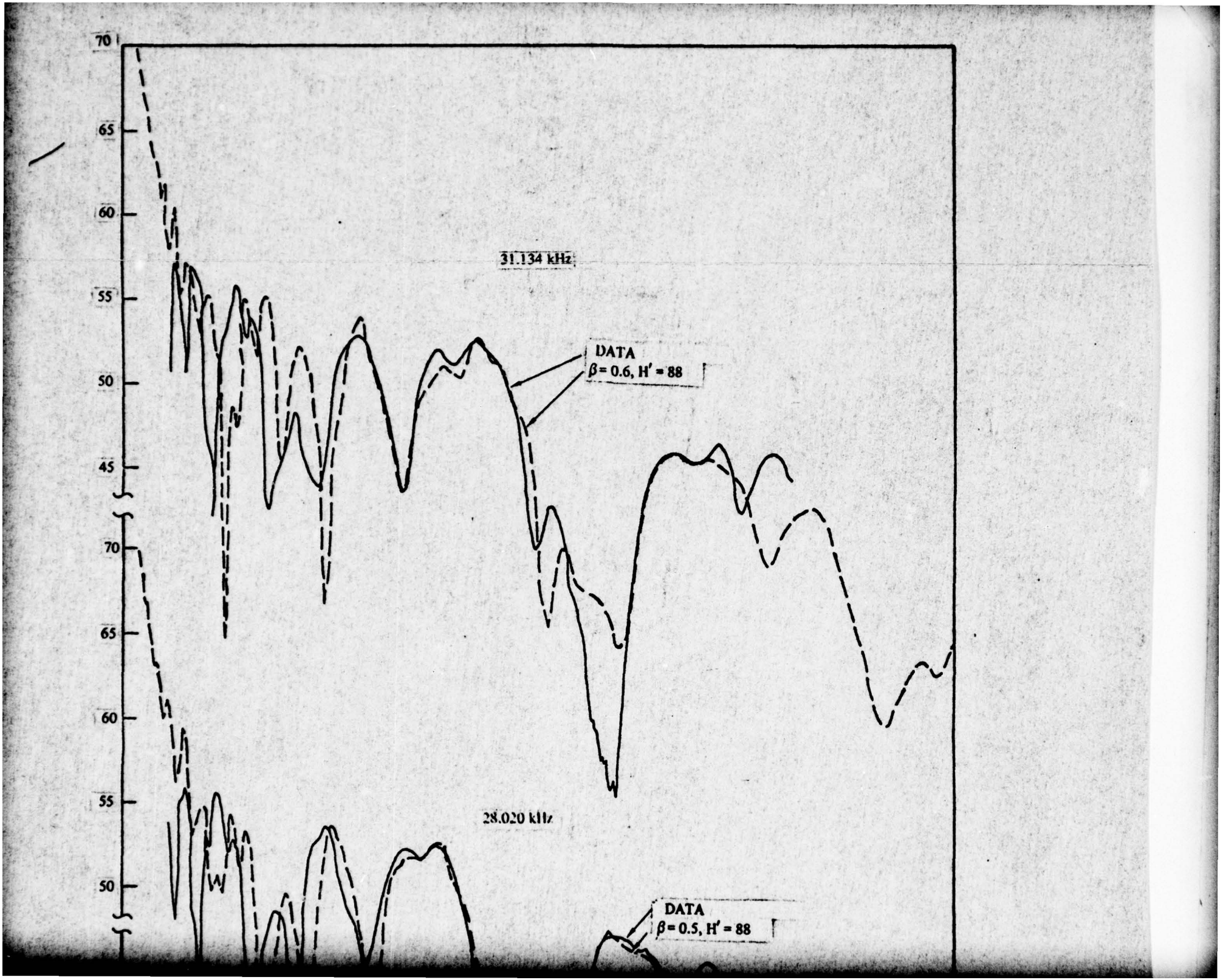
70
65
60
55
50
45
31.134 kHz
DATA
β = 0.6, H' = 88
70
65
60
55
50
28.020 kHz
DATA
β = 0.5, H' = 88

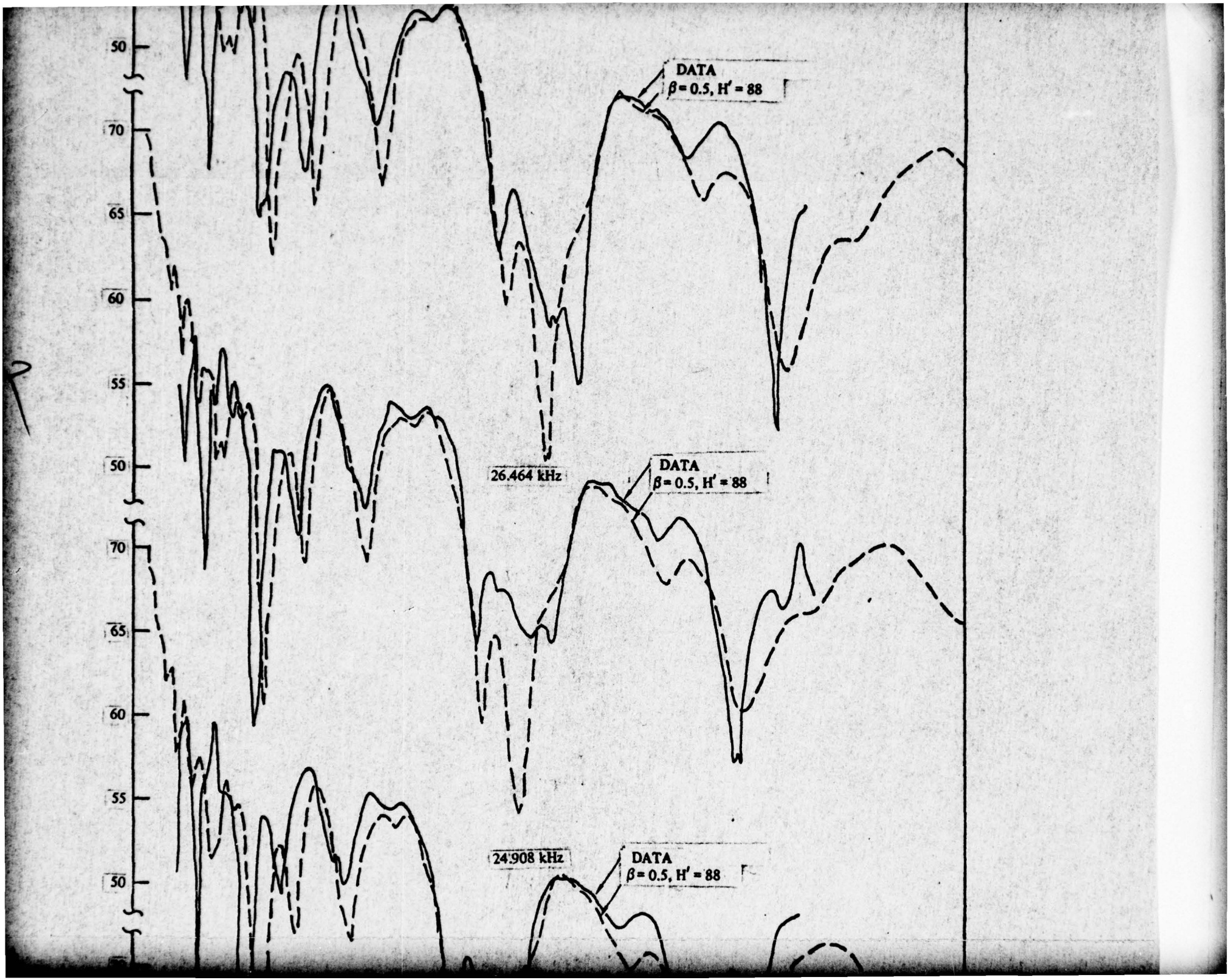
50
70
65
60
55
50
DATA
β = 0.5, H' = 88
26.464 kHz
70
65
60
55
50
DATA
β = 0.5, H' = 88
24.908 kHz
DATA
β = 0.5, H' = 88

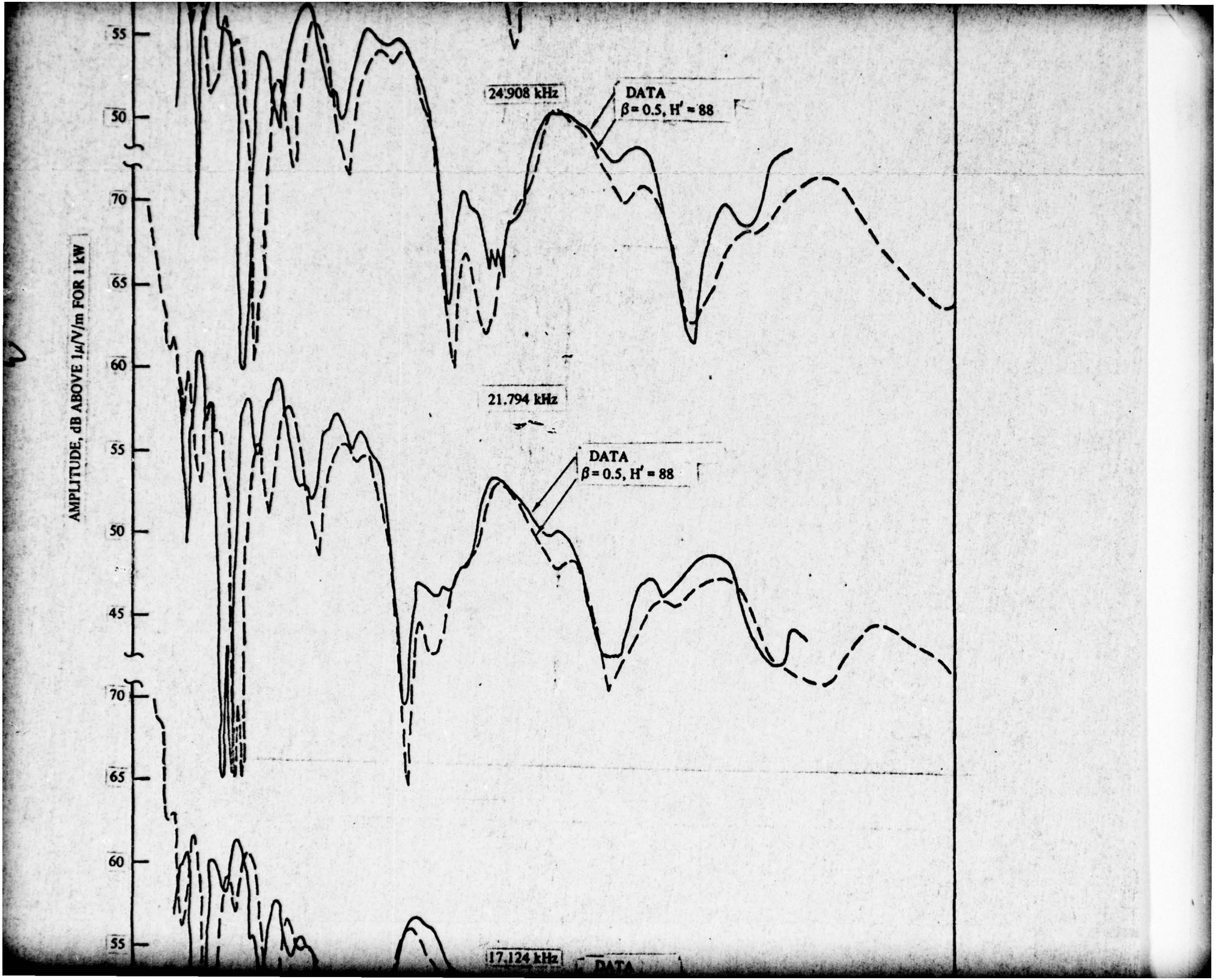
AMPLITUDE, dB ABOVE 1μV/m FOR 1 kW
55
50
70
65
60
55
50
45
70
65
60
55
24.908 kHz
DATA
β = 0.5, H' = 88
21.794 kHz
DATA
β = 0.5, H' = 88
17.124 kHz
DATA

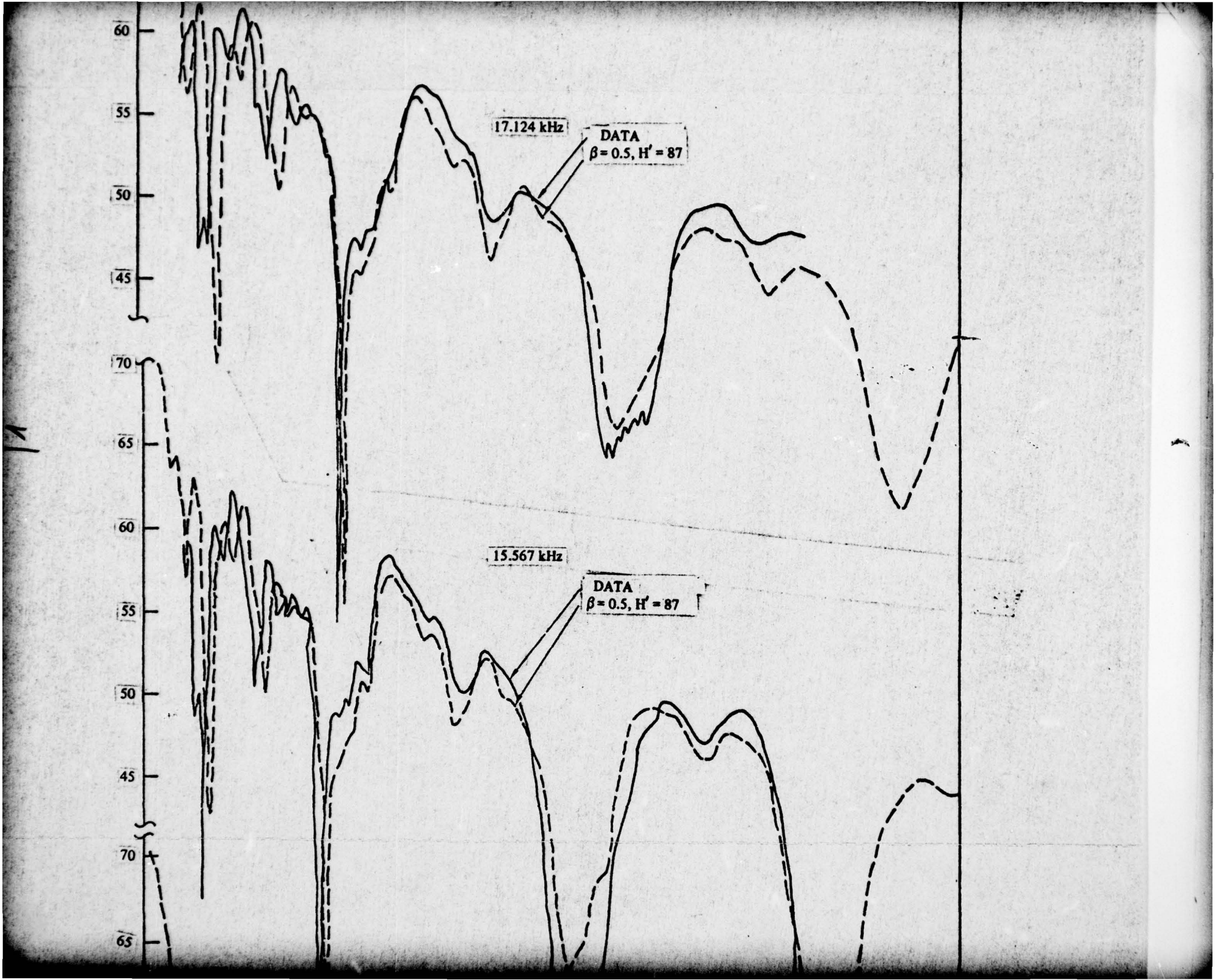
60
55
50
45
17.124 kHz
DATA
β = 0.5, H' = 87
70
65
60
15.567 kHz
DATA
β = 0.5, H' = 87
55
50
45
70
65

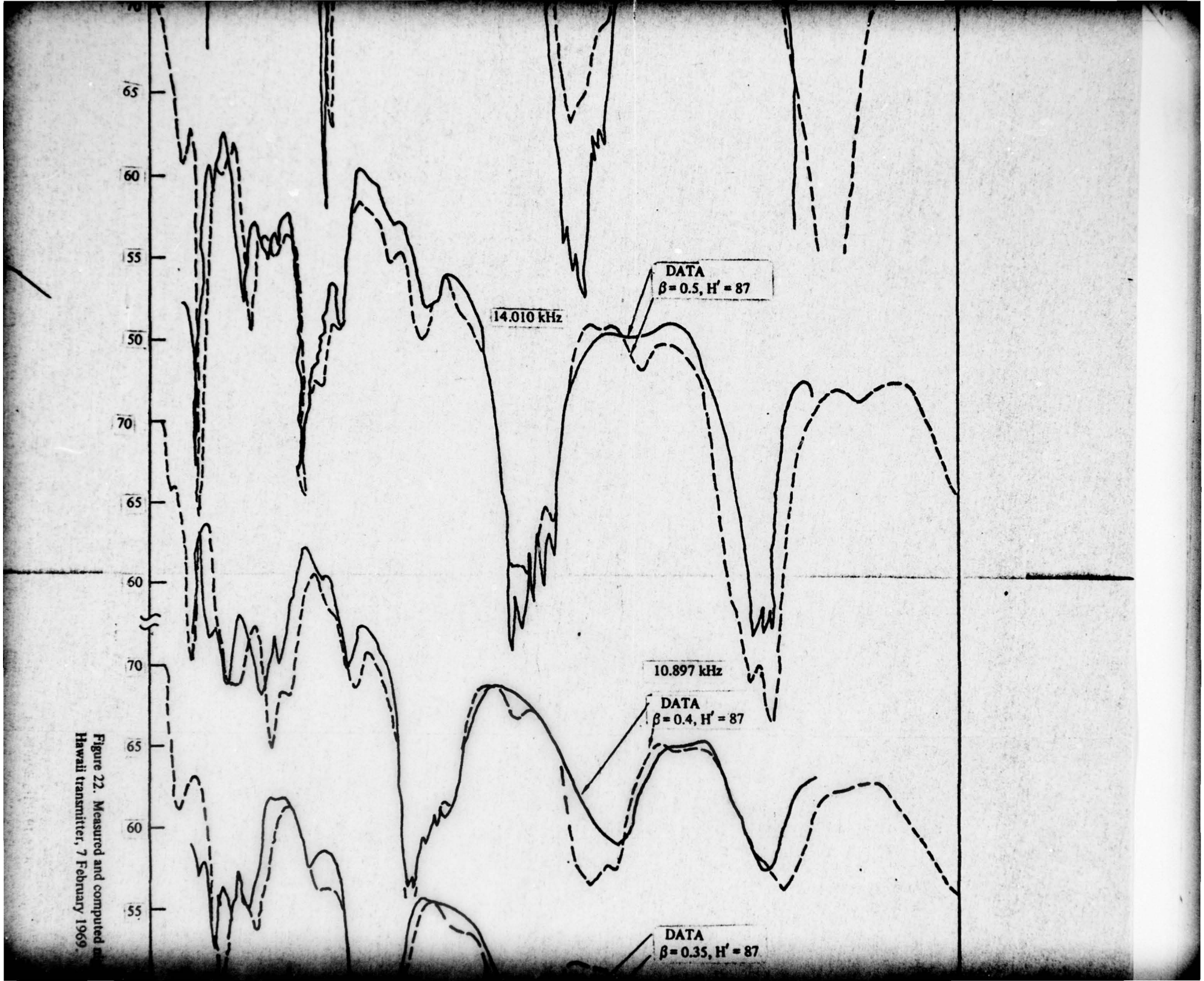

Figure 22. Measured and computed n
Hawaii transmitter, 7 February 1969.

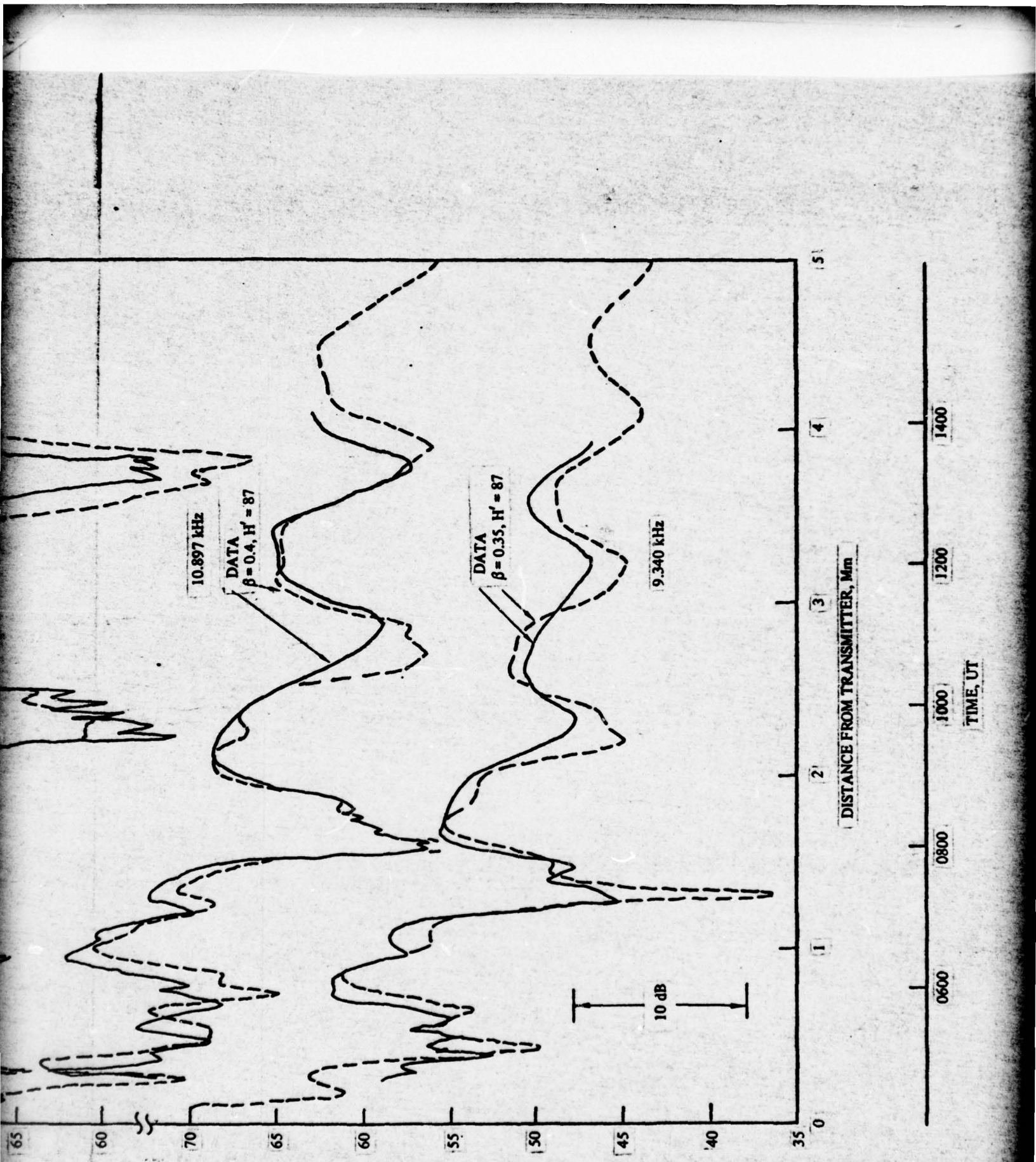

Figure 22. Measured and computed nighttime signal levels on the Hawaii to Ontario, California, path. Hawaii transmitter, 7 February 1969.

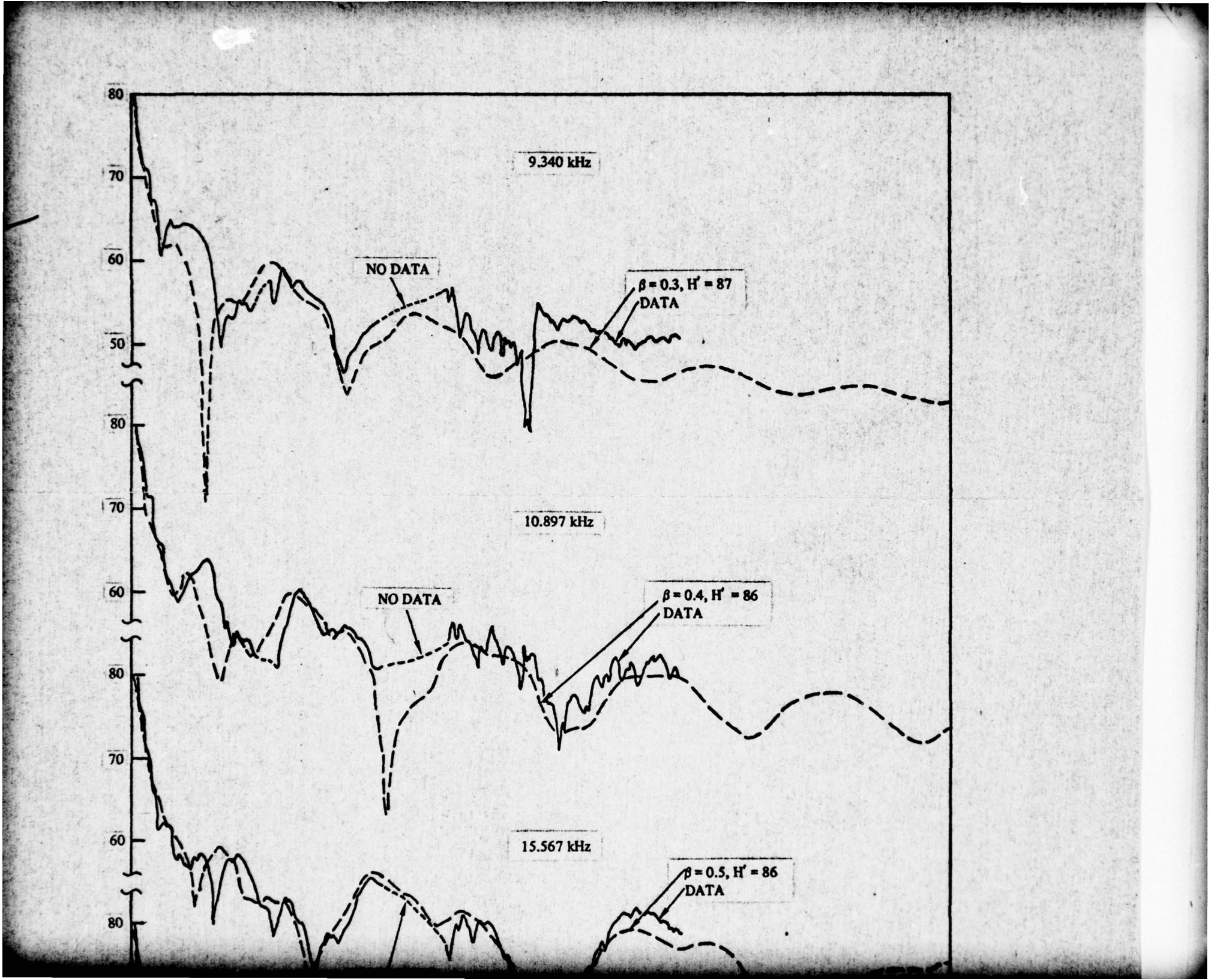
80
70
60
50
80
9.340 kHz
NO DATA
β = 0.3, H' = 87
DATA
70
10.897 kHz
60
NO DATA
β = 0.4, H' = 86
DATA
80
70
60
15.567 kHz
β = 0.5, H' = 86
DATA
80

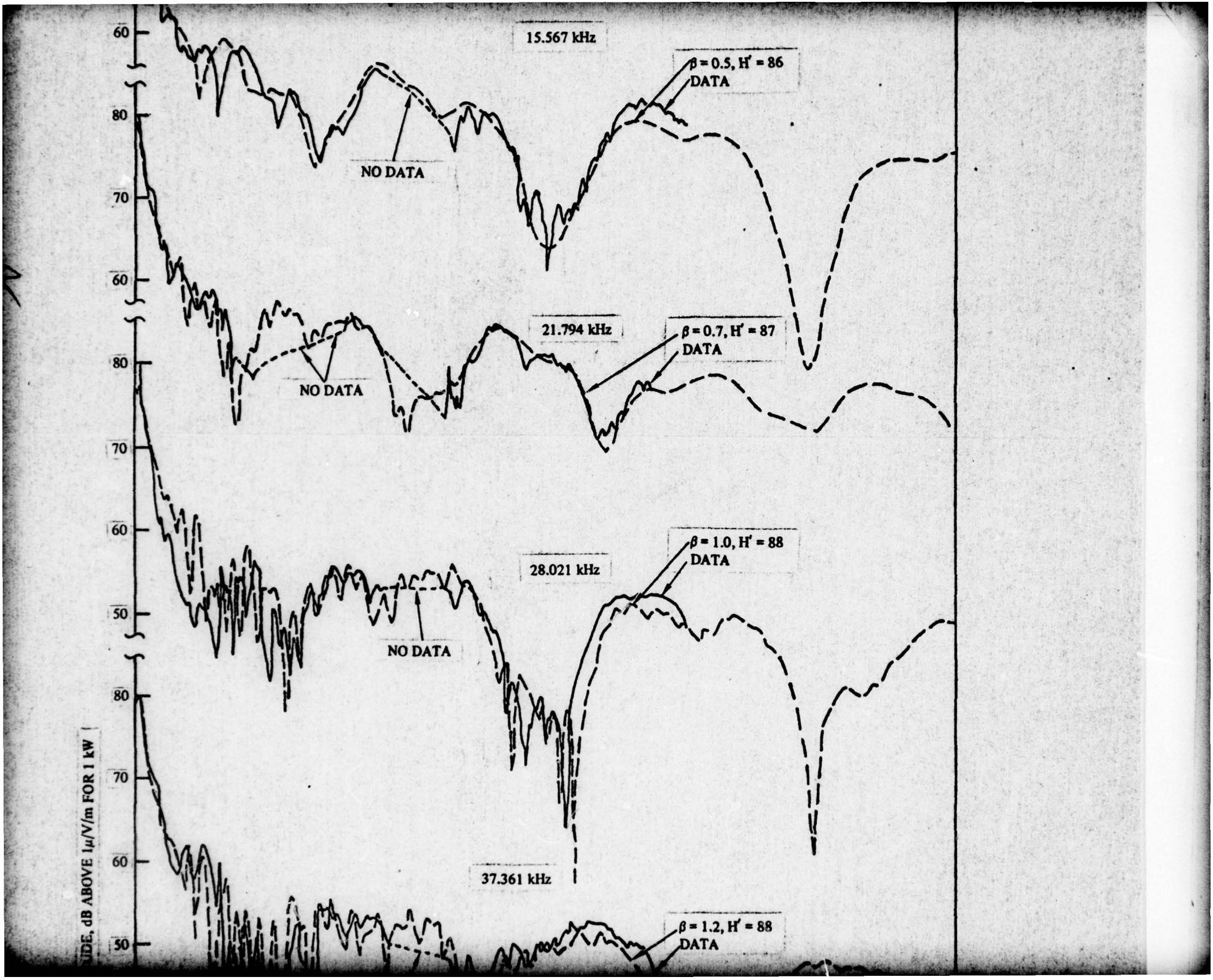
15.567 kHz
β = 0.5, H' = 86
DATA
NO DATA
21.794 kHz
β = 0.7, H' = 87
DATA
NO DATA
28.021 kHz
β = 1.0, H' = 88
DATA
NO DATA
37.361 kHz
β = 1.2, H' = 88
DATA
60
80
70
60
80
70
60
50
80
70
60
50
UDE, dB ABOVE 1μV/m FOR 1 kW

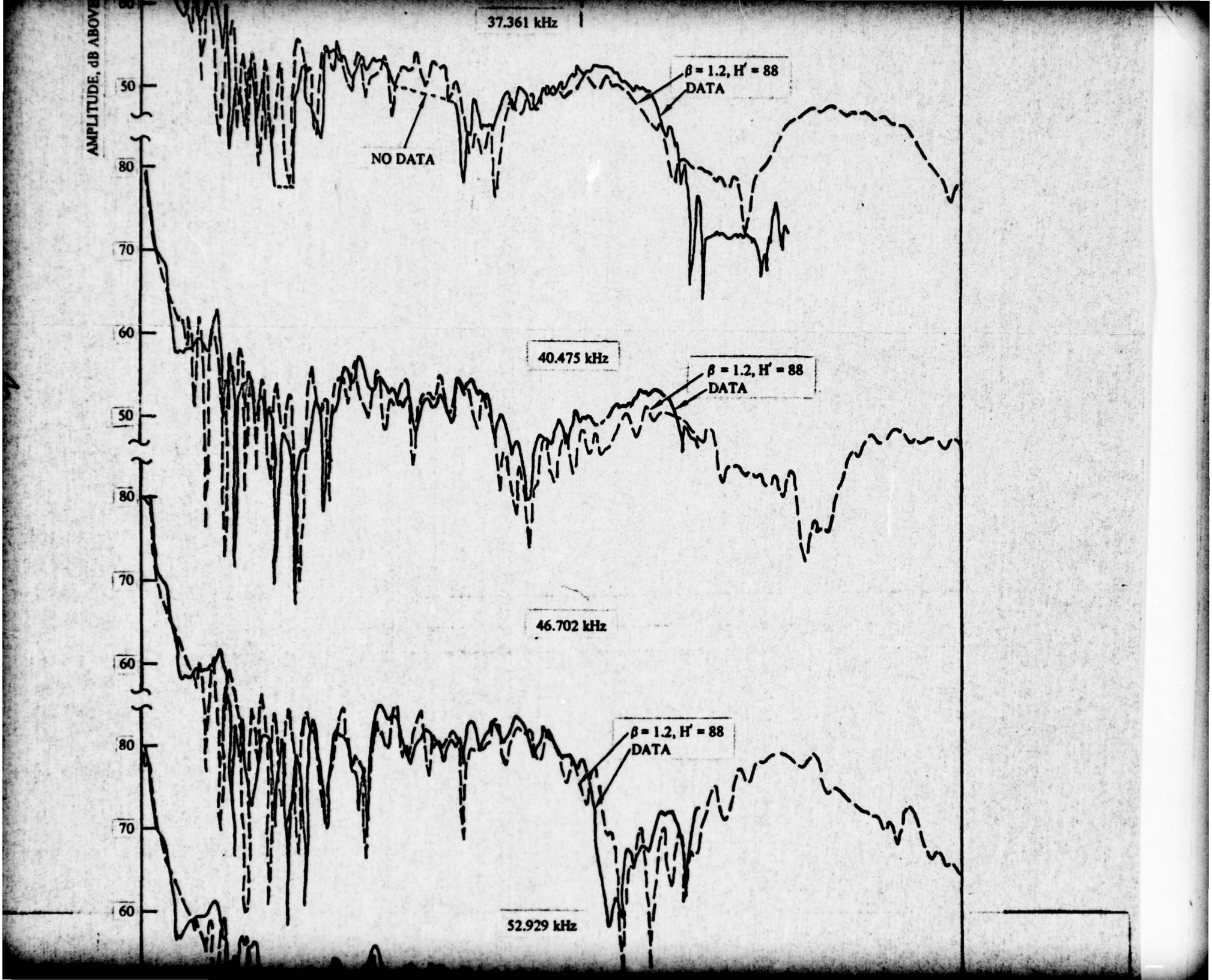
AMPLITUDE, dB ABOVE
37.361 kHz
NO DATA
β = 1.2, H' = 88
DATA
40.475 kHz
β = 1.2, H' = 88
DATA
46.702 kHz
β = 1.2, H' = 88
DATA
52.929 kHz
50
80
70
60
50
80
70
60
80
70
60

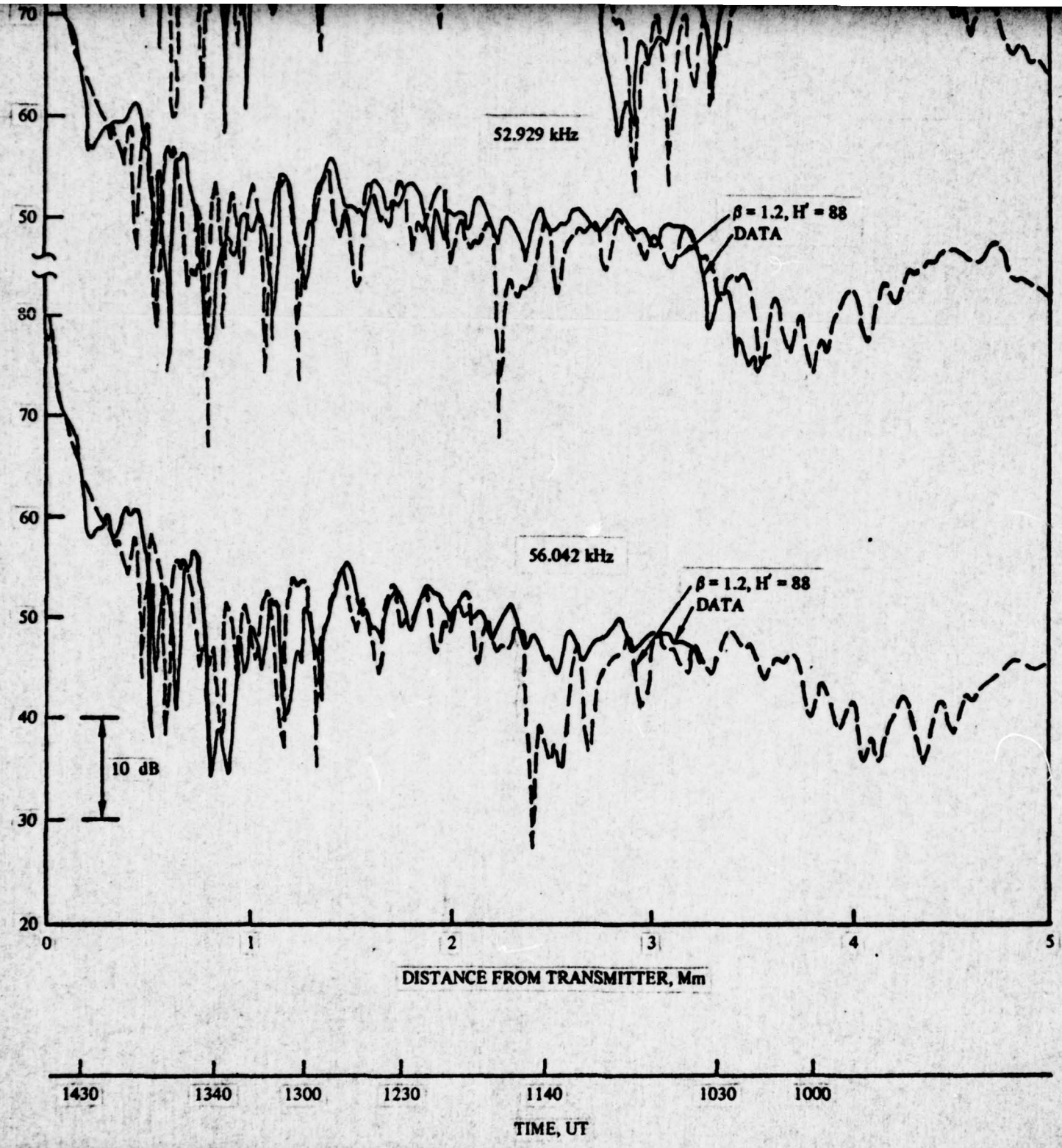

Figure 23. Measured and computed nighttime signal levels on the Hawaii to Sentinel path. Hawaii transmitter, 30 January 1974.

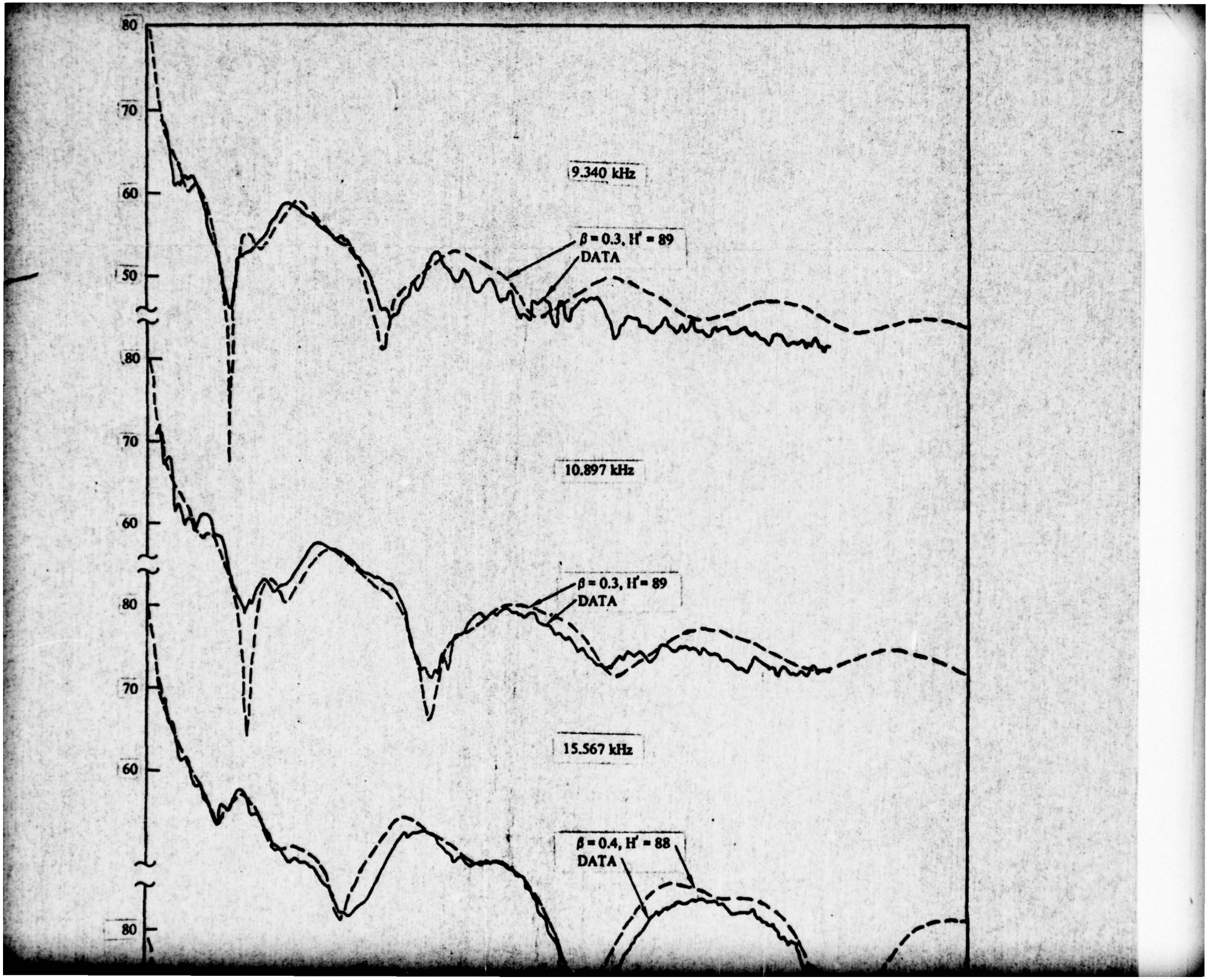
80
70
60
50
80
70
60
9.340 kHz
β = 0.3, H' = 89
DATA
10.897 kHz
β = 0.3, H' = 89
DATA
80
70
60
15.567 kHz
β = 0.4, H' = 88
DATA
80

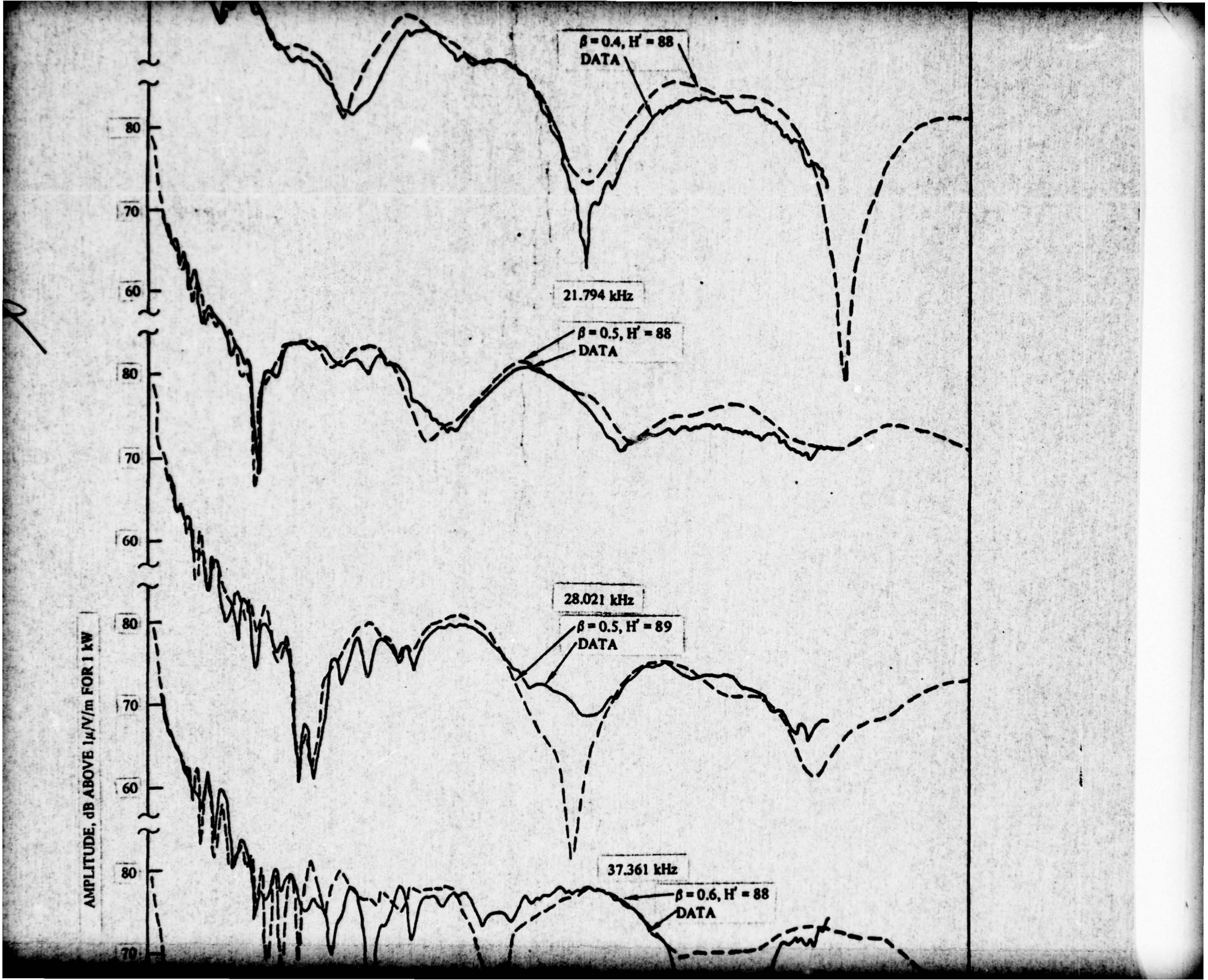
β = 0.4, H' = 88
DATA
21.794 kHz
β = 0.5, H' = 88
DATA
28.021 kHz
β = 0.5, H' = 89
DATA
37.361 kHz
β = 0.6, H' = 88
DATA
AMPLITUDE, dB ABOVE 1μV/m FOR 1 kW
80
70
60
80
70
60
80
70
60
80
70

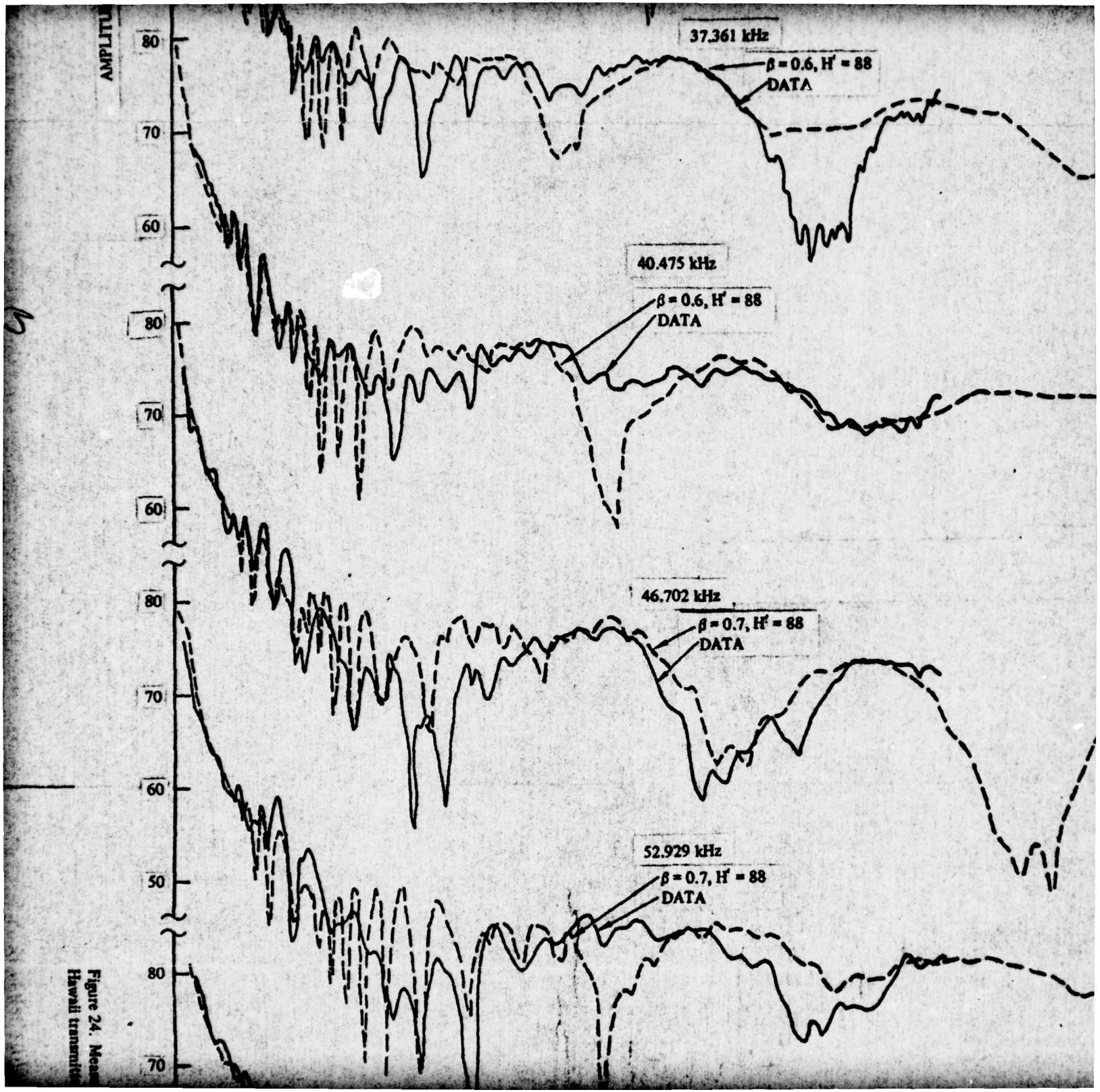

Figure 24. Mea
Hawaii transmitt

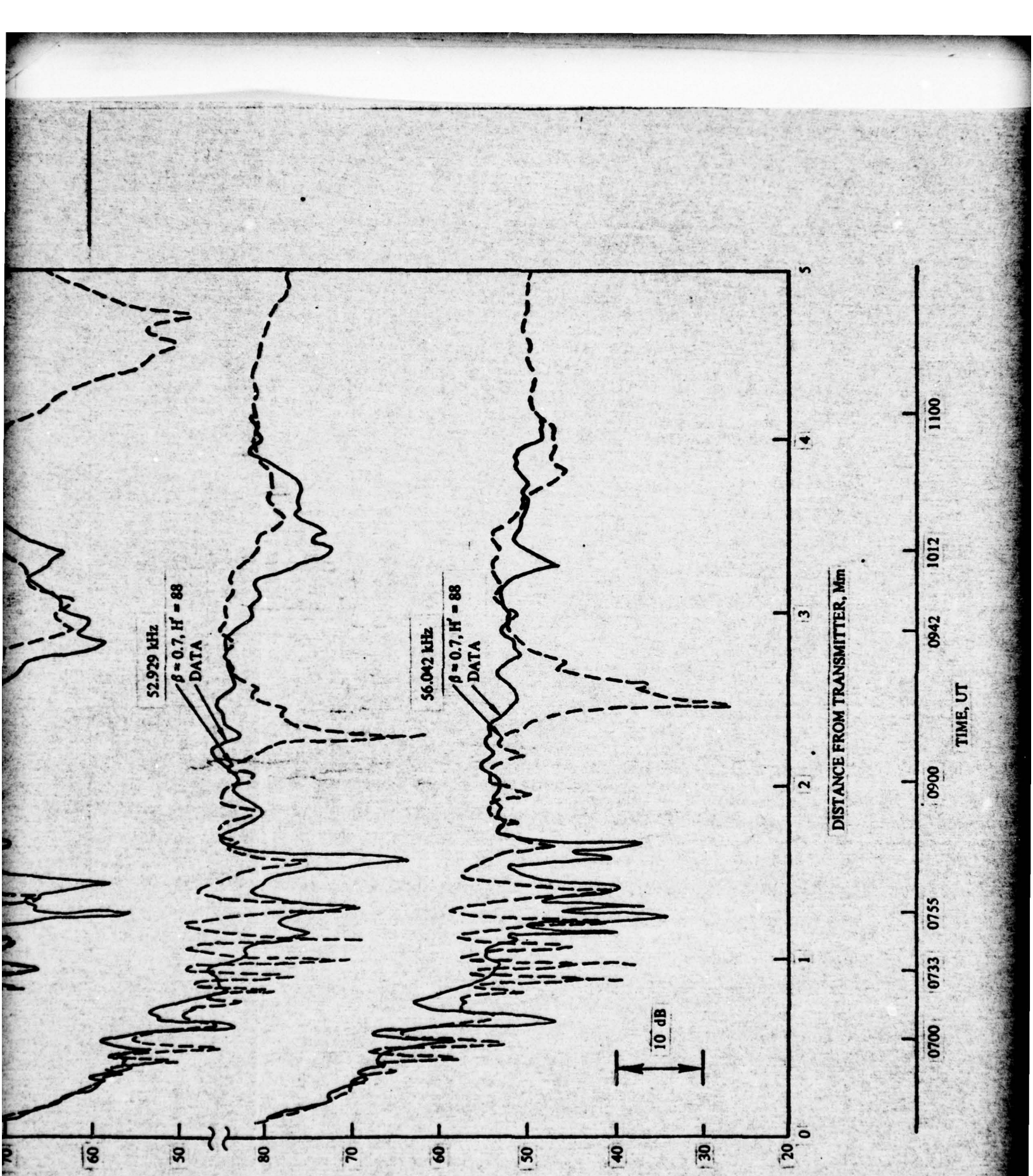

Figure 24. Measured and computed nighttime signal levels on the Hawaii to Sentinel, Arizona, path. Hawaii transmitter, 1 February 1974.

Of interest is the observation that the best-fit exponential profile varies with propagation frequency. As the frequency is increased, the value of the conductivity gradient β is found to increase. The reference height parameter H′, however, is found to remain somewhat constant at the higher frequencies.

The electron density profiles determined to fit both the 7 February 1969 data (fig 22) and the 1974 data from 1 February (fig 24) appear to follow a similar relationship between propagation frequency and the profile gradient parameter β. In the case of the aircraft flight for 30 January 1974 (fig 23), the recorded data tend to require a larger value of β in order to produce an acceptable fit to the field strength levels. The explanation as to the reason for the differences in best-fit electron density profile between the 30 Jan and the 1 Feb data is not completely understood. The results suggest that the effective ionosphere was actualiy different for each of the two nights.

DAYTIME AND NIGHTTIME DATA RECORDED AT FIXED SITES

Propagation measurements made at fixed sites have been reported by several investigators. These measurements almost always have been for one propagation frequency over a given path for a specific time interval. This type of data has not proven useful as far as determining any uniqueness in the form of the electron density profile of the ionosphere through which the radio waves must pass. Estimates, however, of the time and seasonal variability and diurnal changes for a given frequency of propagation over the given path may be obtained. Utilization of this type of data is discussed in reference 22.

Data recorded using the NOSC multifrequency sounder give signal levels at many frequencies simultaneously. With this type of data acquisition, much more data are available at the termination of the single propagation path. Using these additional data values, a more unique form of the electron density of the ionosphere may be obtained (see ref 23).

The NOSC sounder was operated over the path from Hawaii to Southern California during the fall of 1968. The sites chosen to record the propagated data were on the great circle path from the transmitter located on the large island of Hawaii to Vandenburg AFB, California (3281 km) and Johnson Valley, California (4166 km).

The propagated frequencies used for the multifrequency measurements are shown in table 11.

---

22. Naval Electronics Laboratory Technical Memorandum TM-909, Amplitude and Phase of NPM Recorded at San Diego from 9 May to 11 July on Five Very Low Frequencies, by JE Bickel, 10 February 1966
23. Naval Electronics Laboratory Center Technical Report, TR 1854, Computer Techniques for Fitting Electron Density Profiles to Oblique-Path VLF Propagation Data, by DG Morfitt, 16 January 1973

TABLE 11. VLF OBLIQUE INCIDENCE SOUNDER FREQUENCIES.

FREQUENCY, kHz	FREQUENCY kHz
9.340	21.794
10.897	24.908
14.010	26.464
15.567	28.020
17.124	31.134

The sounder data are identified in table 12.

TABLE 12. EXPERIMENTAL SOUNDER DATA FOR FALL, 1968, HAWAII TO SOUTHERN CALIFORNIA PATH.

		Daytime Data			Nighttime Data		
Date	Julian Day	Start (UT)	Stop (UT)	Total Hours	Start (UT)	Stop (UT)	Total Hours
24 Sept	268	1906					
25 Sept	269		0200	7	0500	1300	8
	269	1600	1930	3½			
27 Sept	271	1906					
28 Sept	272		0200	7	0500	1300	8
	272	1600	1930	3½			
Oct 3	277	1900	2100	2			
Oct 4	278	1600	2100	5	0500	1300	8

Note:

Path is totally in sunlight:	1600-0230 UT
Path is totally dark:	0500-1300 UT
Midpath noon:	2130 UT
Midpath midnight:	0930 UT

Examples of the amplitude data recorded for 27–28 September 1968 are shown in figure 25 for the signal levels recorded at the 3821 and 4166 kilometre sites. For these data the path is in total darkness from 0500 to 1300 UT; midpath midnight occurs at 0930 UT. Note in particular the variation in signal amplitude during nighttime on 28.0 kHz at 3821 kilometres and on 15.6 kHz at 4166 kilometres. In these instances, the signal level is seen to decrease greatly and then to recover, thus implying changes throughout the night in the ionospheric profile.

Examples of nighttime signal levels computed as a function of distance for the sounder frequencies are shown in figure 26. These computations illustrate the modal interference – signal-level maxima and minima (or nulls) – which is characteristic of propagation at vlf. The data illustrated in figure 25 were recorded only at the two fixed-site receivers (3821 and 4166 km). Fields computed for these distances are highlighted in figure 26. It may be noted that the level of the 15.567 kHz signal is in the vicinity of a maximum at 3821 kilometres and passes through a strong null at 4166 kilometres. At 28.020 kHz the signal level at 3821 kilometres is located in a null while the 4166 kHz signal is much stronger. These results are also observed in the sounder data presented in figure 25.

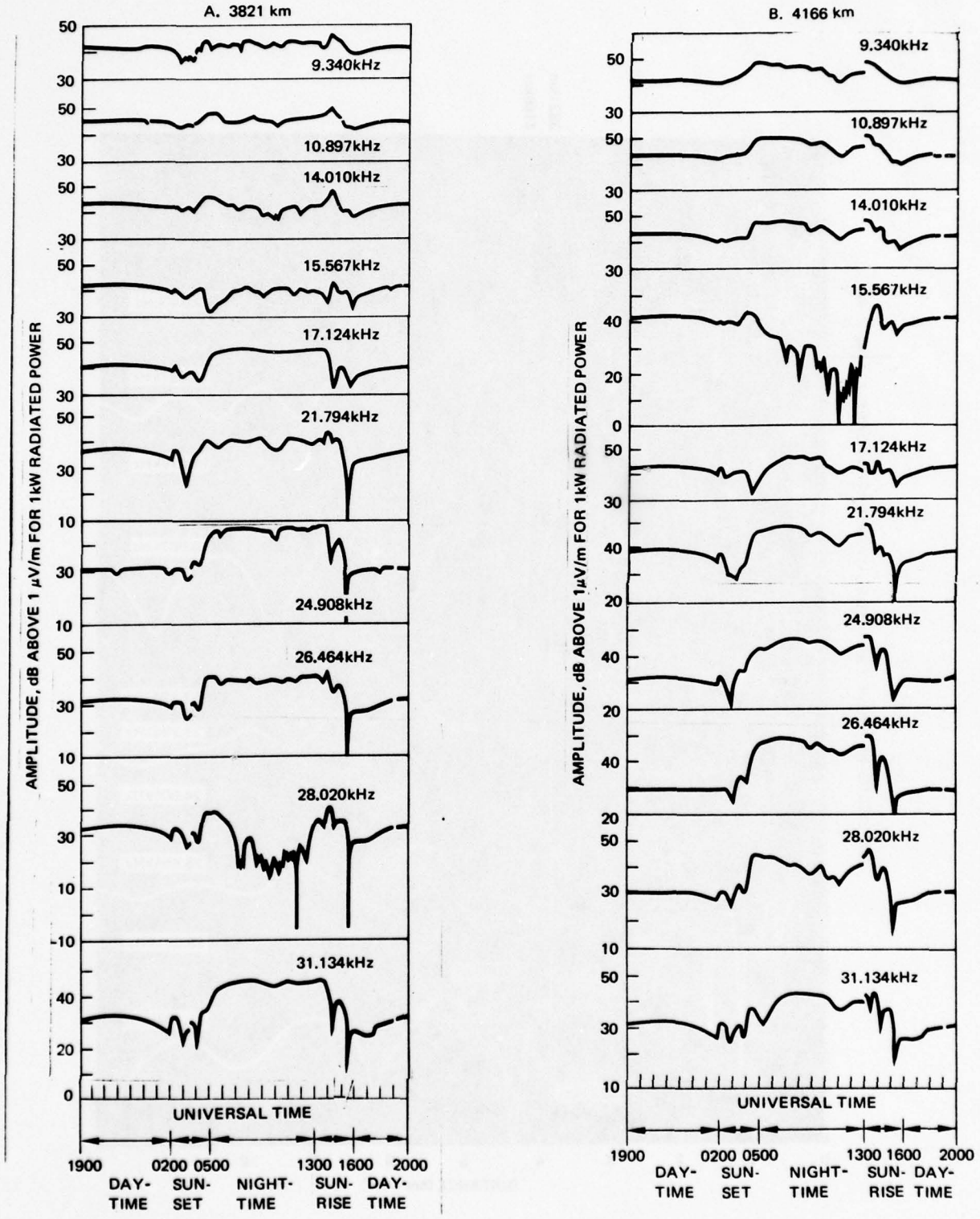

Figure 25. Recorded vlf signal levels for 27-28 September 1968, Hawaii to Southern California.

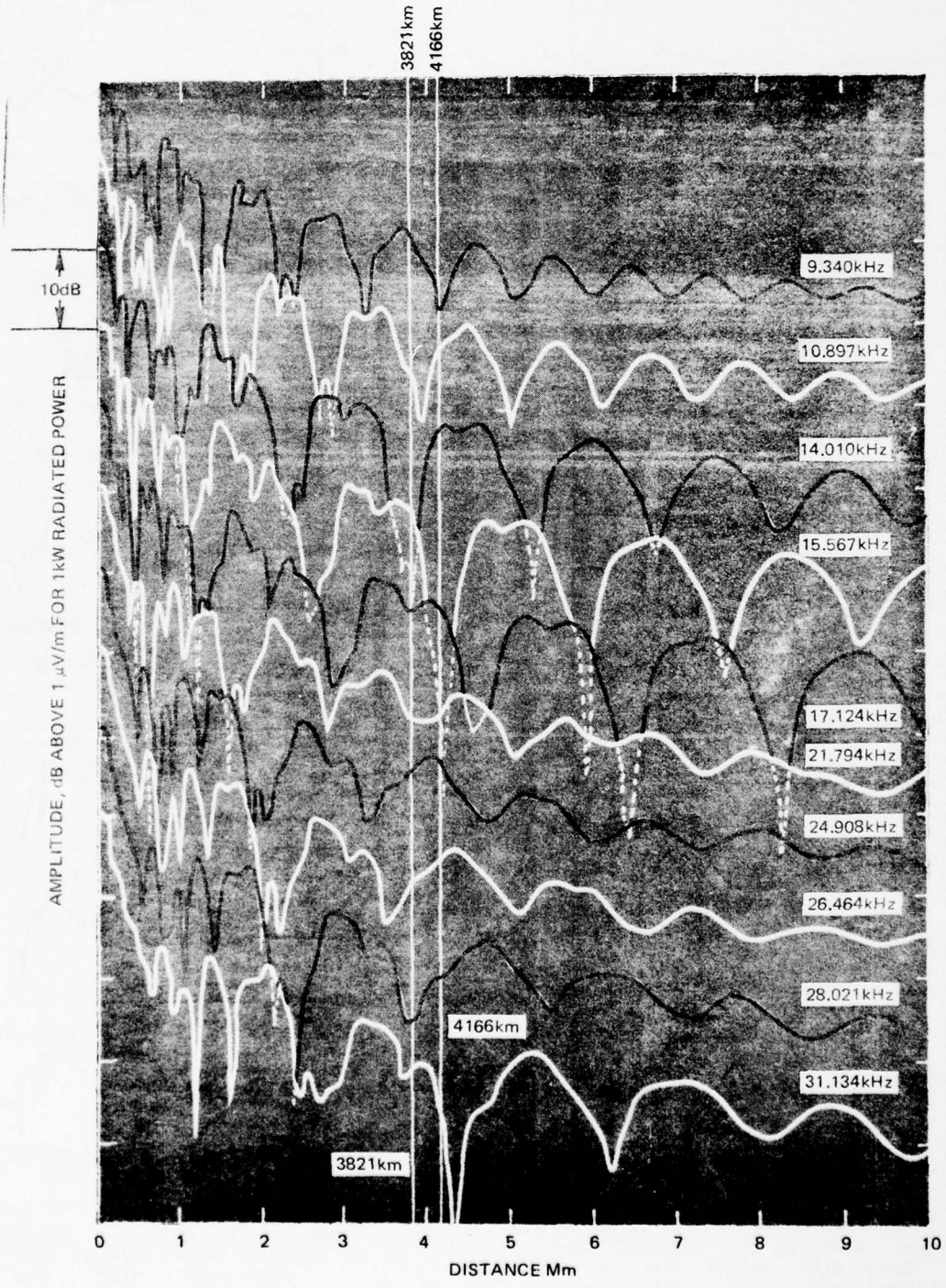

Figure 26. Computed nighttime amplitude for propagation from Hawaii to Southern California.

Figures 27 through 29 are examples of the sounder data listed in table 12. The figures illustrate the variation of signal level possible throughout a given day (or night) over several test periods. Data are shown for Julian days 268–269, 271–272, and 277–278. In particular, figures 27a and 27b for 15.567 kHz demonstrate the variation in signal level recorded simultaneously at the 3821 and 4166 km sites. The nighttime field strength at 4166 kilometres is highly variable because of the modal interference hull in the propagated signal. By comparison, the simultaneous data recorded on 26.464 kHz at the two sites appear to be relatively stable (fig 28a and 28b). At 28.020 kHz (fig 29a and 29b) the effects of the modal interference hull are again strongly evident at the 3821 kilometre site. Between 1100 and 1130 universal time (UT), the signal level drops as much as 25 dB in a short period of time.

The variations of signal level, as shown in figures 27 through 29, are examples of how the propagated vlf signal level can change with time. The degree to which the modal interference characterizes itself at different times throughout a given night and for several nights, is brought about by changes in the ionosphere through which the radio wave propagates.

Tables 13 and 14 represent the relative statistics of the data of table 12. The values in these tables give the signal level in dB above 1 μv/m for 1 kW radiated power. The analysis of the data is broken down into receiver site (Vandenburg AFB, 3821 km or Johnson Valley, California, 4166 km), daytime or night propagation and propagation frequency. Also presented are the dB signal levels exceeded 99%, 90%, and 50% of the time, mean signal level, and the associated standard deviation.

As would be expected from figures 27b and 29a, large standard deviations occur at night at 15.567 kHz for the 4166 kilometre range and at 28.020 kHz for the 3821 kilometre range. The presence of the strong modal interference nulls at the particular receiver site for the above frequencies results in these large values of standard deviation.

Comparison of the NOSC field strength predictions with the sounder data of tables 13 and 14 are shown in figures 30 and 31 for daytime propagation and in figures 32 and 33 for nighttime propagation. In addition, data and predictions for 9 frequencies in the lf range (30–60 kHz) which were recorded for one 30-hour test on 18–19 April 1968 are presented in figure 34 for daytime and in figure 35 for nighttime. This lf data is presented as a mean value together with variation bars as computed from the signal levels computed throughout the daytime or nighttime periods. The profiles used for the model computations were $\beta = 0.5$ km^{-1}, $H' = 70$ km for daytime and $\beta = 0.5$ km^{-1}, $H' = 87$ km for nighttime. The method of computation assumed a horizontally homogenous waveguide. Examination of figures 30 through 35 illustrates that the above profiles for daytime and nighttime tend to simulate the measured propagation data fairly well for this west-to-east propagation path over the Pacific Ocean for frequencies below 20 kHz during daytime propagation and for frequencies below 30 kHz during nighttime propagation. For transmissions at higher frequencies the predicted signal levels are too large to simulate the daytime measurements and the predicted signal levels are too weak to simulate the nighttime levels.

These results are in general agreement with those found using daytime aircraft data (Daytime Aircraft Data section) where it was determined that the $\beta = 0.5$ km^{-1}, $H' = 70$ km profile produced fields are too strong to fit the daytime data above 17 kHz and that a profile such as $\beta = 0.3$ km^{-1}, $H' = 74$ km more accurately describes the data. The section, Nighttime Aircraft Data, illustrates that the fields computed using the $\beta = 0.5$ km^{-1}, $H' = 87$ km profile were too weak to fit the measurements above 30 kHz and that the profiles are needed where the gradient parameter "β" is increased as a function of frequency.

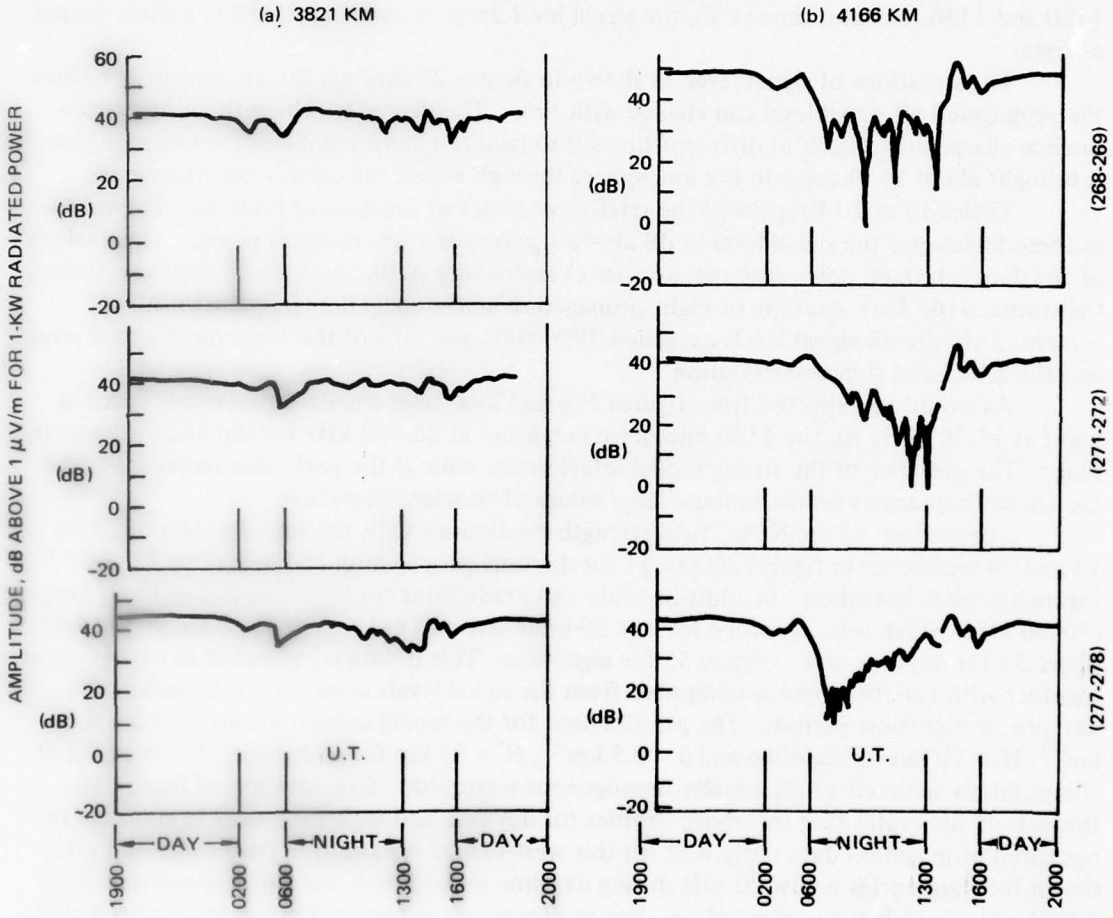

Figure 27. Received signal levels, Hawaii to Southern California (15.567 kHz).

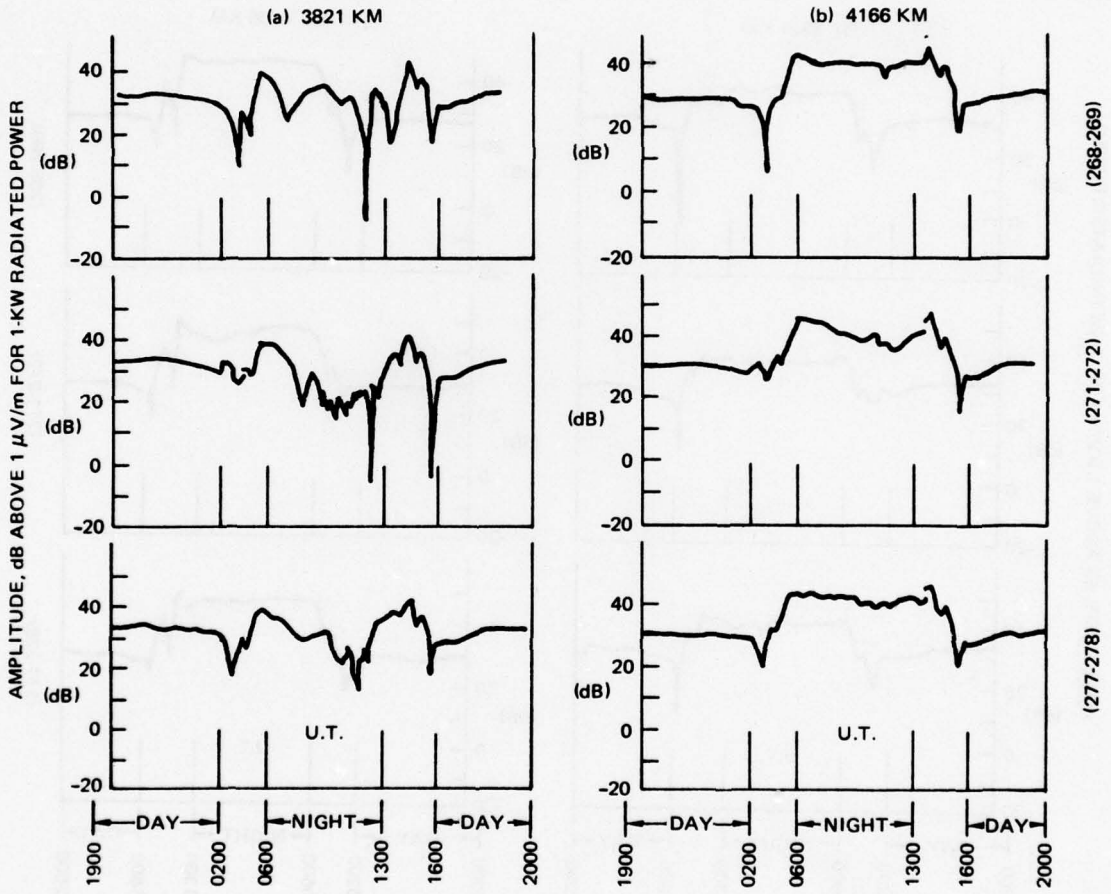

Figure 28. Received signal levels, Hawaii to Southern California (26.464 kHz).

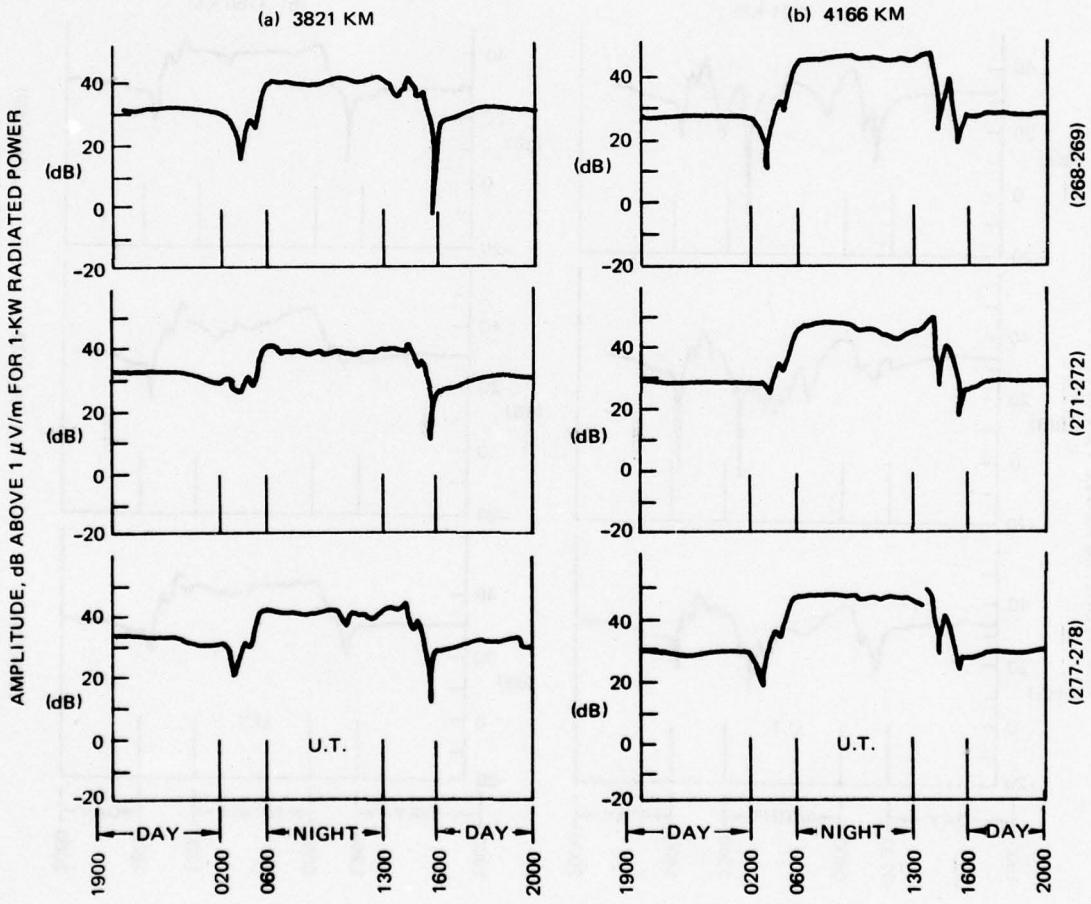

Figure 29. Received signal levels, Hawaii to Southern California (28.020 kHz).

TABLE 13. TIME VARIABILITY FOR SEPTEMBER–OCTOBER 1968 AT 3821 KM.

Frequency kHz	Level (dB) Exceeded for Percent of Time			Mean Signal Level (dB)	Standard Deviation (dB)
	99	90	50		
Daytime					
9.340	37	40	41	42	1.2
10.897	40	42	46	46	1.9
14.010	39	40	44	44	1.8
15.567	37	39	41	42	1.4
17.124	38	39	41	42	1.3
21.794	32	33	36	36	1.5
24.908	28	29	30	31	1.0
26.464	26	28	30	31	1.2
28.020	27	29	31	32	1.5
31.134	24	26	30	31	2.2
Nighttime					
9.340	38	41	43	44	1.4
10.897	39	41	46	46	2.8
14.010	32	35	42	43	4.1
15.567	31	35	38	39	2.5
17.124	44	46	47	48	1.1
21.794	37	37	39	40	1.4
24.908	41	43	45	46	1.3
26.464	35	37	38	39	1.3
28.020	14	20	30	30	6.4
31.134	36	41	44	45	1.9

TABLE 14. TIME VARIABILITY FOR SEPTEMBER–OCTOBER 1968 AT 4166 KM.

Frequency kHz	Level (dB) Exceeded For Percent of Time			Mean Signal Level (dB)	Standard Deviation (dB)
	99	90	50		
Daytime					
9.340	38	40	41	43	1.5
10.897	36	38	39	42	3.5
14.010	38	40	42	43	1.7
15.567	38	39	41	43	3.0
17.124	38	40	42	43	1.9
21.794	34	36	38	39	1.7
24.908	29	30	31	32	1.6
26.464	26	27	28	29	1.3
28.020	26	27	29	30	1.1
31.134	23	26	30	30	2.4
Nighttime					
9.340	37	41	45	46	2.6
10.897	37	40	45	47	4.4
14.010	40	43	46	47	2.2
15.567	10	19	31	30	7.0
17.124	32	37	42	43	4.3
21.794	41	44	46	47	1.7
24.908	40	42	44	45	1.7
26.464	41	44	46	46	1.4
28.020	34	38	41	42	2.4
31.134	27	34	39	40	3.4

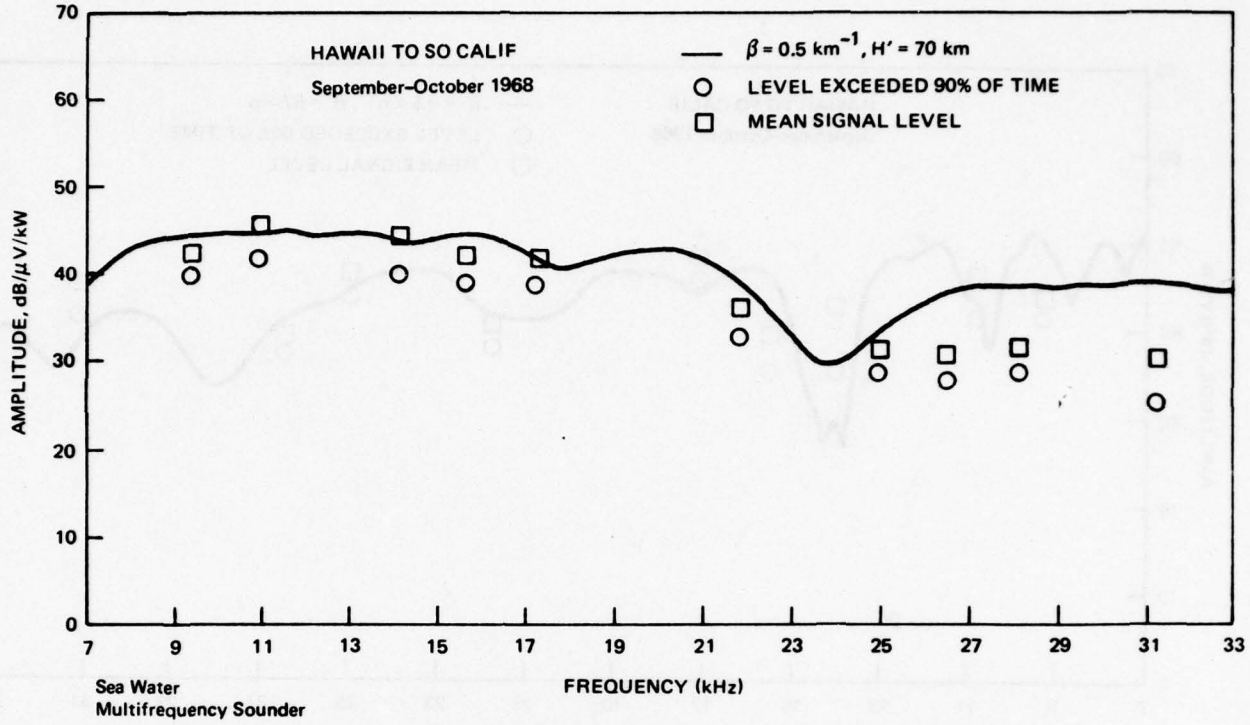

Figure 30. Propagation over the Pacific Ocean to a fixed receiver site at 3821 km (daytime, fall) (vlf).

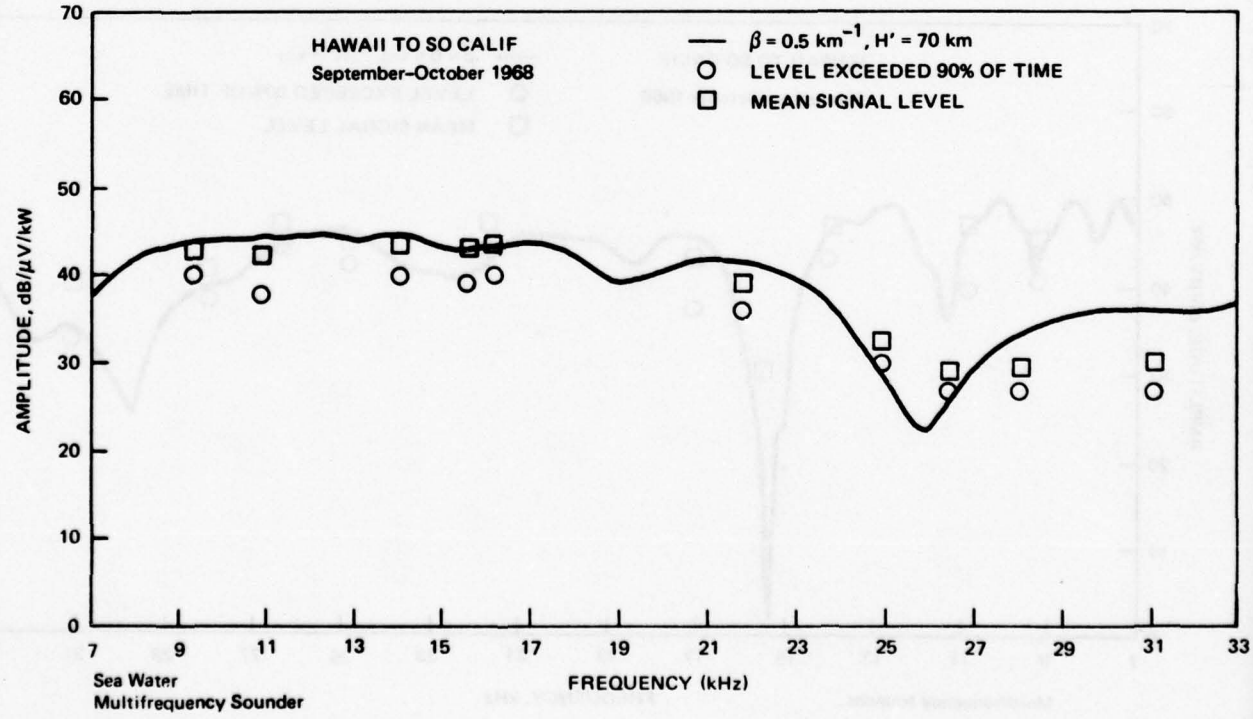

Figure 31. Propagation over the Pacific Ocean to a fixed receiver site at 4166 km (daytime, fall) (vlf).

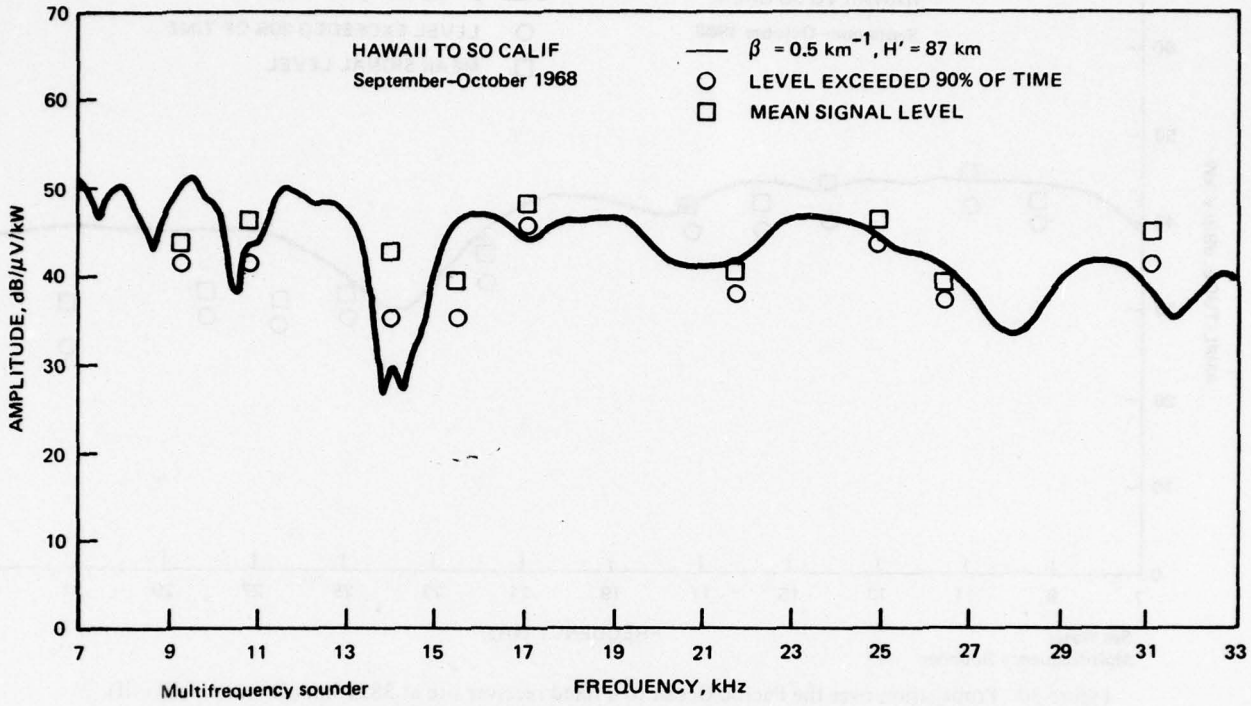

Figure 32. Propagation over the Pacific Ocean to a fixed receiver site at 3821 km (nighttime, fall) (vlf).

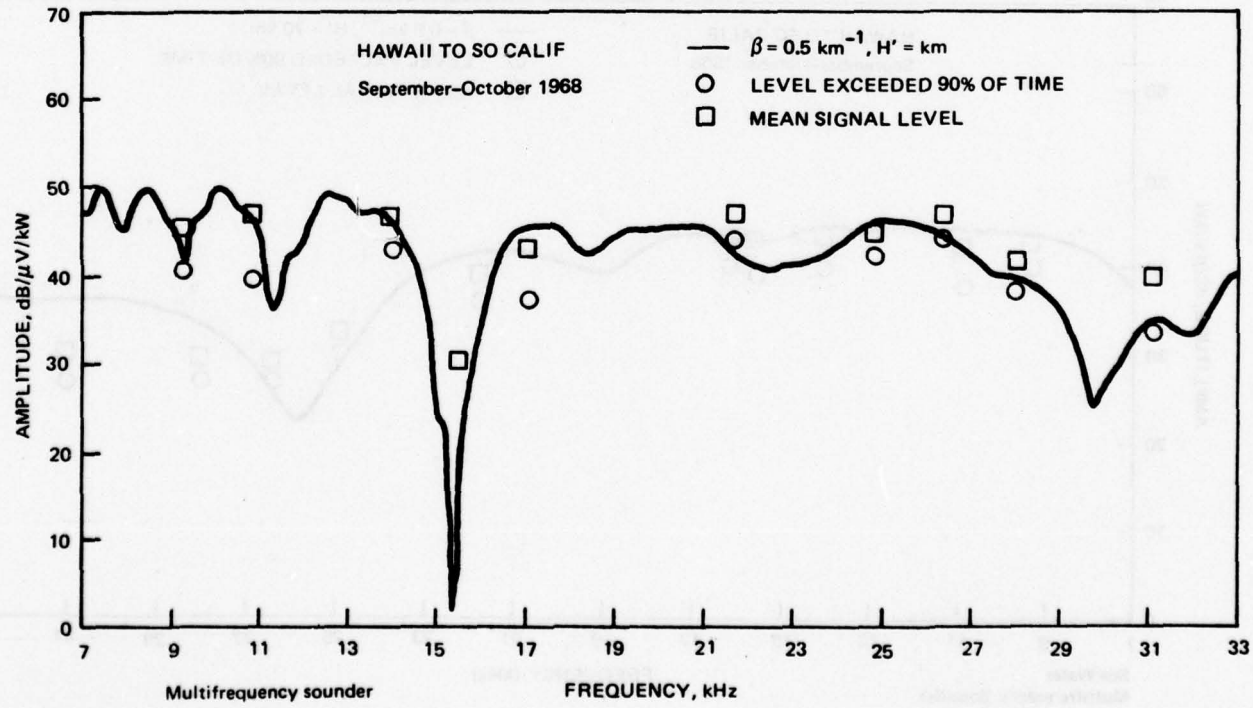

Figure 33. Propagation over the Pacific Ocean to a fixed receiver site at 4166 km (nighttime, fall) (vlf).

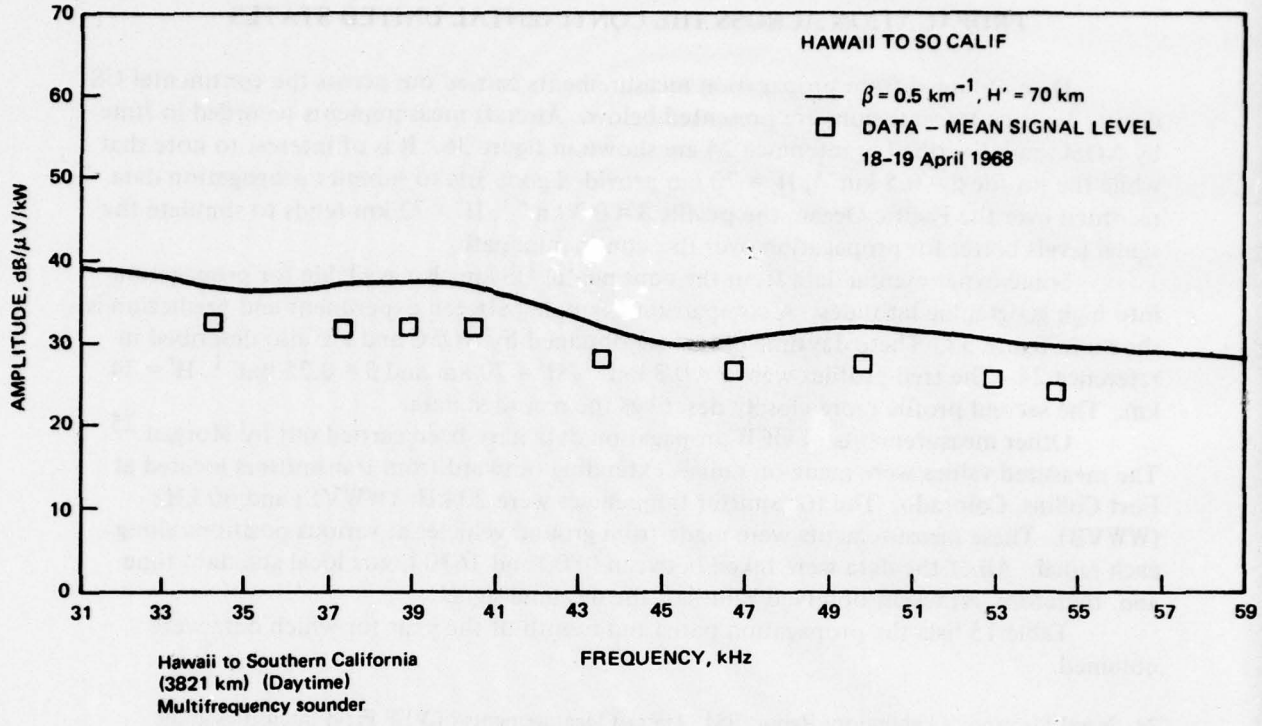

Figure 34. Propagation over the Pacific Ocean to a fixed receiver site at 3821 km (daytime, spring) (lf).

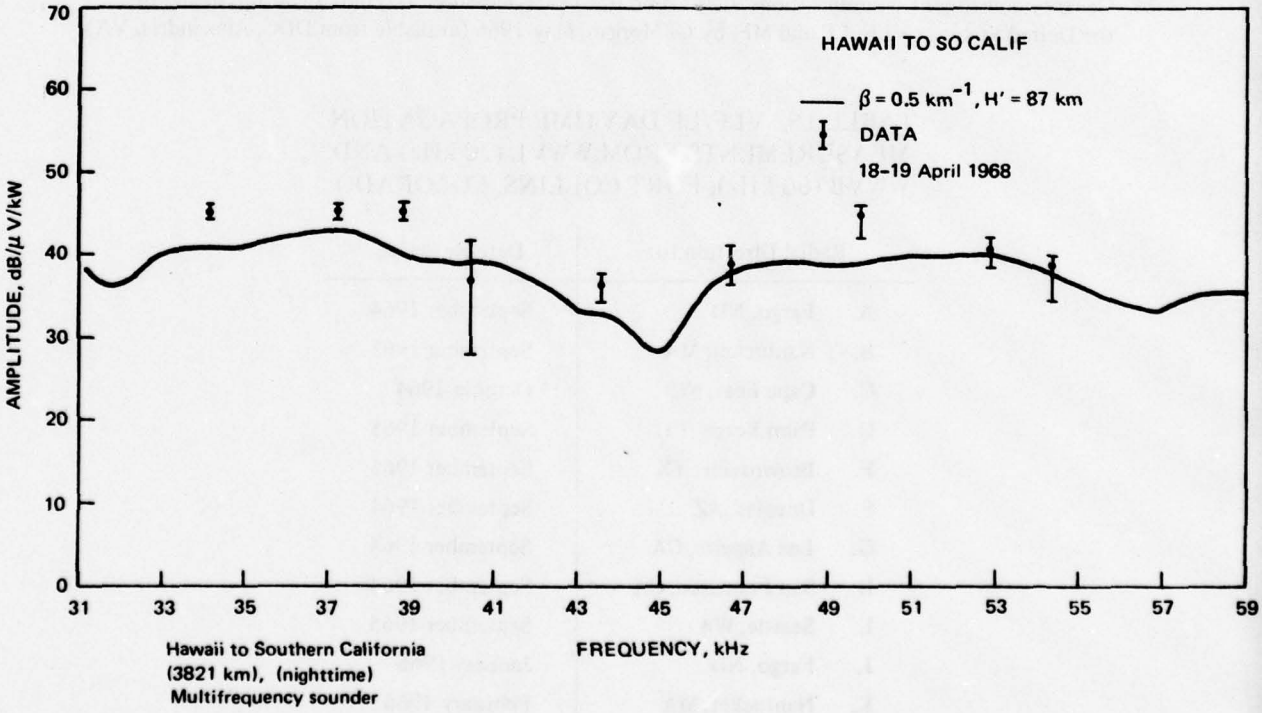

Figure 35. Propagation over the Pacific Ocean to a fixed receiver site at 3821 km (nighttime, spring) (lf).

PROPAGATION ACROSS THE CONTINENTAL UNITED STATES

Data obtained from propagation measurements carried out across the continental US during daytime transmissions are presented below. Aircraft measurements recorded in June by NOSC and described in reference 24 are shown in figure 36. It is of interest to note that while the profile $\beta = 0.5$ km^{-1}, $H' = 70$ km provided good fits to summer propagation data recorded over the Pacific Ocean, the profile $\beta = 0.3$ km^{-1}, $H' = 72$ km tends to simulate the signal levels better for propagation over this continental path.

Some experimental data from the continental US are also available for propagation into high geographic latitudes. A comparison example between experiment and prediction is shown in figure 37. These daytime data were obtained by NOSC and are also described in reference 24. The trial profiles were $\beta = 0.3$ km^{-1}, $H' = 70$ km and $\beta = 0.25$ km^{-1}, $H' = 74$ km. The second profile more closely describes the recorded data.

Other measurements of vlf/lf propagation data have been carried out by Morgan.[25] The measured values were made on radials extending outward from transmitters located at Fort Collins, Colorado. The transmitter frequencies were 20 kHz (WWVL) and 60 kHz (WWVB). These measurements were made from ground vehicles at various positions along each radial. All of the data were taken between 0800 and 1630 hours local standard time and, therefore, represent observed values of the daytime signal.

Table 15 lists the propagation paths and month of the year for which data were obtained.

24. Naval Electronics Laboratory Report 981, Aircraft Measurements of VLF Field Intensities in the Northern Hemisphere, by JE Bickel, 5 August 1960
25. Gautney and Jones Communications, Inc, TR-66.0141 002, Measured Daytime Field Intensities in the United States at VLF, LF and MF, by GI Morga. , May 1966 (available from DDC, Alexandria, VA)

TABLE 15. VLF/LF DAYTIME PROPAGATION MEASUREMENTS FROM WWVL (20 kHz) AND WWVB (60 kHz), FORT COLLINS, COLORADO

Radial Direction to:		Date Recorded
A.	Fargo, ND	September 1964
B.	Nantucket, MA	September 1965
C.	Cape Fear, NC	October 1964
D.	Palm Beach, FL	September 1965
E.	Brownsville, TX	September 1965
F.	Douglas, AZ	September 1964
G.	Los Angeles, CA	September 1964
H.	San Francisco, CA	September 1964
I.	Seattle, WA	September 1965
J.	Fargo, ND	January 1966
K.	Nantucket, MA	February 1966
L.	Brownsville, TX	January 1966

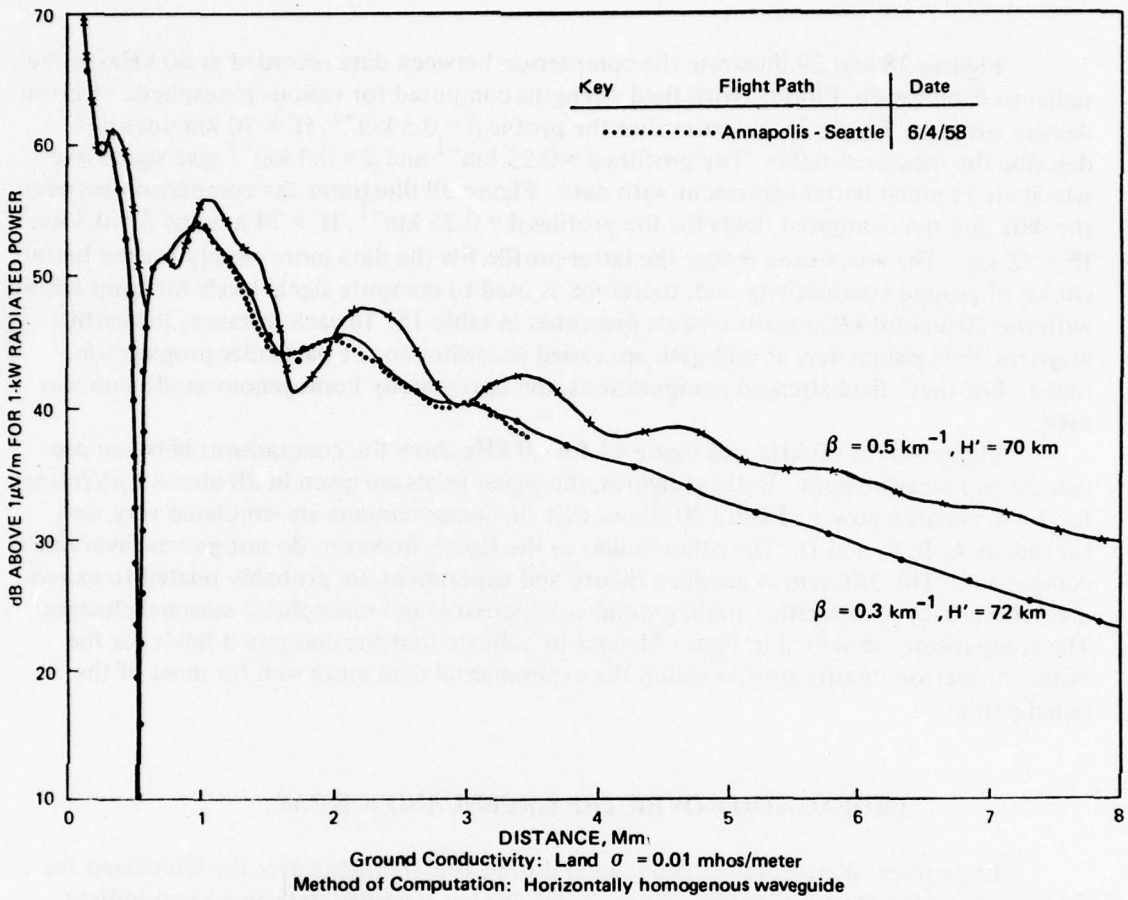

Figure 36. Daytime propagation across the continental United States (NPG/NLK 18.6 kHz).

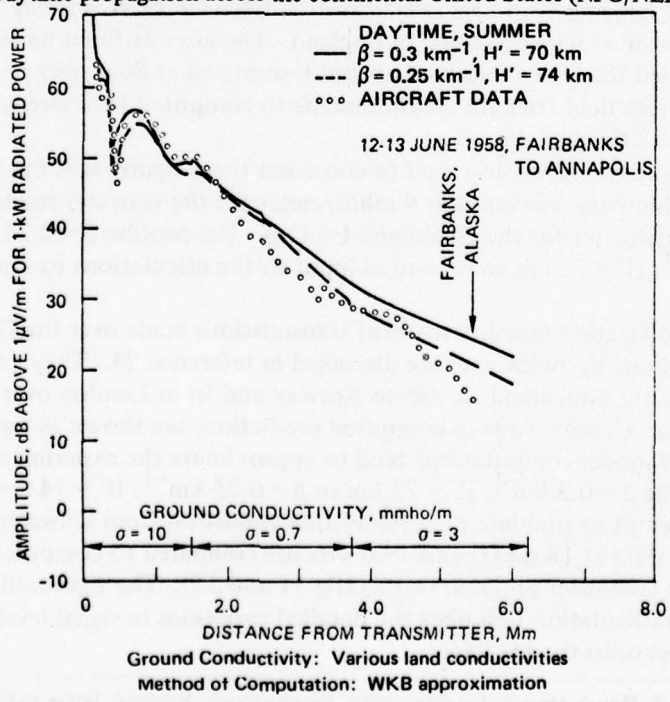

Figure 37. Daytime propagation across the continental United States to high latitudes (NSS 15.5 kHz).

Figures 38 and 39 illustrate the comparison between data recorded at 60 kHz on the radial to Palm Beach, Florida, with field strengths computed for various ionospheric electron density profiles. Figure 38 indicates that the profile $\beta = 0.5$ km^{-1}, $H' = 70$ km does not describe the measured fields. The profiles $\beta = 0.25$ km^{-1} and $\beta = 0.3$ km^{-1} give signal levels which are in much better agreement with data. Figure 39 illustrates the comparison between the data and the computed fields for the profiles $\beta = 0.25$ km^{-1}, $H' = 74$ km and $\beta = 0.3$ km^{-1}, $H' = 72$ km. The conclusion is that the latter profile fits the data more closely for the better choice of ground conductivity and, therefore, is used to compute signal levels for comparison with the 20 and 60 kHz measurements presented in table 15. In each instance, the earth's magnetic field parameters at mid path are varied according to the particular propagation radial. For these field strength computations, the horizontally homogenous mode sum was used.

Figure 40 for 60 kHz and figure 41 for 20 kHz show the comparisons between prediction and measurement. In these figures, the signal levels are given in dB above 1 μV/meter for 1 kW radiated power. Figure 40 shows that the measurements are simulated very well for radials A, B, C, and D. The other radials in the figure, however, do not give as favorable a comparison. The differences between theory and experiment are probably related to experimental accuracy, propagation path, ground conductivity, and ionospheric seasonal changes. The comparisons presented in figure 41 tend to indicate that the computed fields for the assumed electron density profile match the experimental data quite well for most of the radial paths.

PROPAGATION OVER THE GREENLAND ICE CAP

Experimental measurements obtained during aircraft flights over the Greenland Ice Cap are presented for examination. Burgess (ref 26) has recorded data aboard an inflight aircraft at 10.2, 11.3, and 13.6 kHz as transmitted from OMEGA Norway and at 45 and 60 kHz from transmissions originating in England. The aircraft flight paths for recording these data traversed the Greenland Ice Cap and terminated at Sondrestrom, Greenland. Comparison of these field strength measurements to computed field strength predictions is shown in figures 42 through 48.

The method of calculation used to construct these figures was the WKB mode sum. The ground conductivity was input as 4 mhos/meter for the seawater section of the paths and 1×10^{-5} mhos/meter for the Greenland Ice Cap. The profiles $\beta = 0.25$ km^{-1}, $H' = 74$ km and $\beta = 0.3$ km^{-1}, $H' = 72$ km were used as input to the calculations to simulate the measured data.

Other propagation measurements of transmissions made over the Greenland Ice Cap have been carried out by NOSC and are discussed in reference 24. They consist of flights from Seattle over the Greenland ice cap to Norway and from London over the ice cap to Fairbanks, Alaska. Comparisons to computed predictions are shown in figures 49 and 50. In general, the WKB model computations tend to approximate the experimental data quite well using either profile $\beta = 0.3$ km^{-1}, $H' = 72$ km or $\beta = 0.25$ km^{-1}, $H' = 74$ km.

In an attempt to simulate the propagation transition from seawater to Greenland ice, the above NOSC data at 18.6 kHz and 19.6 kHz are compared to computed fields using the mode-conversion computer program (ref 8) (fig 51 and 52). The figures illustrate that the mode-conversion calculation describes the detailed variations in signal level observed as the radio wave crosses onto the Ice Cap.

---

26. Burgess, Boyd R, Royal Aircraft Establishment, Farnborough, England, letter to CO, NELC, 1972

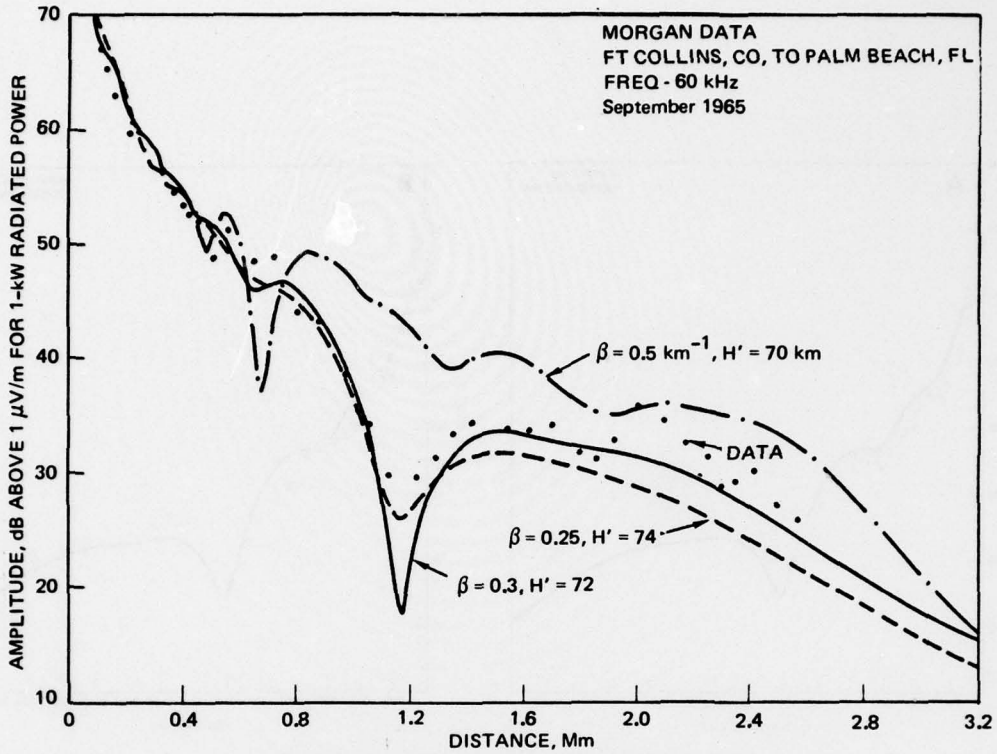

Ground Conductivity: Land, σ = 0.005 mhos/meter
Method of Computation: Horizontally homogenous waveguide

Figure 38. Daytime propagation across the continental United States (WWVB 60 kHz, 5 mmhos/m).

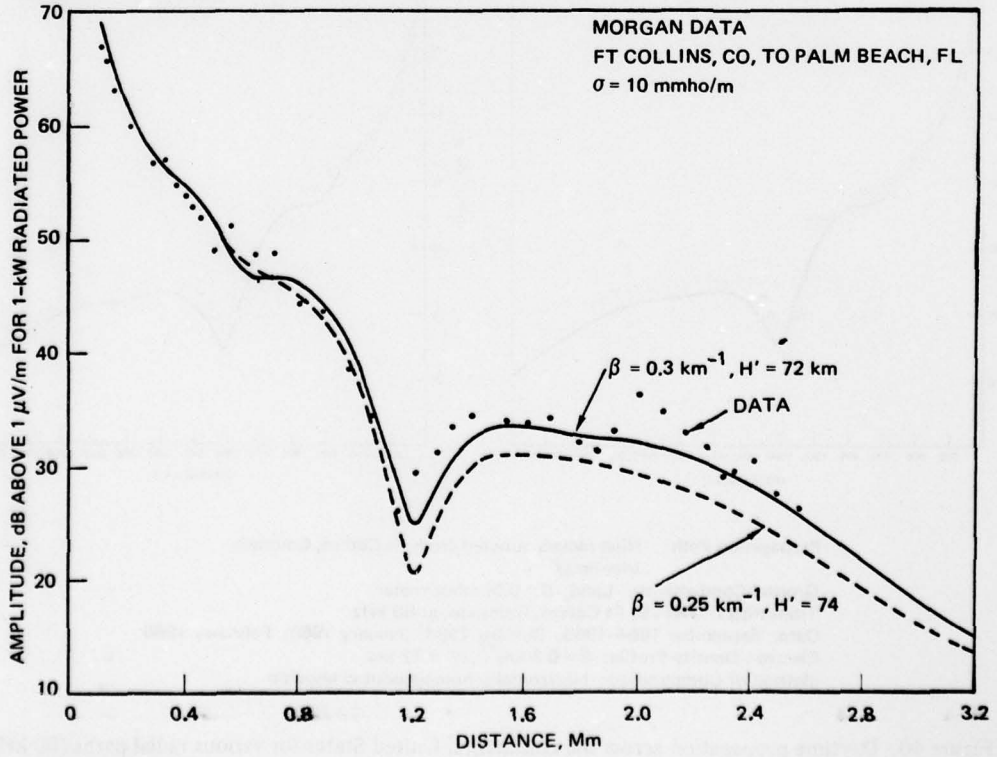

Figure 39. Daytime propagation across the continental United States (60 kHz, 10 mmhos/m).

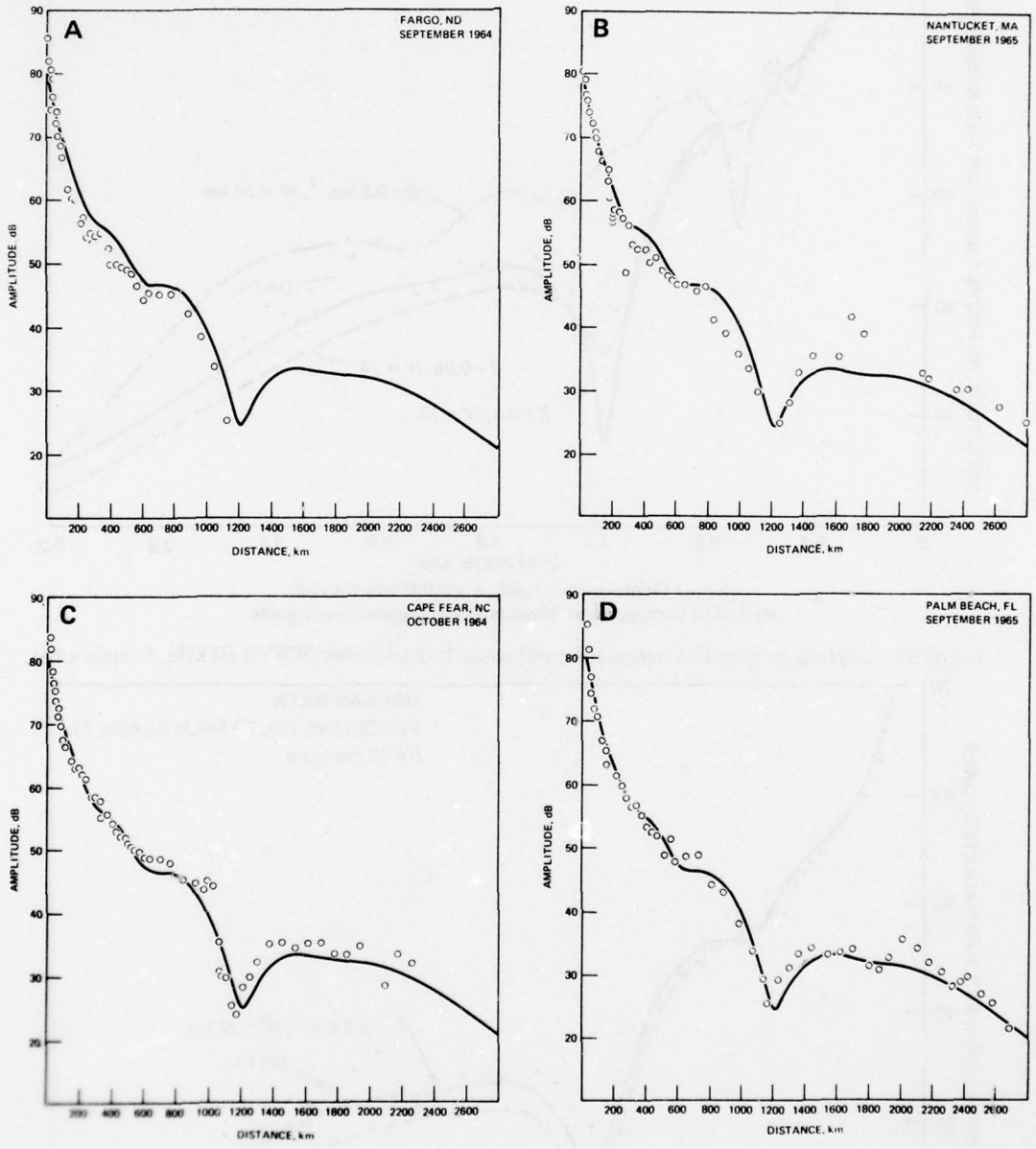

Propagation Path: Nine radials outward from Ft Collins, Colorado (daytime)
Ground Conductivity: Land, σ = 0.01 mhos/meter
Transmitter: WWVB, Ft Collins, Colorado, at 60 kHz
Date: September 1964–1965; October 1964; January 1966; February 1966
Electron Density Profile: $\beta = 0.3\ km^{-1}$, H' = 72 km
Method of Computation: Horizontally homogenous waveguide

Figure 40. Daytime propagation across the continental United States for various radial paths (60 kHz).
(Sheet 1 of 3)

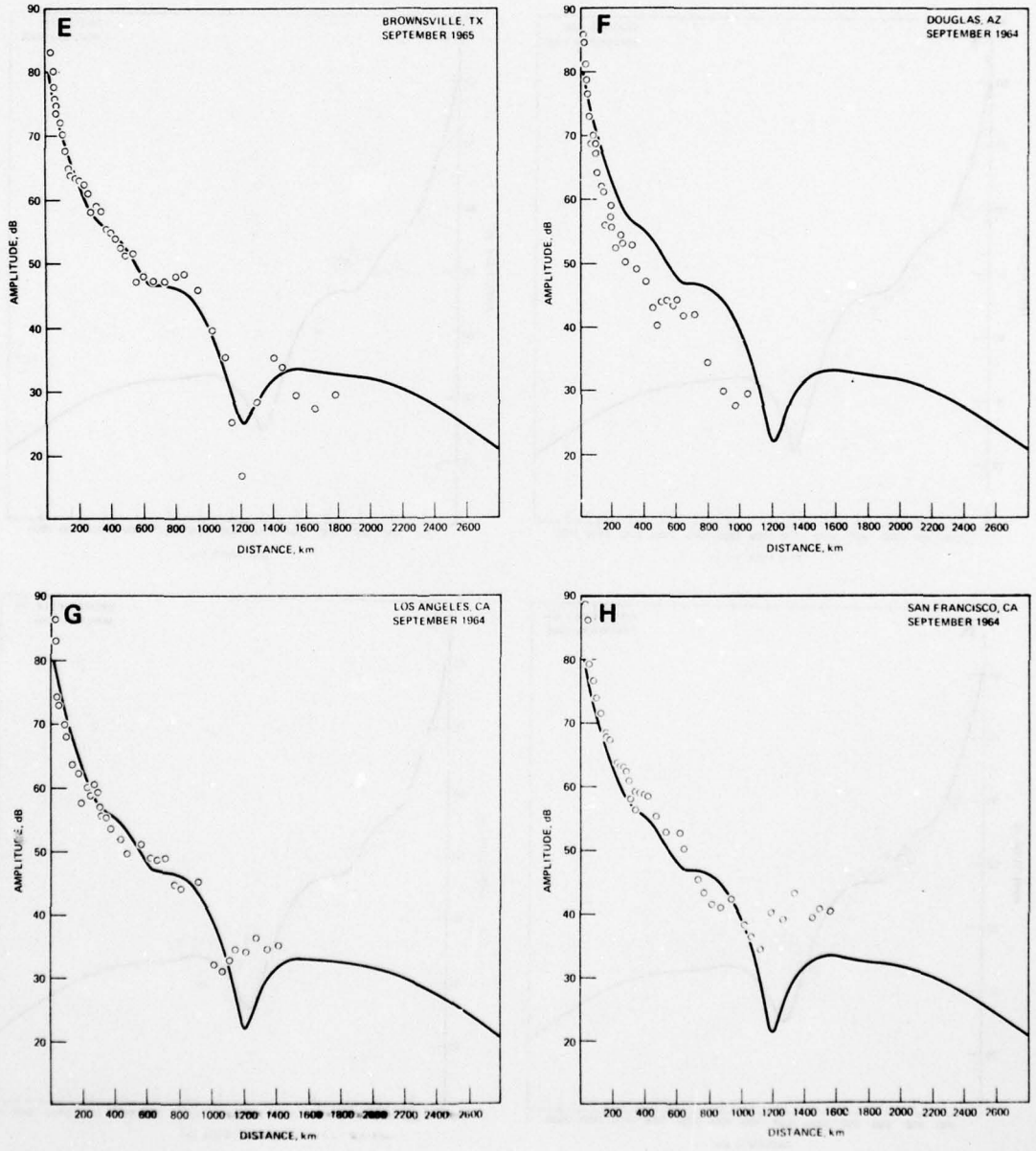

Figure 40. Daytime propagation across the continental United States for various radial paths (60 kHz). (Sheet 2 of 3)

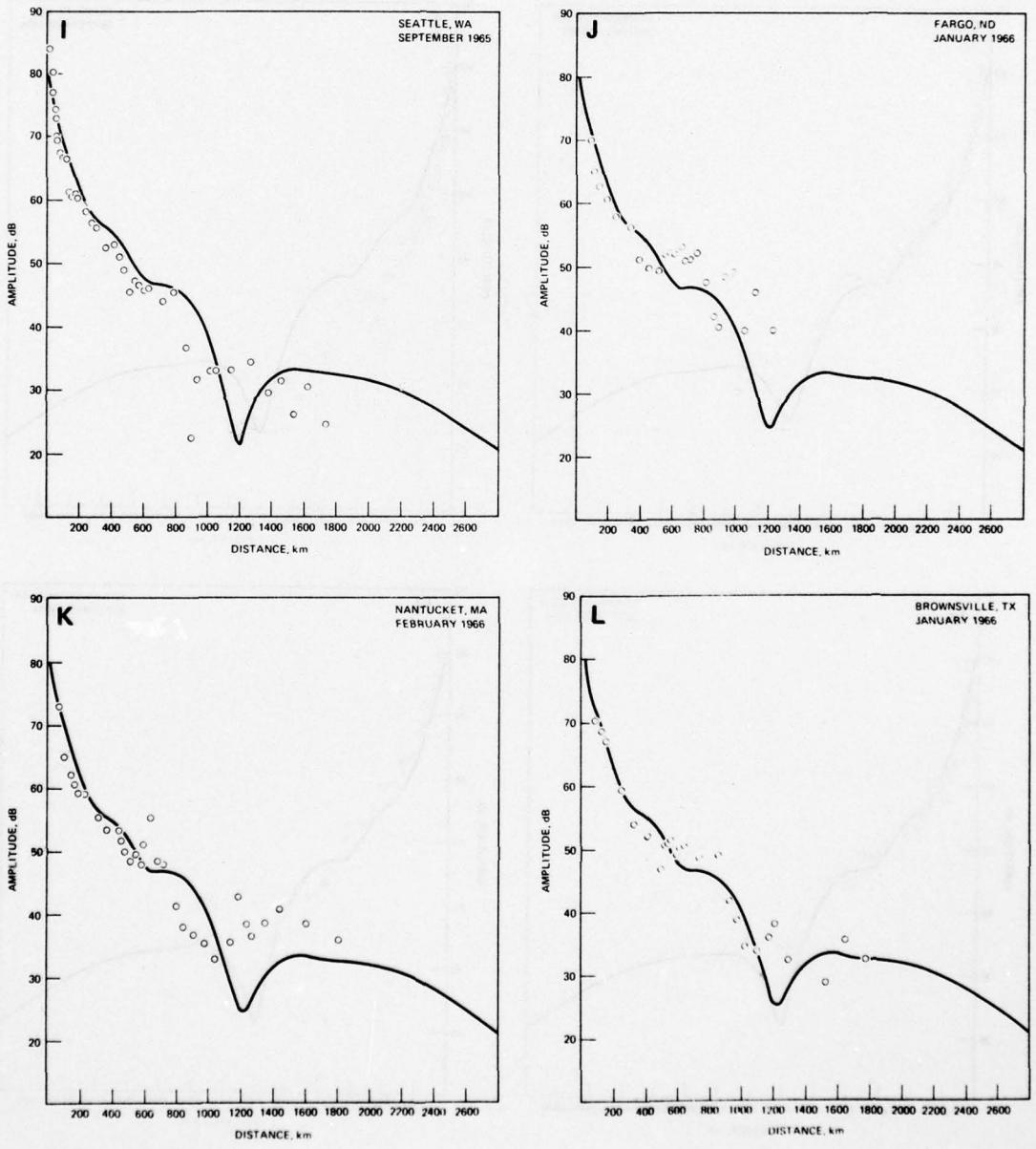

Figure 40. Daytime propagation across the continental United States for various radial paths (60 kHz). (Sheet 3 of 3)

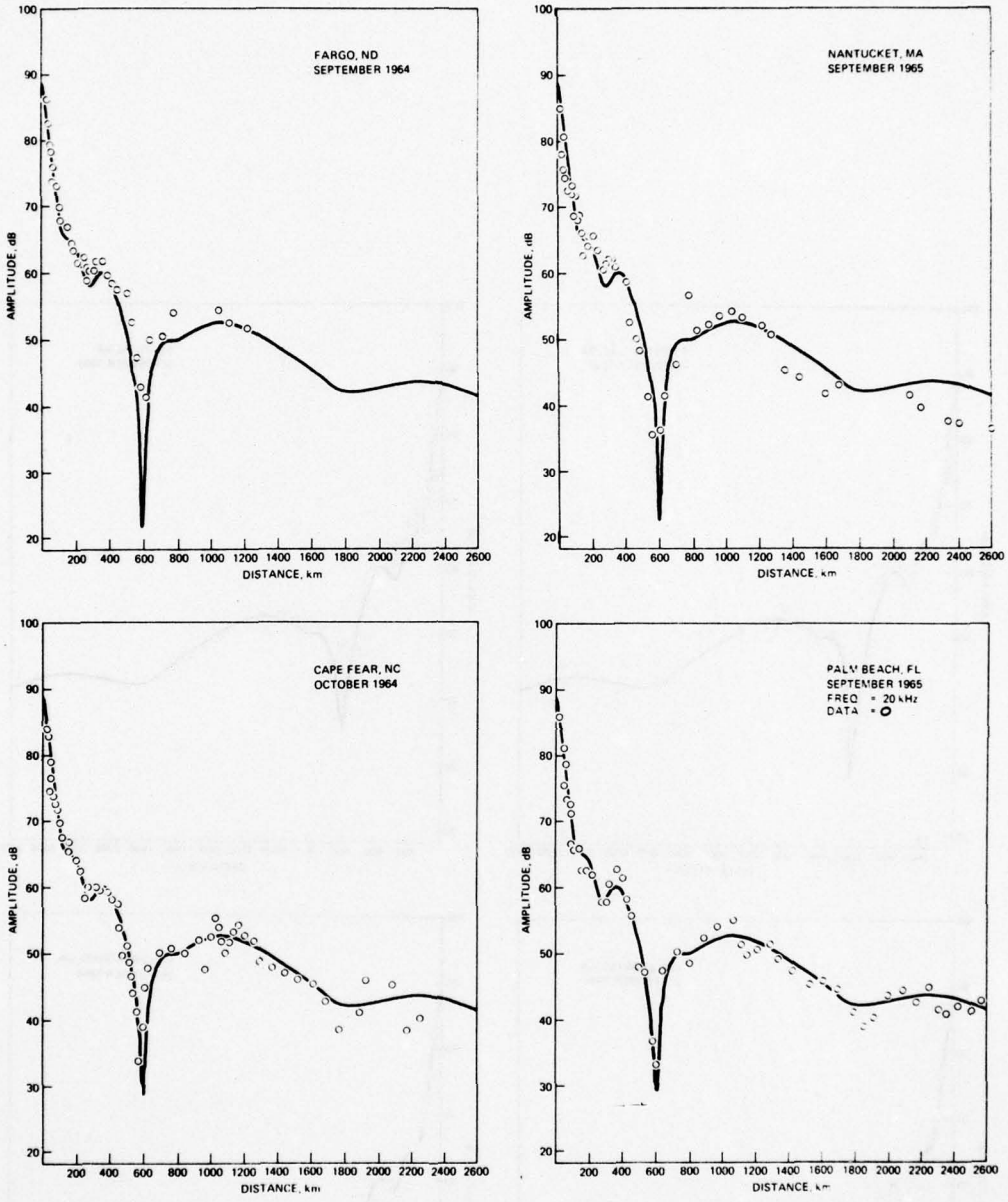

Propagation Path: Nine radials outward from Ft Collins, Colorado (daytime)
Ground Conductivity: Land, σ = 0.01 mhos/meter
Transmitter: WWVL, Ft Collins, Colorado, at 20 kHz
Date: September 1964, 1965; October 1964; January 1966; February 1966
Electron Density Profile: $\beta = 0.3\ km^{-1}$, H' = 72 km
Method of Computation: Horizontally homogenous waveguide

Figure 41. Daytime propagation across the continental United States for various radial paths (20 kHz). (Sheet 1 of 3)

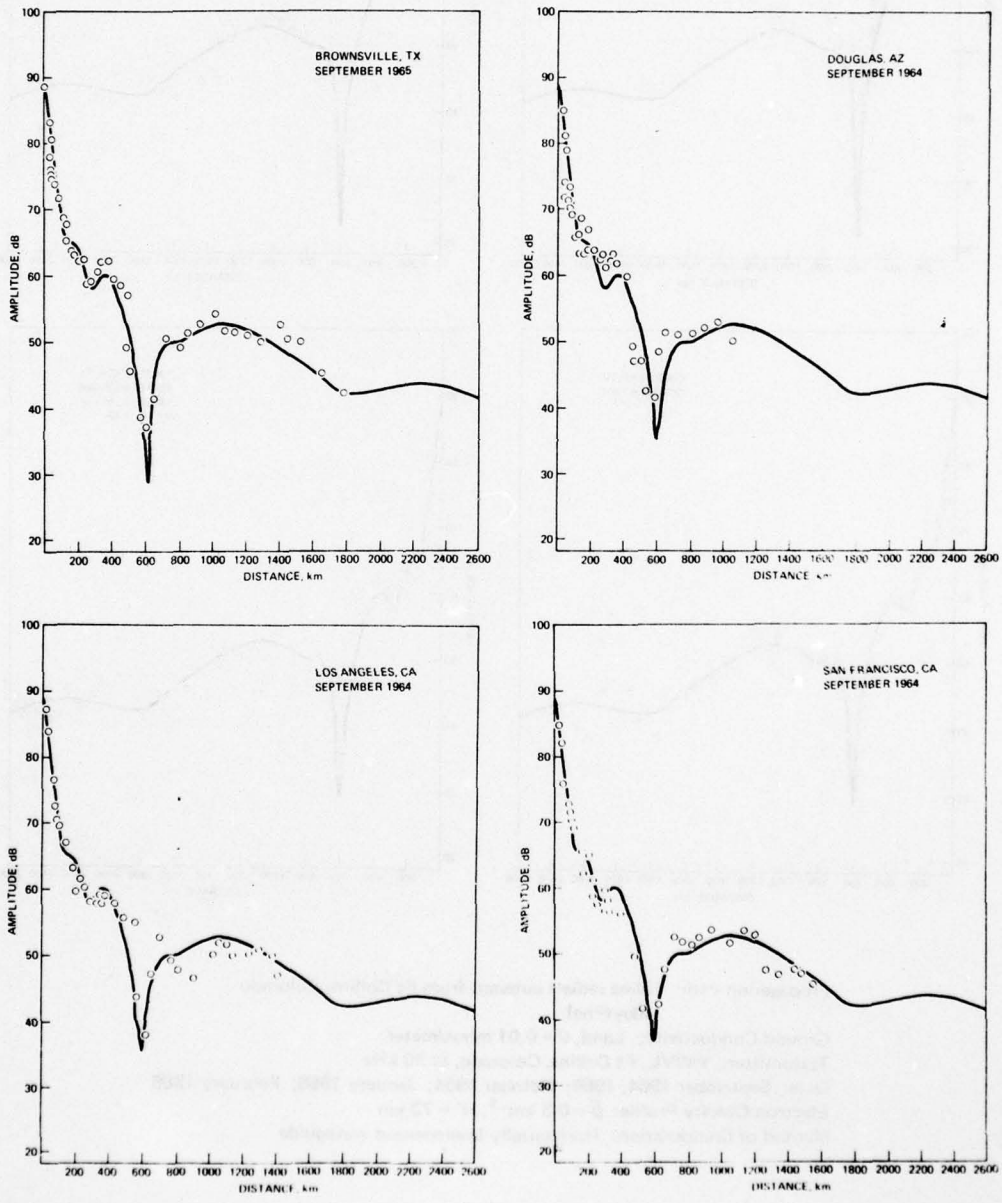

Figure 41. Daytime propagation across the continental United States for various radial paths (20 kHz). (Sheet 2 of 3)

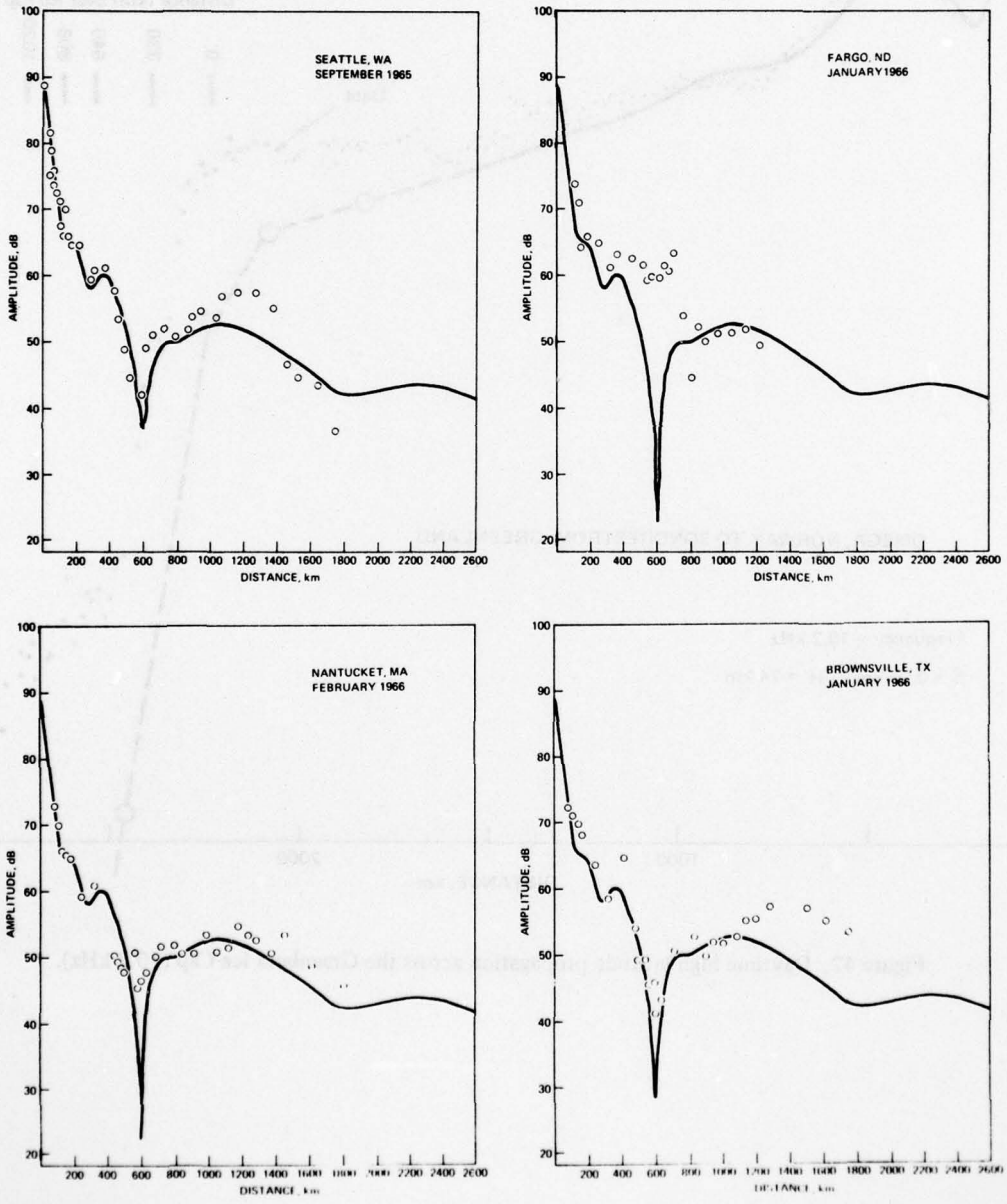

Figure 41. Daytime propagation across the continental United States for various radial paths (20 kHz). (Sheet 3 of 3)

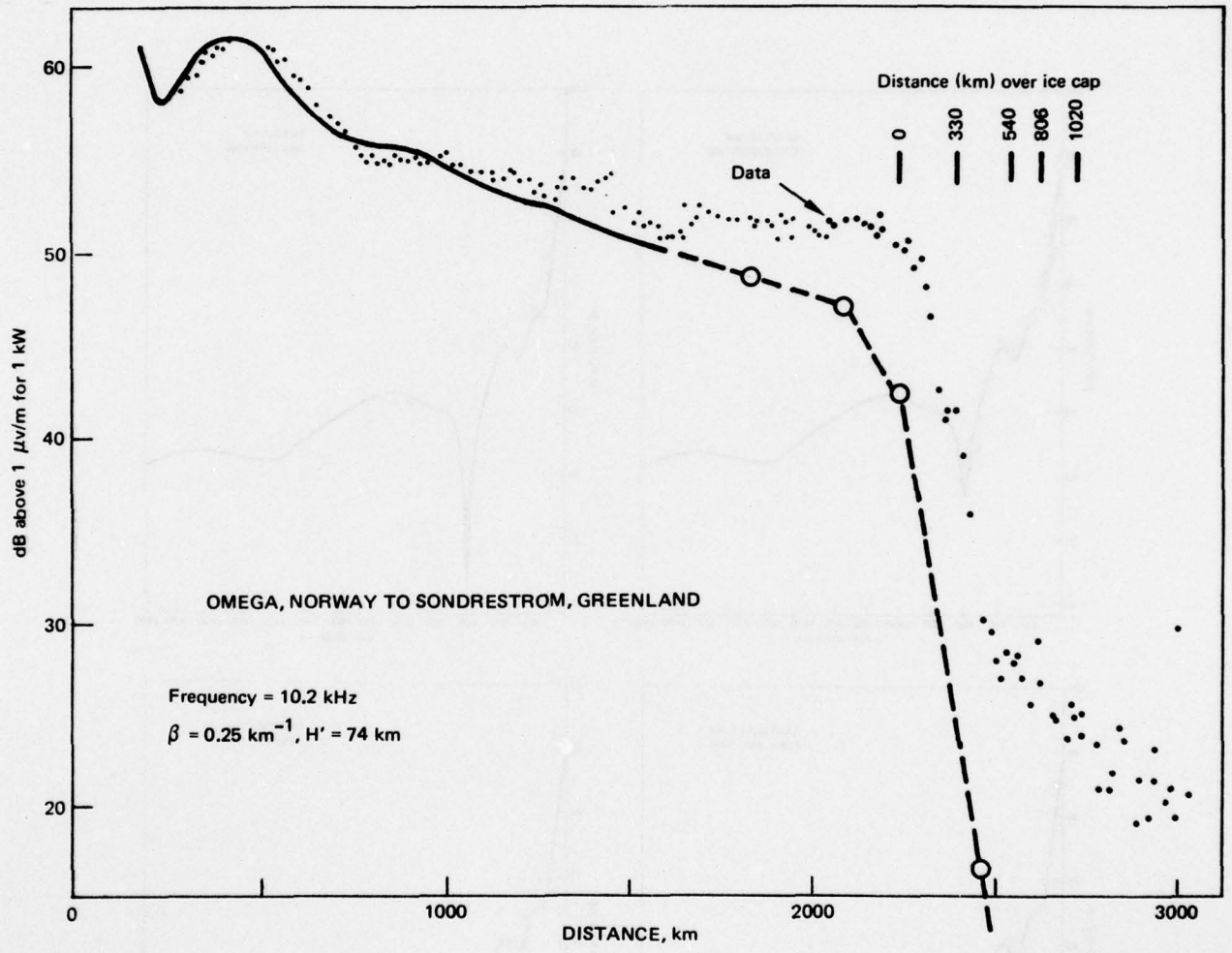

Figure 42. Daytime high latitude propagation across the Greenland Ice Cap (10.2 kHz).

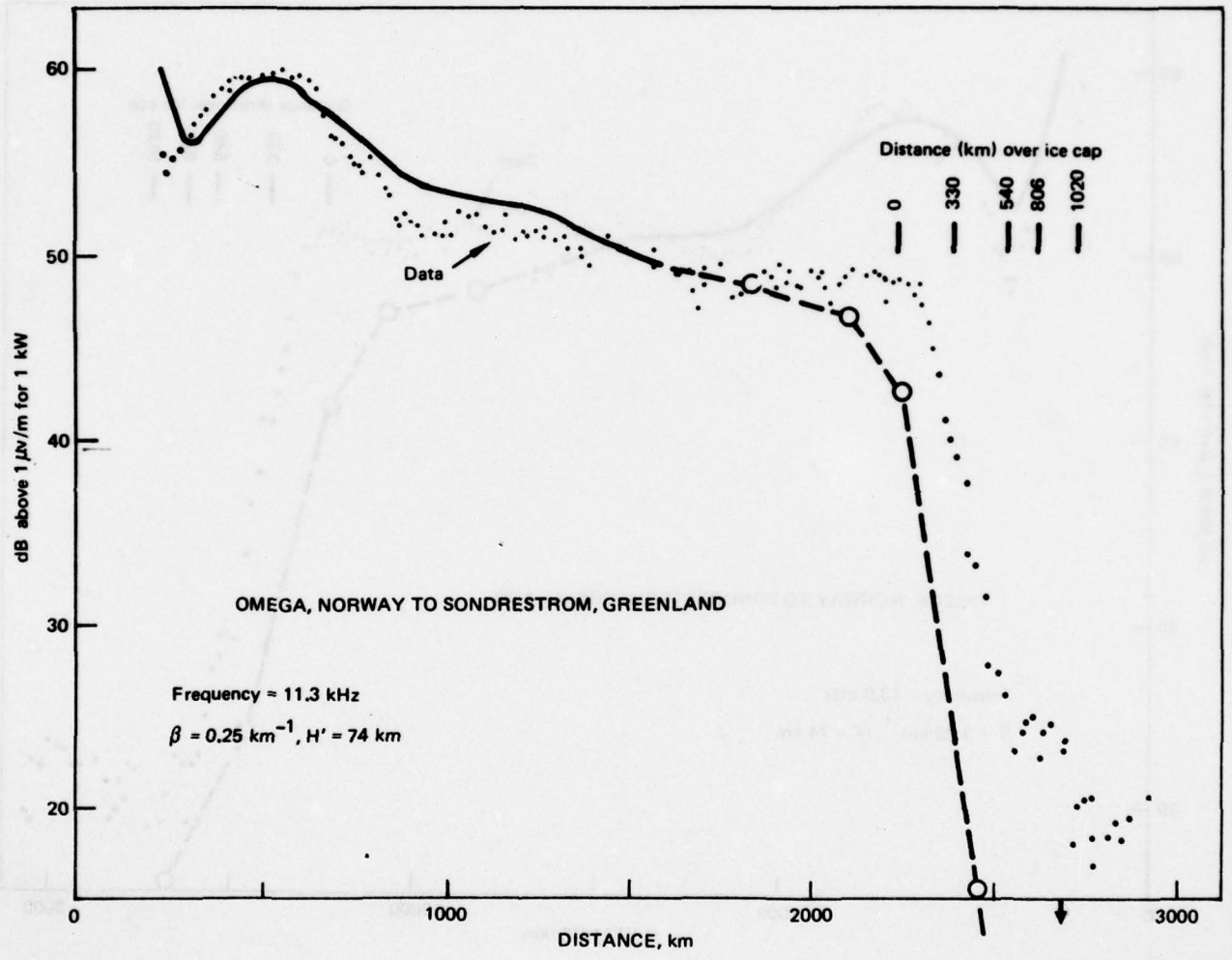

Figure 43. Daytime high latitude propagation across the Greenland Ice Cap (11.3 kHz).

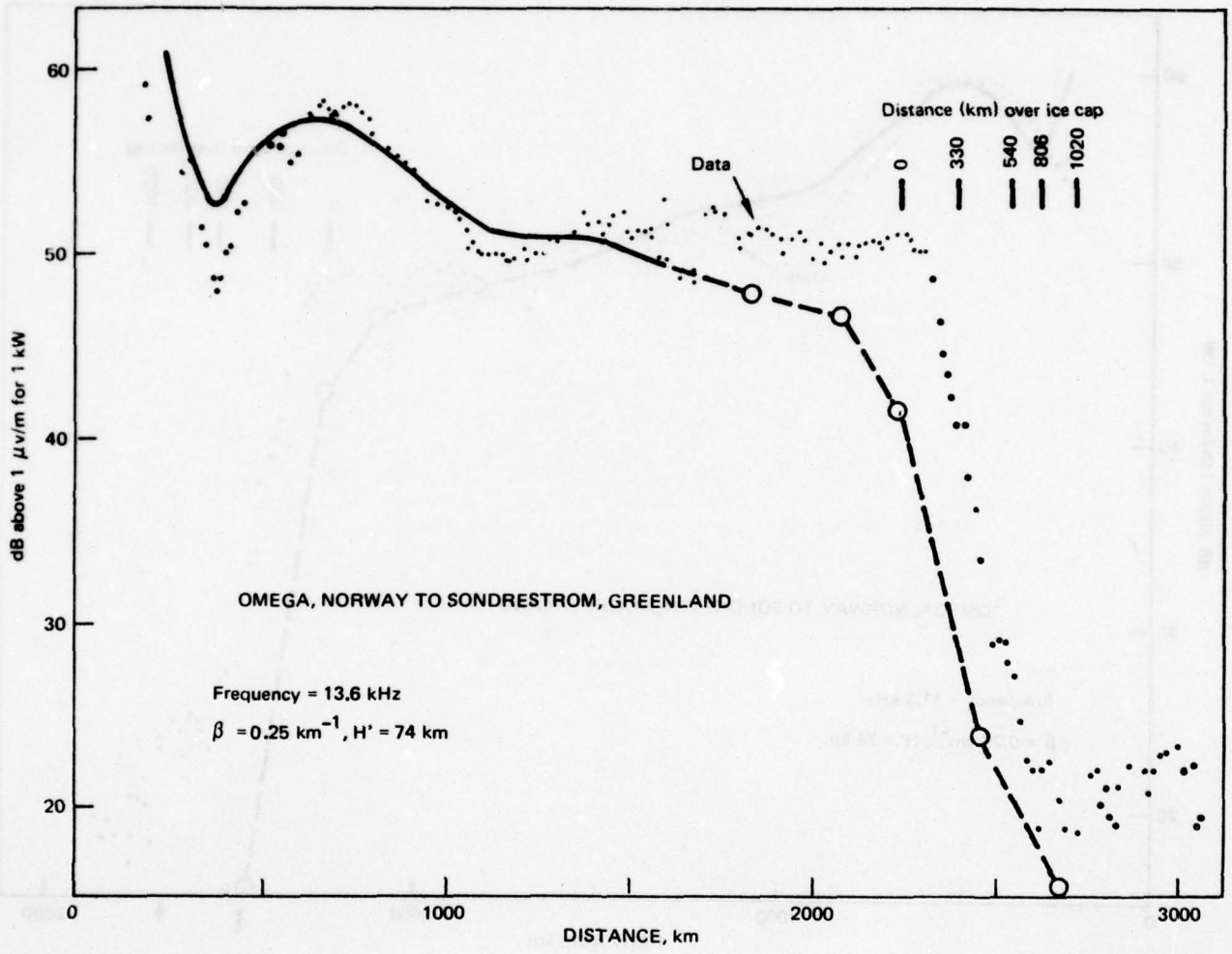

Figure 44. Daytime high latitude propagation across the Greenland Ice Cap (13.6 kHz).

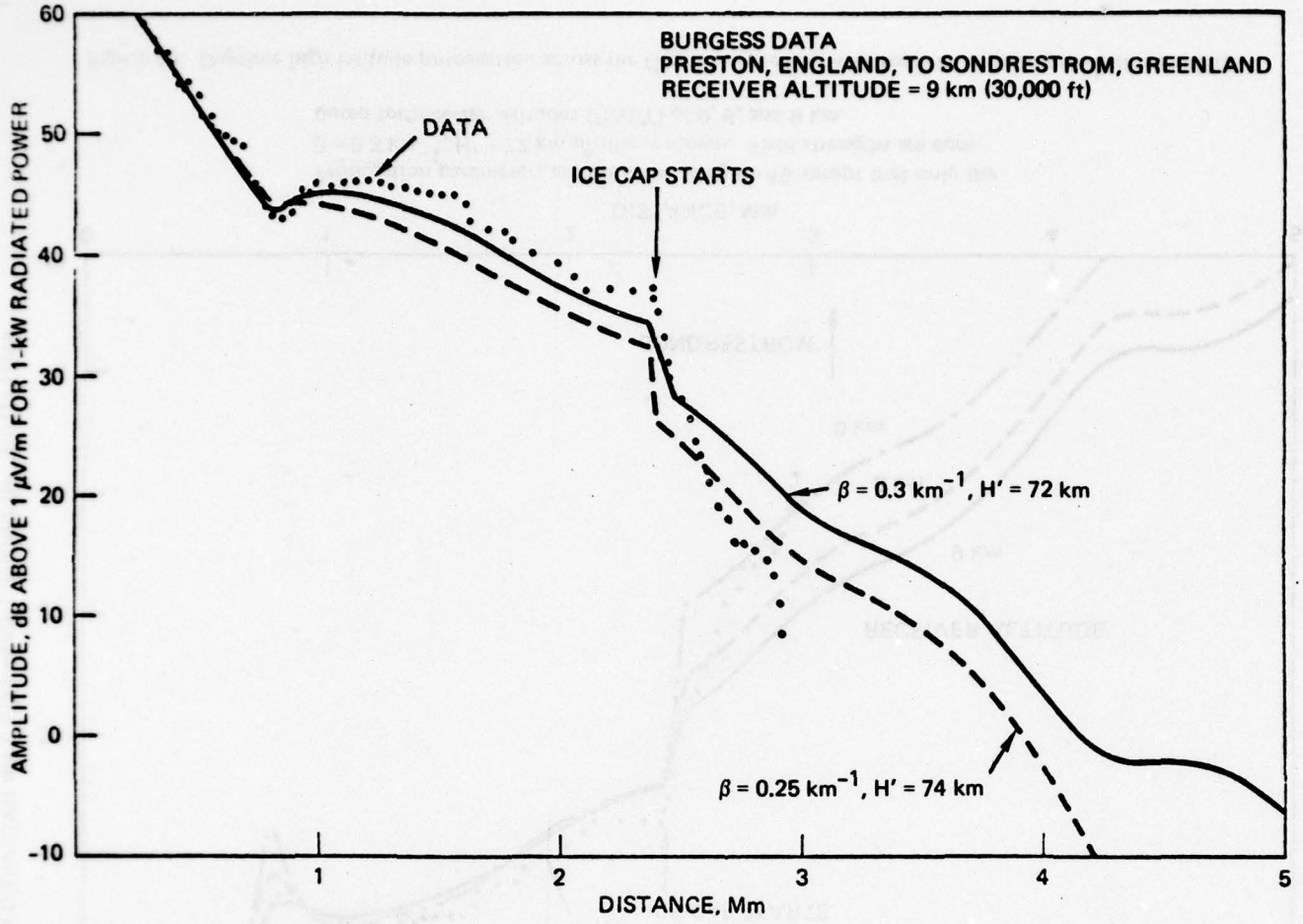

Ground conductivity: Seawater, 4 mhos/meter; Greenland Ice Cap, 10^{-5} mhos/meter
Transmitter: GYN, Preston, England (45 kHz)
Method of Computation: WKB approximation

Figure 45. Daytime high latitude propagation across the Greenland Ice Cap (45 kHz).

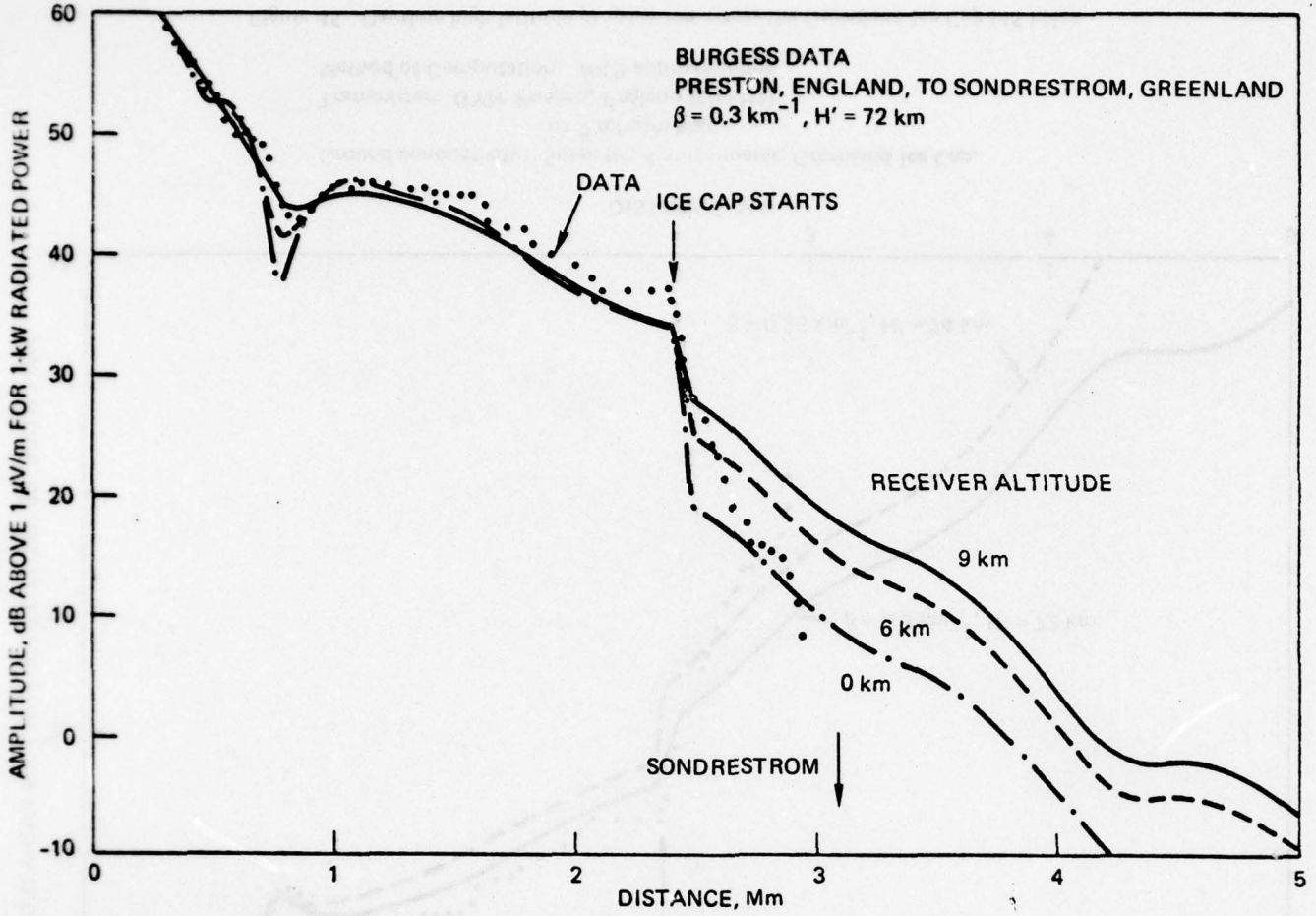

Propagation parameters are the same as figure 45 except that only the $\beta = 0.3\ km^{-1}$, H' = 72 km profile is shown. Field strengths are computed for receiver altitudes (RALT) of 0, 6, and 9 km.

Figure 46. Daytime high latitude propagation across the Greenland Ice Cap with receiver altitude variations (45 kHz).

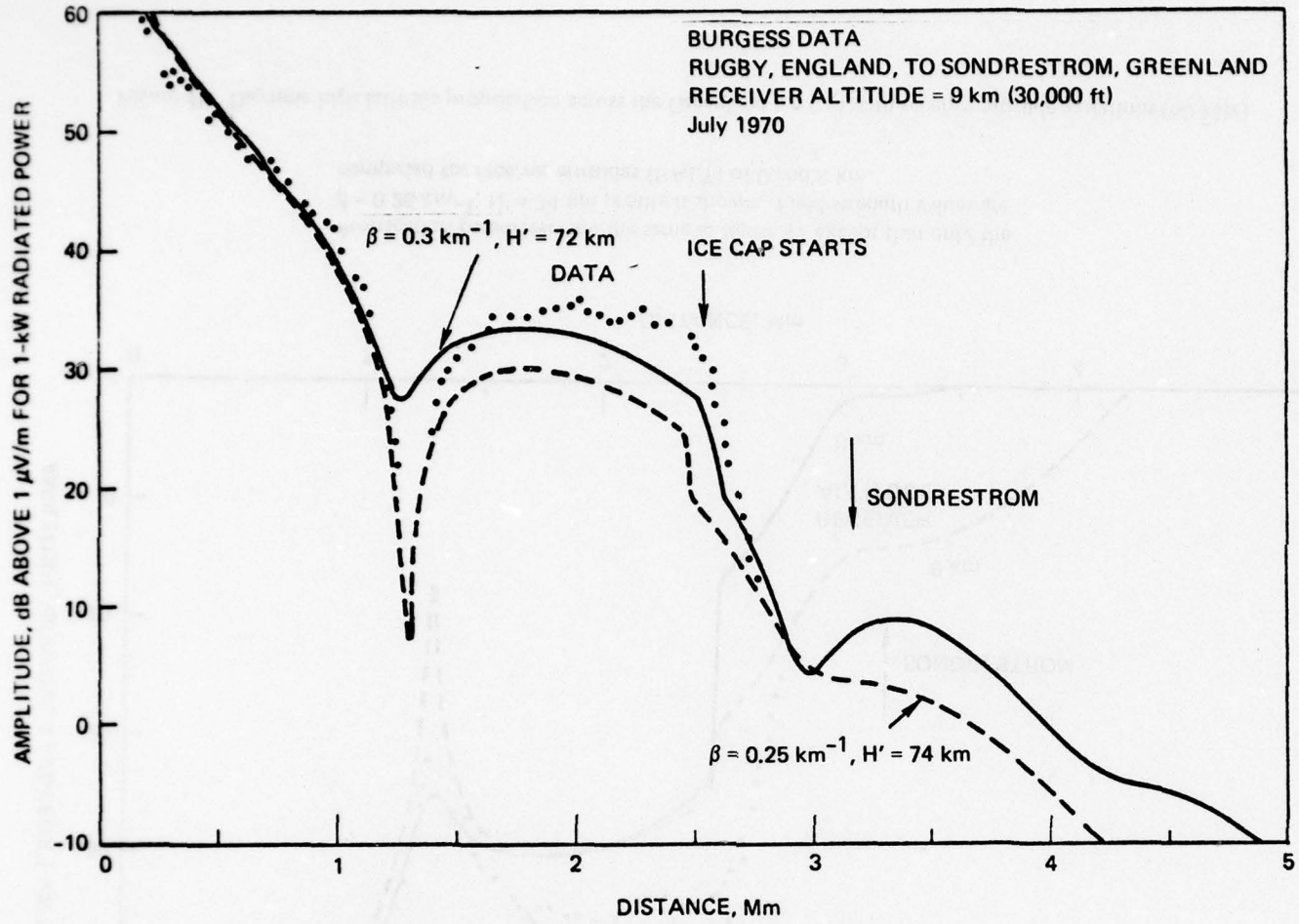

Ground conductivity: Seawater, 4 mhos/meter; Greenland Ice Cap, 10^{-5} mhos/meter
Transmitter: MSF, Rugby, England (60 kHz)
Method of Computation: WKB approximation

Figure 47. Daytime high latitude propagation across the Greenland Ice Cap (60 kHz).

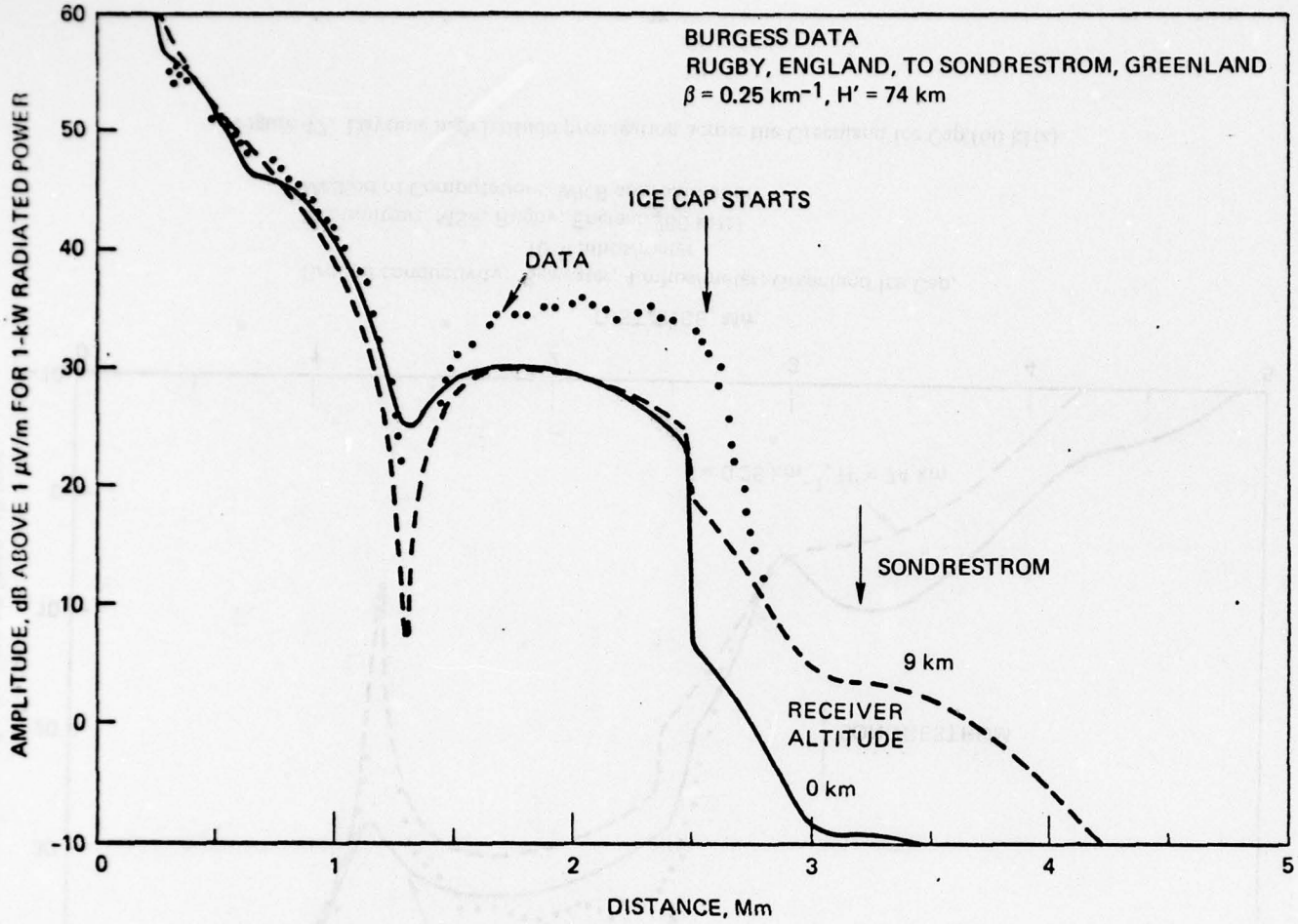

Propagation parameters are the same as figure 47 except that only the $\beta = 0.25\ km^{-1}$, $H' = 74$ km profile is shown. Field strength values are computed for receiver altitudes (RALT) of 0 and 9 km.

Figure 48. Daytime high latitude propagation across the Greenland Ice Cap with receiver altitude variations (60 kHz).

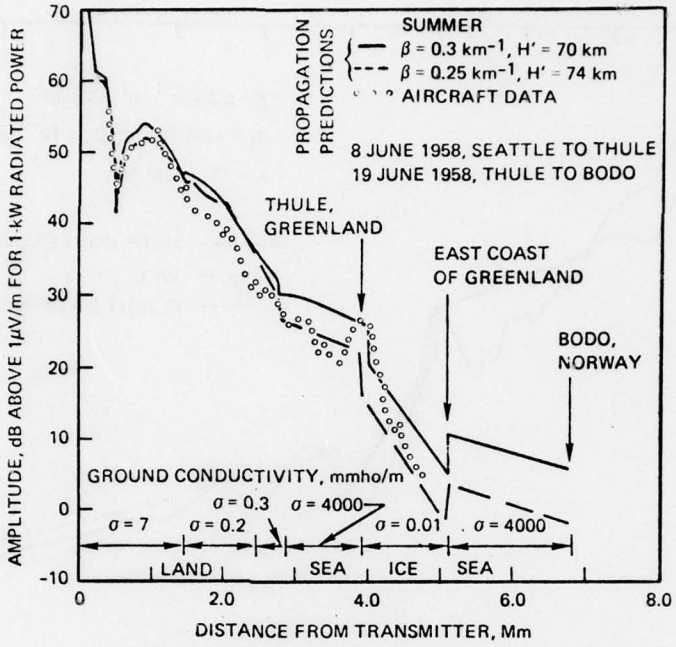

Flight Path: Seattle, Washington across Canada and over the Greenland Ice Cap.
Ground conductivity: Various values of land, sea, and ice along the path.
Method of Computation: WKB approximation.

Figure 49. Daytime high latitude propagation across the Greenland Ice Cap (NLK 18.6 kHz).

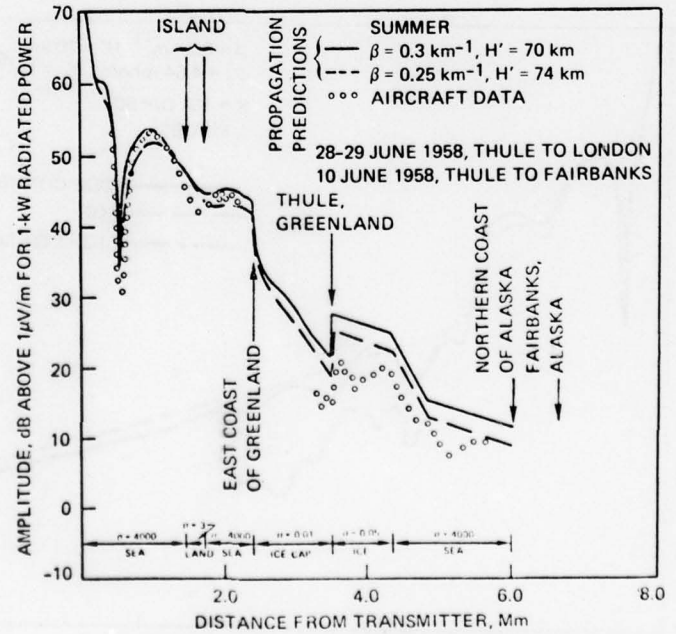

Ground conductivity: Various values of land, sea, and ice along the path.
Transmitter: GBZ, Rugby, England (19.6 kHz)
Method of Computation: WKB approximation.

Figure 50. Daytime high latitude propagation across the Greenland Ice Cap (GBZ 19.6 kHz).

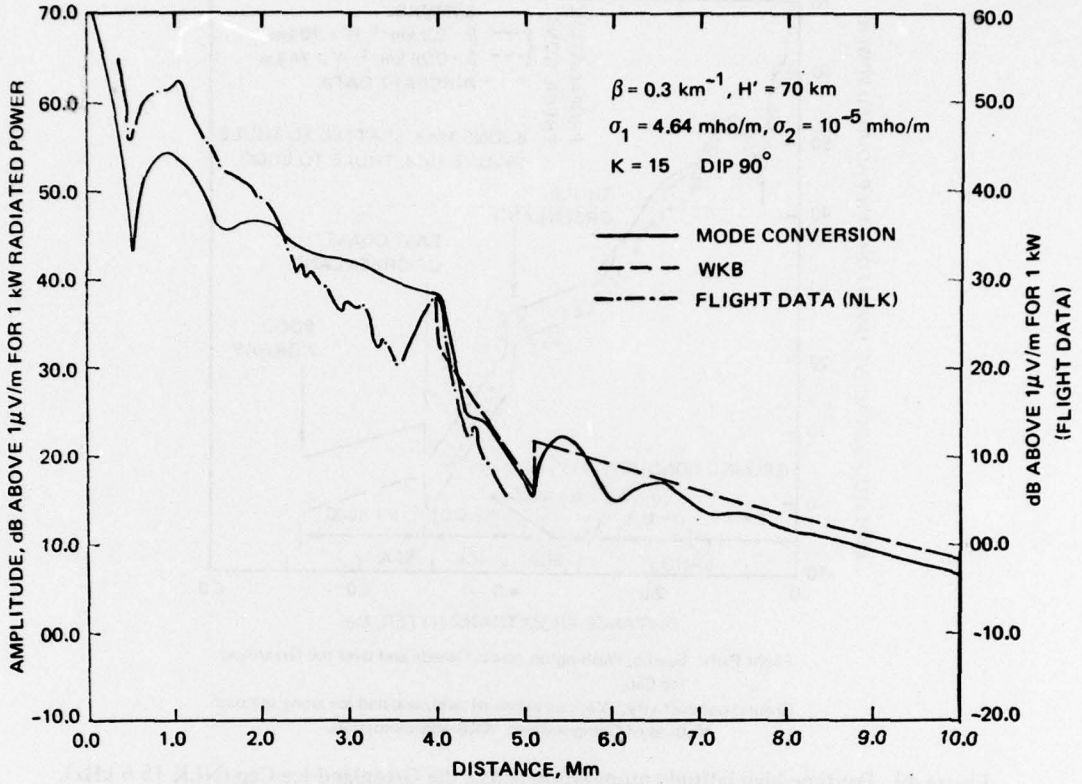

Figure 51. Daytime high latitude propagation across the Greenland Ice Cap with mode conversion (18.6 kHz).

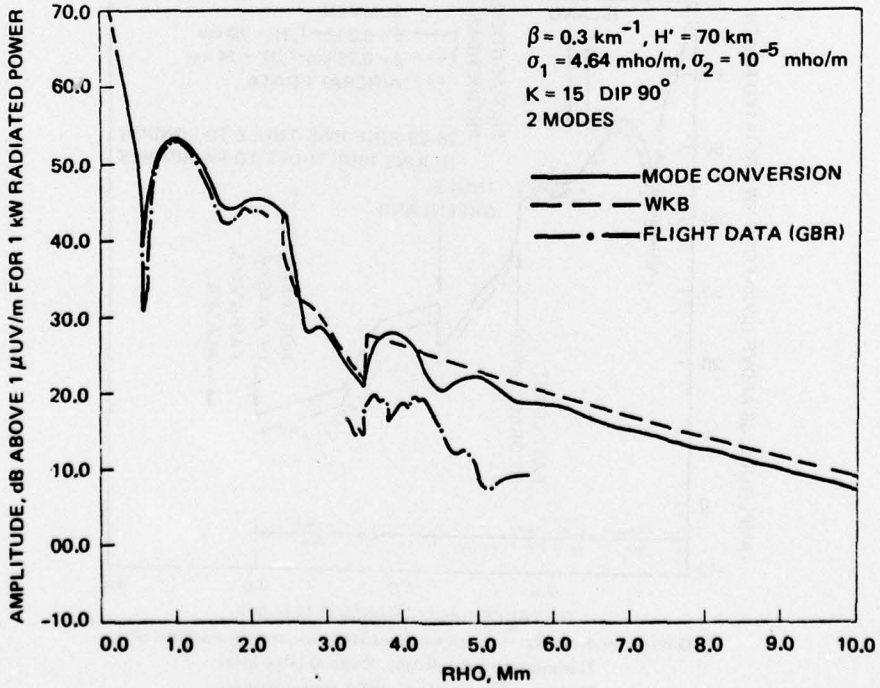

Figure 52. Daytime high latitude propagation across the Greenland Ice Cap with mode conversion (19.6 kHz).

CONCLUSION

This report illustrates the ability of the NOSC field strength computer programs to predict realistic vlf/lf signal levels. Comparisons between predicted and measured values of field strength, as presented in the figures, show that the complicated interference structure characteristic of radio wave propagation at the called out frequencies may be very closely simulated if the propagation parameters are known to be fairly accurate.

It has been determined that the effective electron density profiles, tables 16, 17, and 18, best describe the available propagation data.

Based on the field strength levels recorded over the midlatitude Hawaii to Southern California transmission path, the following exponential profiles most accurately describe the propagation data recorded during winter for daytime and nighttime propagation. Based on the data presented for this path and other Pacific Ocean paths, the choice of profile for daytime summer is listed in table 16.

TABLE 16. EFFECTIVE ELECTRON DENSITY PROFILES FOR USE IN PROPAGATION PREDICTIONS, MIDLATITUDE–PACIFIC.

Daytime		Nighttime	
Frequency (kHz)	Profile β (km^{-1}), H′ (km)	Frequency (kHz)	Profile β (km^{-1}), H′ (km)
Winter		Winter	
9 - 60	$\beta = 0.3$, H′ = 74	below 10	$\beta = 0.3$, H′ = 87
		10 - 15	$\beta = 0.4$, H′ = 87
Summer		15 - 25	$\beta = 0.5$, H′ = 87
16 - 26	$\beta = 0.5$, H′ = 70	25 - 30	$\beta = 0.6$, H′ = 88
		30 - 40	$\beta = 0.7$, H′ = 88
		40 - 60	$\beta = 0.8$, H′ = 88

These ionospheric profiles (table 16) result in winter predictions of signal amplitudes which, on the average, are within 2 dB for daytime and within 3 dB for nighttime of those amplitudes recorded aboard the inflight aircraft.

The nighttime results for 28.0, 37.4, 40.5, 46.7, 52.9, and 56.0 kHz are illustrated in figures 53 through 58. In these figures, the differences between computed signal amplitudes and measured data are plotted as a function of propagation distance. The computed values are obtained first by using the profile $\beta = 0.5$ km^{-1}, H′ = 87 km for all frequencies and then as a function of frequency by using the profiles presented in table 16. The measured values are derived by taking the average signal level as a function of propagation range from the recorded data listed in table 9. The figures (53–58) show the improvement made in predicting signal levels using the profiles from table 9 over what is obtained when the single profile $\beta = 0.5$ km^{-1}, H′ = 87 km is used over the 15–60 kHz frequency band.

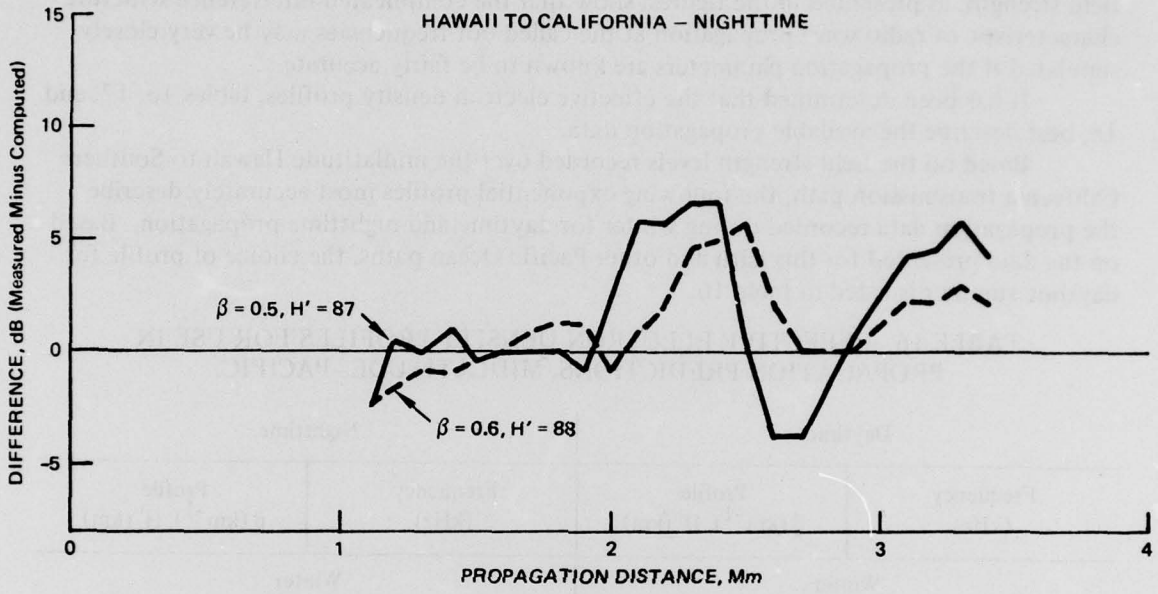

Figure 53. Improvement in propagation predictions at 28.0 kHz.

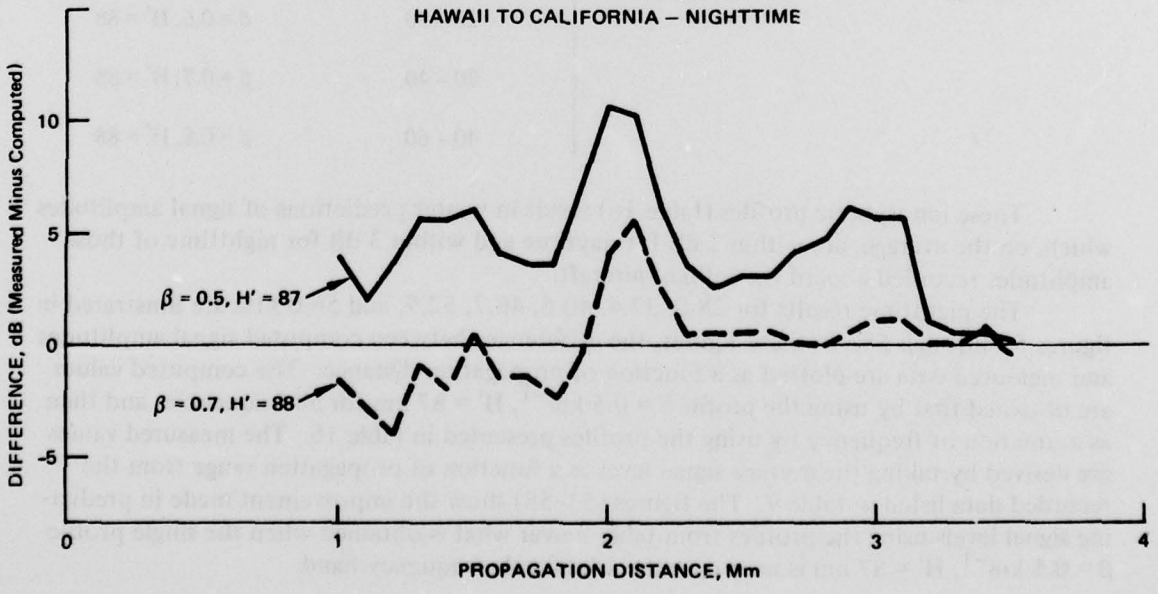

Figure 54. Improvement in propagation predictions at 37.4 kHz.

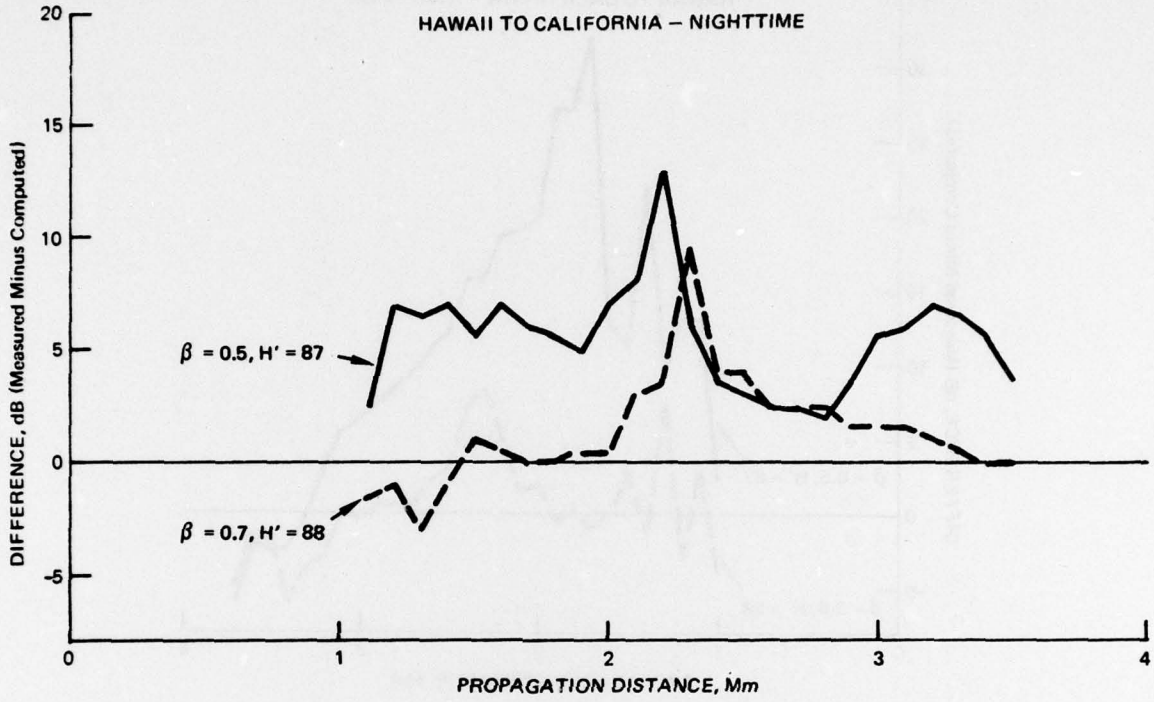

Figure 55. Improvement in propagation predictions at 40.5 kHz.

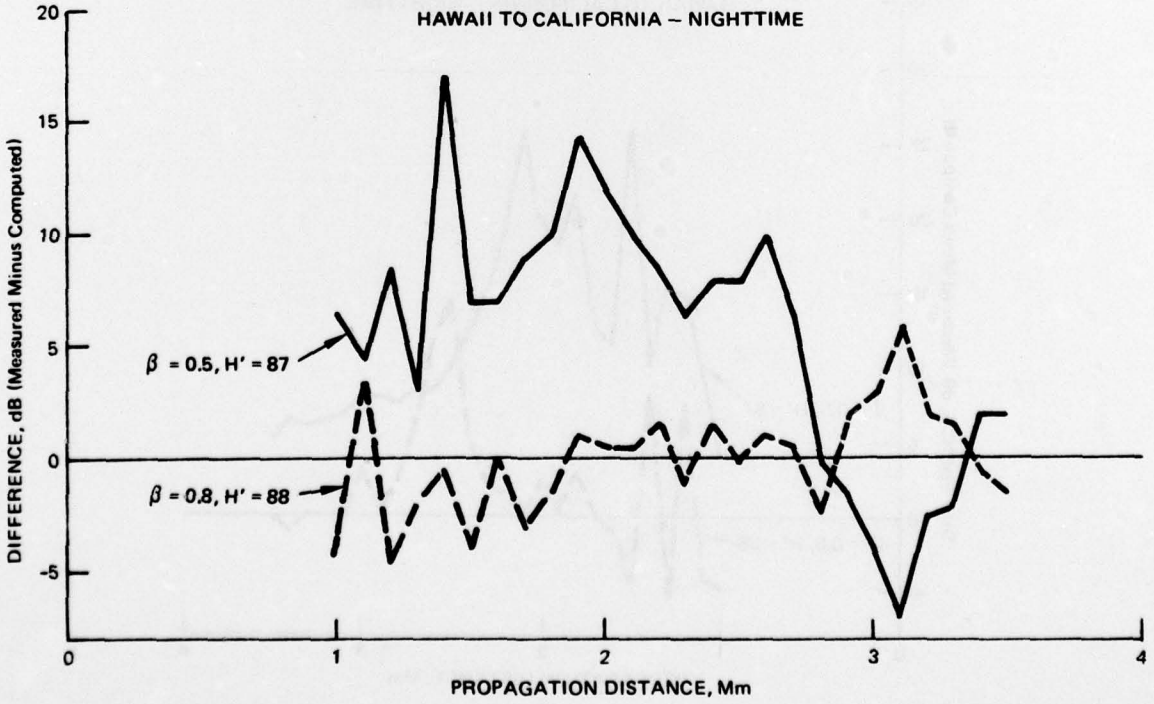

Figure 56. Improvement in propagation predictions at 46.7 kHz.

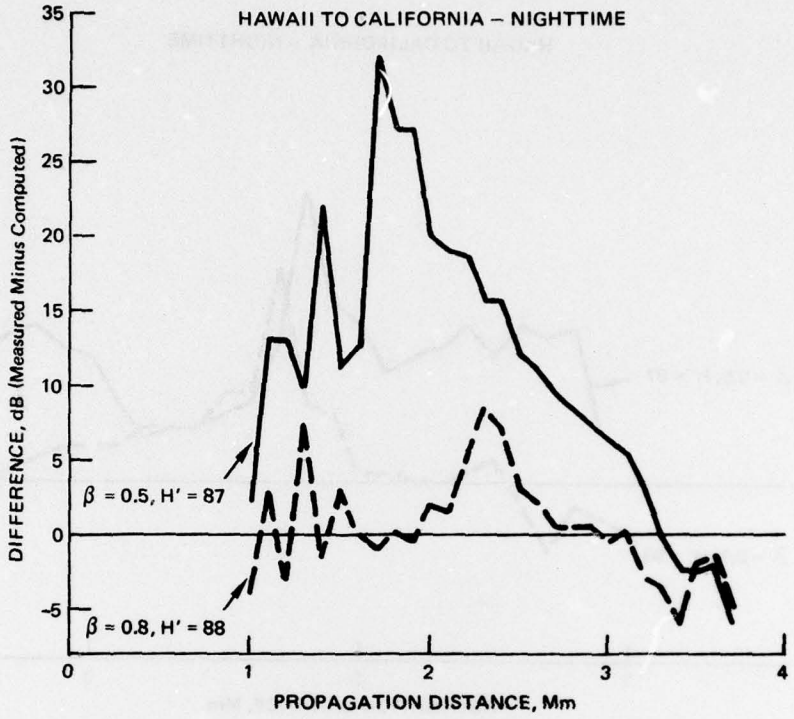

Figure 57. Improvement in propagation predictions at 52.9 kHz.

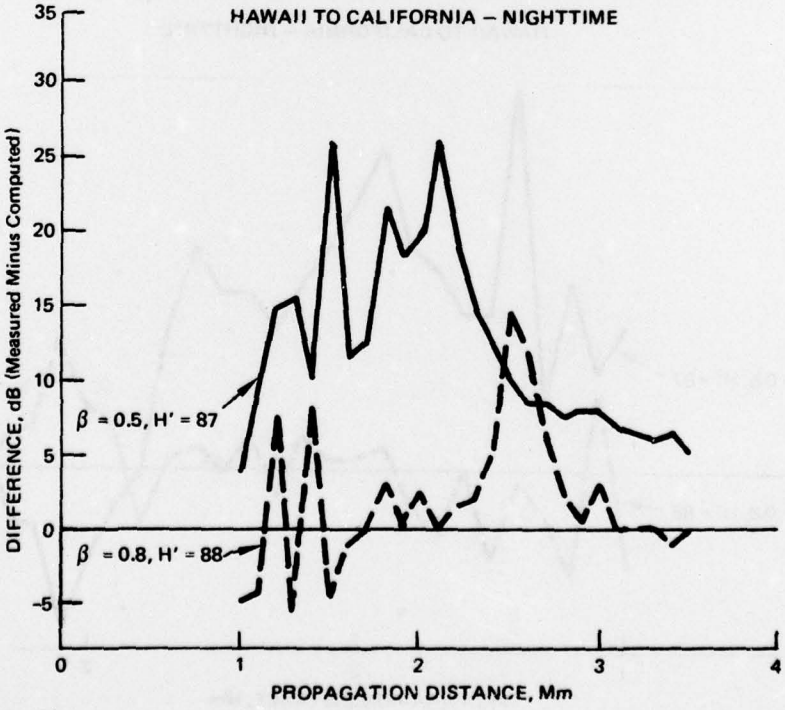

Figure 58. Improvement in propagation predictions at 56.0 kHz.

Table 17 summarizes the results for propagation predictions as compared to data measurements for transmissions across the continental United States.

TABLE 17. EFFECTIVE ELECTRON DENSITY PROFILES FOR USE IN DAYTIME PROPAGATION PREDICTIONS ACROSS THE CONTINENTAL UNITED STATES.

"Best-fit" Profile	Month	Frequency (kHz)
$\beta = 0.3\ km^{-1}$, $H' = 72\ km$	June, Sept-Oct, Jan	20
$\beta = 0.3\ km^{-1}$, $H' = 72\ km$	Sept-Oct, Jan	60

No analysis was carried out for nighttime propagation across the continental US due to the lack of experimental measurements.

For propagation over high latitudes the choice of "best-fit" exponential electron density profiles is given in table 18.

TABLE 18. EFFECTIVE ELECTRON DENSITY PROFLIES FOR USE IN DAYTIME PROPAGATION ACROSS THE GREENLAND ICE CAP AND AT HIGH LATITUDES.

"Best-fit" Electron Density Profile	Season	Frequency (kHz)
$\beta = 0.25\ km^{-1}$, $H' - 74\ km$	Summer	10.2, 11.3, 13.6
$\beta = 0.25\ km^{-1}$, $H' = 74\ km$ / $\beta = 0.3\ km^{-1}$, $H' = 72\ km$	Summer	20
$\beta = 0.3\ km^{-1}$, $H' = 72\ km$	Summer	45.0, 60.0

Again no analysis was carried out for nighttime propagation at high latitudes due to the lack of experimental data.

It is possible that other choices of electron density profiles could be found that would fit the propagation data more closely in some instances. The exponential form of the profiles in this report was chosen for computations in our analysis because attempts to find more complex shapes would likely require much additional research. The state of the art in analysis procedures allows for an almost infinite variety of profile shapes to be examined. Also, since the propagation paths being considered are quite long, any profile determined to produce a "best-fit" to the data is really an average profile for the total path.

The results of the analysis described in this report demonstrate the need for changing the gradient of the nighttime exponential profile as a function of frequency. Further investigation should lead to a multiparameter profile which will simultaneously describe the propagation at all vlf/lf frequencies.

RECOMMENDATIONS

In the past, much of the vlf/lf propagation data reported in the literature have consisted of measurements made at a single receiver site on one propagation frequency over a given path. This type of data has not proven useful as far as determining any uniqueness in the form of the electron density profile of the ionosphere through which the radio wave must pass. Data recorded using the NOSC multifrequency sounder, on the other hand, give signal levels at many frequencies simultaneously. With this type of data acquisition, much more data are available at the termination of a single propagation path. In the case where a receiver is placed aboard an inflight recording aircraft, multifrequency data are obtained as a continuous function of distance. The availability of such multiple frequency data provides a facility for determining a much more unique form of the ionospheric electron density than has previously been possible.

The propagation theory implemented in existing computer programs is probably sufficient for computing signal levels as a function of frequency and distance. This theory requires that very little additional effort needs to be expended on the analytical aspect of the propagation. However, in order to make accurate predictions of vlf/lf signal levels on a global basis the propagation environment—particularly the electron density profile of the ionosphere—must be known more precisely than it is at this time. The ionosphere itself is sufficiently variable with respect to geographic longitude and latitude. As to diurnal and seasonal changes, the ability to make precise predictions of propagated fields for all propagation paths and for all seasons has been quite limited. If only existing data are considered in determining ionospheric profiles, propagation predictions must be based on relatively few, isolated data sources. To produce more reliable and accurate vlf/lf propagation predictions for utilization in the development of Navy and Air Force operational systems, additional data in all geophysical environments are needed. This includes measurements of propagation data over many propagation paths at many frequencies during the four seasons and should include measurements of signal amplitude and phase as recorded versus time and/or distance on several frequencies simultaneously. These measurements will allow us to obtain the most reliable and definitive information concerning the effective long path propagation medium. Signals to be measured should include those radiated by airborne long-trailing wire antennas, fixed site operational vlf/lf communication, and navigation systems and experimental transmitting facilities such as the NOSC multifrequency sounder which permits data to be recorded on 10 to 20 frequencies simultaneously ranging from 9 to 60 kHz.

The most important propagation paths over which data should be obtained are:

- Those involving primarily seawater at nearly constant geomagnetic latitude where the propagation paths may be assumed to be horizontally homogenous, thus simplifying interpretation and analysis of the data.

- High latitude paths, ie, those passing through polar cap region and auroral zone. Only a very limited amount of information and data are available concerning the effective ionospheric profiles that support long distance vlf/lf propagation in the higher latitudes. Paths which pass through these regions will provide an opportunity to determine the electron density profiles as produced by solar-geophysical phenomena, ie, PCA events, solar flares, and geomagnetic storms.

- Paths which contain highly varying ground conductivities, such as propagation across Canada and over the Greenland Ice Cap, should also be included to examine further the utility of the prediction model in simulating these propagation conditions.

Once a sufficient amount of experimental data has been acquired, the ionospheric parameters, ie, electron density profiles, which describe the propagation environment may be determined with sufficient accuracy to ensure reliable predictions of vlf/lf signal levels. These predictions can be used, together with data on signal variability, atmospheric noise, and system parameters, to compute the time availability of MEECN vlf/lf links.

REFERENCES

1. Budden, KG, Radio Waves in the Ionosphere, Cambridge University Press, 1961

2. Budden, KG, The Waveguide Mode Theory of Wave Propagation, Prentice Hall, Inc, Englewood Cliffs, NJ, 1961

3. Wait, JR, Electromagnetic Waves in a Stratified Media, Pergamon Press, Inc, Elmsford, NY 1962

4. Galejs, J, Terrestrial Propagation of Long Electromagnetic Waves, Pergamon Press, Inc, Elmsford, NY, 1972

5. Pappert, RA, EE Gossard, and IJ Rothmuller, A Numerical Investigation of Classical Approximations Used in VLF Propagation, Radio Science, v 2, p 387–400, April 1967

6. Wait, JR, Two-Dimensional Treatment of the Mode Theory of the Propagation of VLF Radio Waves, Radio Science, v 68D, p 81–95, January 1964

7. Bickel, JE [illegible]erguson, and GV Stanley, Experimental Observation of Magnetic Field [illegible]on VLF Propagation at Night, Radio Science, p 19–25, January 1970

8. Naval [illegible]tronics Laboratory Center Interim Report 722, Mode Conversion Program for an Inhomogeneous Anisotropic Ionosphere, by RA Pappert and LR Shockey, 1 May 1972

9. Pappert, RA and FP Snyder, Some Results of a Mode-Conversion Program for VLF, Radio Science, v 7, p 913–923, October 1972

10. Pappert, RA, Effects of Elevation and Ground Conductivity on Horizontal Dipole Excitation of the Earth-Ionosphere Waveguide, Radio Science, v 5, p 579–590, March 1970

11. Pappert, RA and JE Bickel, Vertical and Horizontal VLF Fields Excited by Dipoles of Arbitrary Orientation and Elevation, Radio Science, v 5, p 1445–1452, December 1970

12. Naval Electronics Laboratory Center Technical Report 1833, Measurements of Vertical and Horizontal VLF Fields Excited by an Elevated, Arbitrarily Oriented Antenna, by JE Bickel, 21 July 1972

13. Naval Electronics Laboratory Center Interim Report 702, A Fortran Program for Waveguide Propagation Which Allows for Both Vertical and Horizontal Dipole Excitation, by RA Pappert and LR Shockey, 15 June 1970

14. Naval Electronics Laboratory Center Interim Report 713, WKB Mode Summing Program for VLF/ELF Antennas of Arbitrary Length, Shape and Elevation, by RA Pappert and LR Shockey, 2 June 1971

15. Wait, JR and KP Spies, Characteristics of the Earth-Ionosphere Waveguide for VLF Radio Waves, National Bureau of Standards Technical Note 300, 30 December 1964

16. Naval Ordance Laboratory Corona Report 722, Multiple-Frequency Oblique-Incidence VLF Ionospheric Sounder, by DA Wulfing and VE Hildebrand, 5 May 1967

17. Naval Weapons Center TWC TP 5038, VLF-Propagation Measurement Technique Using Repetitive-Pulse Spectral Lines, by VE Hildebrand and DJ Adrian, February 1971

18. Naval Research Laboratory Report 6359, An Investigation of the Modal Interference of Very-Low-Frequency Radio Waves, by FJ Rhoads and WE Garner, 27 October 1965

19. Rhoads, FJ and WE Garner, An Investigation of the Modal Interference of VLF Radio Waves, Radio Science, v 2, p 539–546, June 1967

20. Naval Electronics Laboratory Report 767, An Experimental Measurement of VLF Field Strength as a Function of Distance, Using an Aircraft, by JE Bickel, JL Heritage, and S Weisbrod, 28 January 1957

21. Naval Electronics Laboratory Report 1798, Analysis of a Multimode Propagation Concept for Predicting VLF Signal Strengths at Night, by DG Morfitt, 9 December 1971

22. Naval Electronics Laboratory Technical Memorandum TM-909, Amplitude and Phase of NPM Recorded at San Diego from 9 May to 11 July on Five Very Low Frequencies, by JE Bickel, 10 February 1966

23. Naval Electronics Laboratory Center Technical Report, TR 1854, Computer Techniques for Fitting Electron Density Profiles to Oblique-Path VLF Propagation Data, by DG Morfitt, 16 January 1973

24. Naval Electronics Laboratory Report 981, Aircraft Measurements of VLF Field Intensities in the Northern Hemisphere, by JE Bickel, 5 August 1960

25. Gautney and Jones Communications, Inc, TR-66.0141.002, Measured Daytime Field Intensities in the United States at VLF, LF and MF, by GI Morgan, May 1966 (available from DDC, Alexandria, VA)

26. Burgess, Boyd R, Royal Aircraft Establishment, Farnborough, England, letter to CO, NELC, 1972